

# Role of polycation promoters in the cobalt phthalocyanine-catalyzed autoxidation of thiols

**Citation for published version (APA):**

Schipper, E. T. W. M. (1994). *Role of polycation promoters in the cobalt phthalocyanine-catalyzed autoxidation of thiols*. [Phd Thesis 1 (Research TU/e / Graduation TU/e), Chemical Engineering and Chemistry]. Technische Universiteit Eindhoven. <https://doi.org/10.6100/IR410007>

**DOI:**

[10.6100/IR410007](https://doi.org/10.6100/IR410007)

**Document status and date:**

Published: 01/01/1994

**Document Version:**

Publisher's PDF, also known as Version of Record (includes final page, issue and volume numbers)

**Please check the document version of this publication:**

- A submitted manuscript is the version of the article upon submission and before peer-review. There can be important differences between the submitted version and the official published version of record. People interested in the research are advised to contact the author for the final version of the publication, or visit the DOI to the publisher's website.
- The final author version and the galley proof are versions of the publication after peer review.
- The final published version features the final layout of the paper including the volume, issue and page numbers.

[Link to publication](#)

**General rights**

Copyright and moral rights for the publications made accessible in the public portal are retained by the authors and/or other copyright owners and it is a condition of accessing publications that users recognise and abide by the legal requirements associated with these rights.

- Users may download and print one copy of any publication from the public portal for the purpose of private study or research.
- You may not further distribute the material or use it for any profit-making activity or commercial gain
- You may freely distribute the URL identifying the publication in the public portal.

If the publication is distributed under the terms of Article 25fa of the Dutch Copyright Act, indicated by the "Taverne" license above, please follow below link for the End User Agreement:

[www.tue.nl/taverne](http://www.tue.nl/taverne)

**Take down policy**

If you believe that this document breaches copyright please contact us at:

[openaccess@tue.nl](mailto:openaccess@tue.nl)

providing details and we will investigate your claim.

Role of Polycation Promoters in the  
Cobalt Phthalocyanine-Catalyzed  
Autoxidation of Thiols

Eugène T.W.M. Schipper

**Role of Polycation Promoters in the  
Cobalt Phthalocyanine-Catalyzed  
Autoxidation of Thiols**

CIP-GEGEVENS KONINKLIJKE BIBLIOTHEEK, DEN HAAG

Schipper, Eugène Theodorus Wilhelmus Maria

Role of polycation promoters in the cobalt  
phthalocyanine-catalyzed autoxidation of thiols / Eugène

Theodorus Wilhelmus Maria Schipper. - [S.l. : s.n.]

Proefschrift Eindhoven. - Met lit. opg.

ISBN 90-386-0113-1

Trefw.: polymeren / katalyse.



# **Role of Polycation Promoters in the Cobalt Phthalocyanine-Catalyzed Autoxidation of Thiols**

PROEFSCHRIFT

ter verkrijging van de graad van doctor aan de  
Technische Universiteit Eindhoven, op gezag van  
de Rector Magnificus, prof.dr. J.H. van Lint,  
voor een commissie aangewezen door het College  
van Dekanen in het openbaar te verdedigen op  
woensdag 19 januari 1994 om 16.00 uur

door

EUGÈNE THEODORUS WILHELMUS MARIA SCHIPPER  
Geboren te Helmond

Dit proefschrift is goedgekeurd door

de promotoren:            prof.dr.ir. A.L. German  
                                  prof.dr. J. Reedijk

en de co-promotor:        P. Piet

*Aan mijn ouders*

# Contents

## Chapter 1 Introduction

1.1	General Introduction	1
1.2	Polymer Catalysis	2
1.3	Backgrounds of this Thesis	3
1.4	Objectives and Survey of this Thesis	4
	References	6

## Chapter 2 Theoretical background

2.1	Mechanism of the Cobalt Phthalocyanine-Catalyzed Thiol Autoxidation	9
2.2	Polymeric Effects on the Mechanism of the Cobalt Phthalocyanine-Catalyzed Thiol Oxidation	11
	References	16

## Chapter 3 Experimental Section

3.1	Materials	19
3.1.1	Phthalocyanines	19
3.1.2	Synthesis of Ionene Polymers	21
3.1.3	Preparation of Monodisperse Ionene Oligomers	22
3.2	Experimental Techniques	24
3.2.1	Catalytic Activity Measurements	24
3.2.2	UV-Vis Spectroscopy	25
	References	26

## Chapter 4 Influence of the Molecular Weight of Ionenes on the Cobalt Phthalocyanine-Catalyzed Autoxidation of Mercaptoethanol

4.1	Introduction	28
4.2	Influence of the Molecular Weight of 2,4-Ionene on Cobalt Phthalocyanine Dimerization	29
4.3	Effects of the Molecular Weight of 2,4-Ionene on the Mercaptoethanol Oxidation Rate	32
4.4	Conclusions	41
	References	42

**Chapter 5 Role of Polycation Promoters in the Cobalt(II) Phthalocyanine-tetracarboxylic and -Octacarboxylic Acid-Catalyzed Autoxidation of 2-Mercaptoethanol**

5.1	Introduction	44
5.2	Effects of 2,4-Ionene on the Spectroscopic Behaviour of $\text{CoPc}(\text{COOH})_4$ and $\text{CoPc}(\text{COOH})_8$	45
5.3	Influence of 2,4-Ionene on the Catalytic Properties of $\text{CoPc}(\text{COOH})_4$ and $\text{CoPc}(\text{COOH})_8$	47
5.4	Conclusions	53
	References	55

**Chapter 6 Effects of Complexation of Oppositely Charged Water-Soluble Cobalt Phthalocyanines on the Catalytic Mercaptoethanol Autoxidation**

6.1	Introduction	58
6.2	Spectroscopic Properties of Mixtures of Oppositely Charged Cobalt Phthalocyanines	59
6.3	Catalytic Properties of Different Mixtures of Cobalt Phthalocyanines with and without Polymers	63
6.4	Discussion	68
6.5	Conclusions	71
	References	72

**Chapter 7 Synthesis of Amphiphilic Polystyrene-Ionene Diblock Copolymers with Controlled Block Lengths**

7.1	Introduction	75
7.2	Experimental Section	80
7.3	Preparation of 3-(Dimethylamino)propyllithium-Initiated Polystyrene	84
7.4	End-Coupling of Dimethylamino Functionalized Polystyrene with Ionene Oligomers	87
7.5	Conclusions	91
	References	93

**Chapter 8 Synthesis and Co-Catalytic Properties of Polystyrene-Ionene Stabilized Latices**

8.1	Introduction	95
8.2	Experimental Procedures	97
8.3	Emulsion Polymerization of Polystyrene-Ionene Diblock Copolymer Stabilized Polystyrene Latices	99
	8.3.1 Mechanism of the Emulsion Polymerization	99
	8.3.2 Surface Charge Density	103

8.4	Catalytic Activities of Latex-Supported $\text{CoPc}(\text{NaSO}_3)_4$ Catalysts in the Mercaptoethanol Autoxidation	104
8.5	Conclusions	110
	References	112
<b>Chapter 9 Co-Catalytic Properties of Amphiphilic Diblock Copolymers on the Cobalt Phthalocyanine-Catalyzed Oxidation of 1-Dodecanethiol</b>		
9.1	Introduction	116
9.2	Experimental Procedures	117
	9.2.1 Synthesis of End-Capped Ionenics	117
	9.2.2 Catalytic Activity Measurements	118
9.3	Influence of the Molecular Weight of 2,4-Ionene on the $\text{CoPc}(\text{NaSO}_3)_4$ -Catalyzed Oxidation of 1-Dodecanethiol	118
9.4	Influence of Amphiphilic Polystyrene-Ionene Diblock Copolymers on the $\text{CoPc}(\text{NaSO}_3)_4$ -Catalyzed Oxidation of 1-Dodecanethiol	123
9.5	Conclusions	126
	References	128
<b>Chapter 10 Effects of Solvents on the Cobalt Phthalocyanine-Catalyzed Oxidation of Hydrophobic Thiols</b>		
10.1	Introduction	130
10.2	Experimental Section	131
10.3	Results and Discussion	131
10.4	Conclusions	141
	References	143
<b>Chapter 11 Molecular Mechanics Calculations on Cobalt Phthalocyanine Dimers</b>		
11.1	Introduction	145
11.2	Experimental Section	146
11.3	Results and Discussion	147
	11.3.1 Modelling of Cobalt(II) Phthalocyanine	147
	11.3.2 Modelling of Cobalt(II) Phthalocyanine Dimer	153
11.4	Conclusions	163
	References	164
	<b>Epilogue</b>	167
	<b>Summary</b>	171
	<b>Samenvatting</b>	175
	<b>Dankwoord</b>	179
	<b>Curriculum Vitae</b>	181

# Chapter 1

## Introduction

### 1.1 General Introduction

Nowadays more than 90 % of industrial chemical processes contact a catalyst. Besides, catalysis plays a key role in living organisms, where in almost all biological reactions a catalyst is involved. In all cases, application of catalysts facilitates more efficient processes in high selectivity and conversion, leading to a reduction of environmental problems. It appears that polymers can play different roles on catalytic reactions. Merrifield first introduced the use of insoluble polymers as support for reagents in the solid-phase technique for peptide synthesis<sup>1</sup>. Since his pioneering work, initially polymers were mainly used as support for many catalysts in order to retain the high activity of the catalyst in combination with the advantages of immobilization, which are improvement of separation, reduced toxicity, and intrinsic possibilities for continuous operation, isolation and purification. Some appearing disadvantages of polymer-bound catalysts are: leaching of the catalyst from the support, higher costs compared with low molar mass analogues and occurrence of diffusional problems resulting in lower activities. Likewise, immobilization of enzymes on polymer carriers has received considerable attention<sup>2-5</sup>.

Apart from macromolecular-supported catalysts, the interest in polymer-anchored species increased enormously, and polymers have since been used as polymeric reagents, polymeric protecting groups and polymeric mediators<sup>6,7</sup>. In each case a reactive species is bound to a polymer in order to make convenient manipulation possible. Also polymeric reagents are used as acid catalysts and as ion-exchange resins in several industrial processes<sup>8,9</sup>. Poly(styrenesulfonic acid) for example is used as a catalyst on large

industrial scale in the synthesis of methyl tert-butyl ether from methanol and isobutene, and in the preparation of 2-propanol from propene and water.

## 1.2 Polymer Catalysis

Besides acting as support for a catalyst, or functioning as catalysts themselves, polymers can exert different types of promoting effects on catalytic reactions<sup>10-15</sup>. When polymers are used as support for a catalyst, reaction rate, selectivity and even the reaction mechanism can be changed by polymeric effects. The fact that polymers can be tailor-made, offers the opportunity to influence these effects due to specific macromolecular ligation.

Applications of polymers have been reported, in which polymers achieve site isolation of the catalyst, a change in the chemical microenvironment, steric and structural effects, local concentration effects, and reduction of side-reactions, thus resulting in a higher reactivity and/or selectivity of the supported catalyst<sup>10-15</sup>. For example, site isolation, due to a restricted motion of the polymer-attached catalyst, resulted in higher activities due to prevention of the formation of less active dimers<sup>16</sup>. Jongasma studied the steric hindrance in relation to the site isolation of a rhodium-based hydroformylation catalyst, which was achieved by immobilization<sup>17</sup>. The influence of site isolation of polystyrene-bound thiazolium salts was investigated by Van den Berg *et al.*<sup>18</sup>. Koning *et al.* reported in the case of polymer-catalyzed oxidative coupling of 2,6-dimethylphenol a promoting effect due to desired site-site interactions<sup>19</sup>. Schoo found a 70-fold rate increase, as compared with the low molecular weight analogue, by adjusting the chemical micro-environmental conditions of a polyanion-bound flavin complex<sup>20</sup>. Polymers with chiral cavities, exhibiting molecular recognition, have been used for several stereoselective reactions<sup>21-23</sup>.

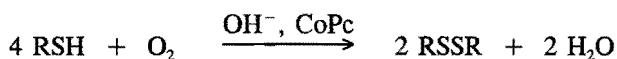
One of the important polymeric effects is substrate enrichment caused by electrostatic or hydrophobic interactions. This effect results in higher local substrate concentrations and therefore leads to higher reaction rates<sup>24-26</sup>. For example, due to hydrophobic interactions with the polysiloxane chain higher oxidation rates were realized in the cobalt phthalocyanine-catalyzed oxidation of 3-methyl indole<sup>27</sup>. Both hydrophobic and electro-



static interactions influenced the oxidation of hydroquinone, catalyzed by pyridine-Cu(II) complexes attached to polysiloxanes<sup>28</sup>. Furthermore, polymer-attached metallo-porphyrins have been applied for the development of model systems to mimic enzymatic systems<sup>29,30</sup>.

### 1.3 Backgrounds of this Thesis

A very interesting system, in which polymers have shown a strong influence and exhibit polymeric promoting effects, is the cobalt(II) phthalocyanine-catalyzed autoxidation of thiols to disulfides (Scheme 1.1). Various researchers have paid attention to the effects of polycations on the cobalt(II) phthalocyaninetetrasodiumsulfonate- (CoPc(NaSO<sub>3</sub>)<sub>4</sub>) catalyzed thiol oxidation and to the immobilization of the catalytic system, and have performed mechanistic and kinetic studies<sup>31-38</sup>.



where : RSH = thiol and CoPc = cobalt(II) phthalocyanine

#### *Scheme 1.1*

Due to the application of metal complexes attached to water-soluble polymers, this catalytic system is very interesting, from a mechanistic point of view, for the study of purely polymeric effects. Additionally, in homogeneous systems transport limitations are most unlikely to occur.

Furthermore, the importance of the thiol oxidation is apparent in different fields. First of all, in industry light oil fractions, which contain undesirable thiols, are treated by the so-called UOP Merox (mercaptan oxidation) process in order to remove these contaminants<sup>39-42</sup>. After extraction from the light hydrocarbon fractions, the mercaptans are oxidized, using an active carbon-supported cobalt phthalocyanine catalyst. Compared to a variety of other compounds, these cobalt(II) phthalocyanines proved to be the most active catalysts in the autoxidation of thiols<sup>43-48</sup>. Moreover, the phthalocyanine-catalyzed

oxidation of thiols has found its way in several commercialized deodorization applications<sup>49-52</sup>.

The interest in the thiol oxidation is also enhanced by the biological relevance of sulfhydryl groups and by the role of disulfide linkages in living organisms<sup>53,54</sup>. Besides, there is also a growing interest in the application of polymers in other cobalt(II) phthalocyanine-catalyzed reactions<sup>27,55</sup>. Additionally, in photodynamic cancer therapy polymer-phthalocyanine interactions have demonstrated to be promising<sup>56</sup>.

Despite the performed studies on various effects polymers exhibit on the  $\text{CoPc}(\text{NaSO}_3)_4$ -catalyzed thiol autoxidation, many questions still remain.

## 1.4 Objectives and Survey of this Thesis

The main objective of this thesis is to gain a better understanding of the role of polycation promoters in the cobalt phthalocyanine-catalyzed autoxidation of hydrophilic, as well as hydrophobic thiols.

In Chapter 2 the state of investigations on the catalytic mechanism of the thiol autoxidation is briefly reviewed. Also, an overview of previously obtained results on the effects of polymers on the cobalt phthalocyanine-catalyzed autoxidation of thiols is presented. In Chapter 3 the experimental procedures, materials, and synthesis of the different polymers and phthalocyanines used throughout this thesis, are described. Furthermore, the preparative procedures for monodisperse oligomers of 2,4-ionene, which are the most promising polycationic promoters of the  $\text{CoPc}(\text{NaSO}_3)_4$ -catalyzed thiol oxidation, are specified.

Chapter 4 will address the question, whether the use of these oligomers requires a minimum molecular weight of the 2,4-ionene in order to obtain the highly active aggregated form of the catalyst. This chapter further deals with the dependence of the  $\text{CoPc}(\text{NaSO}_3)_4$ -catalyzed mercaptoethanol oxidation rate on the molecular weight of 2,4-ionene.

Another aim is to obtain insight into the separate polycation-promoting contributions to the reaction mechanism. Therefore, Chapter 5 will emphasize on one separate promoting contribution, *i.e.* substrate enrichment, which was investigated by applying a water-soluble octa-substituted cobalt phthalocyanine catalyst in the mercaptoethanol oxidation. Chapter 6 focuses on the spectroscopic and catalytic properties of mixtures of oppositely charged water-soluble cobalt phthalocyanines, which offer the possibility to study exclusively the contribution of dimerization of the catalyst to the overall activity. Eventually, based on the obtained insights into the different promoting effects, a revised reaction mechanism will be proposed.

The application of the gathered knowledge to the immobilization of polymeric catalytic systems on latices, necessary to allow continuous operation, is the next objective. For this reason, a new synthetic route leading to tailor-made amphiphilic monodisperse polystyrene-ionene diblock copolymers is presented in Chapter 7. The use of these highly defined diblock copolymers as stabilizer in the emulsion polymerization of styrene is discussed in Chapter 8. Additionally, their co-catalytic properties are examined after immobilization of the  $\text{CoPc}(\text{NaSO}_3)_4$  catalyst on the pertaining latex particles.

Chapter 9 contains mechanistic information concerning the dependence on the 2,4-ionene chain length of the more complex mechanism of the catalytic autoxidation of the hydrophobic 1-dodecanethiol. Furthermore, the influence of the block lengths of ionene-containing diblock copolymers as co-catalyst on the dodecanethiol oxidation will be unravelled. One of the apotheoses of this thesis is found in Chapter 10, where the remarkable results are presented of the effects of adding organic (polar and apolar) solvents on the reaction mechanism of the oxidation of water-insoluble thiols.

Finally, in the last chapter molecular mechanics calculations on cobalt phthalocyanine dimers are outlined, in an attempt to provide more insight into the optimal geometry of the catalytically most active species.

Parts of this thesis have already been published or will be in the near future: Chapters 4<sup>57)</sup>, 5<sup>58)</sup>, 6<sup>59)</sup>, 7<sup>60,61)</sup>, 8<sup>62)</sup>, 9<sup>60,63)</sup>, 10<sup>64)</sup> and 11<sup>65)</sup>.

## References

1. R.B. Merrifield, *J. Am. Chem. Soc.*, **85** (1963) 2149.
2. H. Kitano, K. Nakamura, N. Ise, *J. Appl. Biochem.*, **4** (1982) 34.
3. H. Kitano, N. Ise, *Biotechnol. and Bioeng.*, **31** (1988) 507.
4. W. Marconi, *React. Polymers*, **11** (1989) 1.
5. S. Takeuchi, I. Omodaka, K. Hasegawa, Y. Maeda, H. Kitano, *Makromol. Chem.*, **194** (1993) 1991.
6. D.C. Sherrington, *Chem. Ind.*, **1** (1991) 15.
7. D.C. Sherrington, in *"High Value Polymers"*, A.H. Fawcett, Ed., The Royal Society of Chemistry, Cambridge, 1991.
8. A. Guyot, P. Hodge, D.C. Sherrington, H. Widdecke, *React. Polymers*, **16** (1991/1992) 233.
9. A. Chakrabarti, M.M. Sharma, *React. Polymers*, **20** (1993) 1.
10. E. Tsuchida, *Macromol. Rev.*, **16** (1982) 397.
11. G. Challa, *J. Mol. Catal.*, **21** (1983) 1.
12. W.T. Ford, Ed., *"Polymeric Reagents and Catalysts"*, *ACS Symp. Ser.*, **308**, 1986.
13. D.C. Sherrington, P. Hodge, Eds., *"Synthesis and Separations Using Functional Polymers"*, Wiley, Chichester, 1988.
14. D.C. Sherrington, *Pure Appl. Chem.*, **60** (1988) 401.
15. F. Ciardelli, C. Carlini, P. Pertici, G. Valentini, *J. Macromol. Sci. Chem.*, **A26** (1989) 327.
16. R.H. Grubbs, C. Gibbons, L.C. Kroll, W.D. Bond Jr., C.H. Brubaker Jr., *J. Am. Chem. Soc.*, **95** (1973) 2373.
17. T. Jongsma, Ph.D. Thesis, Groningen State University, Groningen, 1992.
18. H.J. van den Berg, G. Challa, U.K. Pandit, *React. Polymers*, **11** (1989) 101.
19. C.E. Koning, J.J.W. Eshuis, F.J. Viersen, G. Challa, *React. Polymers*, **4** (1986) 293.
20. H.F.M. Schoo, Ph.D. Thesis, Groningen State University, Groningen, 1991.
21. G. Wulff, in *"Polymeric Reagents and Catalysts"*, *ACS Symp. Ser.*, W.T. Ford, Ed., **308** (1986) 186.
22. G. Wulff, B. Heide, G. Helfmeier, *React. Polymers*, **6** (1987) 299.
23. G. Wulff, *Makromol. Chem., Macromol. Symp.*, **70/71** (1993) 285.
24. N. Ise, in *"Polyelectrolytes and Their Applications"*, A. Rembaum, E. Sélégny, Eds., Reidel, Dordrecht, 1975.
25. J.H. Fendler, E.J. Fendler, *"Catalysis in Micellar and Macromolecular Systems"*, Academic Press, New York, 1975.
26. J. Jager, Ph.D. Thesis, Groningen State University, Groningen, 1987.

27. N. Nemoto, M. Asano, T. Asakura, I. Hongo, Y. Ueno, K. Ikeda, N. Takamiya, *J. Inorg. and Organomet. Polymers*, **1** (1991) 211.
28. N. Nemoto, H. Ishii, Y. Ueno, K. Ikeda, N. Takamiya, *Makromol. Chem.*, **193** (1992) 59.
29. A.W. van der Made, J.W.H. Smeets, R.J.M. Nolte, W. Drenth, *J. Chem. Soc., Chem. Commun.*, (1983) 1204.
30. J. van Esch, M.F.M. Roks, R.J.M. Nolte, *J. Am. Chem. Soc.*, **108** (1986) 6093.
31. J. Zwart, Ph.D. Thesis, Eindhoven University of Technology, Eindhoven, 1978.
32. J.H. Schutten, Ph.D. Thesis, Eindhoven University of Technology, Eindhoven, 1981.
33. W.M. Brouwer, Ph.D. Thesis, Eindhoven University of Technology, Eindhoven, 1984.
34. J. van Welzen, Ph.D. Thesis, Eindhoven University of Technology, Eindhoven, 1989.
35. K.H. van Streun, Ph.D. Thesis, Eindhoven University of Technology, Eindhoven, 1990.
36. J.W. Hof, *Post-Graduate Research Training Program*, Eindhoven University of Technology, Eindhoven, 1990.
37. F. Twigt, *Post-Graduate Research Training Program*, Eindhoven University of Technology, Eindhoven, 1990.
38. M.T. Ratering, *Post-Graduate Research Training Program*, Eindhoven University of Technology, Eindhoven, 1990.
39. K.M. Brown, W.K.T. Gleim, P. Urban, *Oil Gas*, **57** (1959) 73.
40. W.K. Gleim, P. Urban Jr., *U.S. Patent*, **2,988,500** (1961).
41. R.R. Frame, *U.S. Patent*, **4,498,977** (1985).
42. *Hydrocarbon. Processing*, **71(4)** (1992) 120.
43. N.N. Kundo, N.P. Keier, C.V. Glazneva, E.K. Mamaeva, *Kin. Katal.*, **8** (1967) 1325.
44. C.F. Cullis, J.D. Hopton, C.J. Swan, D.L. Trimm, *J. Appl. Chem.*, **18** (1968) 335.
45. C.J. Swan, D.L. Trimm, *J. Appl. Chem.*, **18** (1968) 340.
46. I.G. Dance, R.C. Conrad, *Austr. J. Chem.*, **30** (1977) 305.
47. D.H.F. Carlson, T.A. Verachert, J.E. Sobel, *U.S. Patent*, **4,028,269** (1977).
48. W.M. Douglas, *U.S. Patent*, **4,088,569** (1978).
49. J. Fukui, Y. Sakai, K. Hosaka, T. Yamashita, A. Ogawa, H. Shirai, *J. Am. Geriatr. Soc.*, **38** (1990) 889.
50. H. Shirai, K. Hanabusa, T. Koyama, H. Tsuiki, E. Masuda, *Makromol. Chem., Macromol. Symp.*, **59** (1992) 155.
51. H. Shirai, in "*Phthalocyanines, Properties and Applications*", **Vol. 2**, C.C. Leznoff, A.B.P. Lever, Eds., VCH Publishers, Weinheim, 1993.
52. Y. Takahashi, T. Shimomura, N. Shirane, *Eur. Pat. Appl.*, **386,723** (1990).

53. P.C. Jocelyn, "*Biochemistry of the SH-group*", Academic Press, New York, 1972, p. 94.
54. M. Friedman, "*The Chemistry and Biochemistry of the Sulfhydryl Group in Amino-Acids, Peptides and Proteins*", Pergamon, Oxford, 1973.
55. H. Turk, W.T. Ford, *J. Org. Chem.*, **53** (1988) 460.
56. D. Wöhrle, A. Ardeshirpur, A. Heuermann, S. Müller, G. Grasczew, H. Rinneberg, M. Kohl, J. Neukammer, *Makromol. Chem., Macromol. Symp.*, **59** (1992) 17.
57. E.T.W.M. Schipper, A.H.C. Roelofs, P. Piet, A.L. German, *Polym. Int.*, accepted for publication.
58. E.T.W.M. Schipper, J.P.A. Heuts, R.P.M. Pinckaers, P. Piet, A.L. German, *in preparation*.
59. E.T.W.M. Schipper, J.P.A. Heuts, P. Piet, T.P.M. Beelen, A.L. German, *J. Mol. Catal.*, accepted for publication.
60. E.T.W.M. Schipper, J.C.M. van Hest, P. Piet, A.L. German, *Makromol. Chem.*, **193** (1992) 2807.
61. E.T.W.M. Schipper, J.C.M. van Hest, A.H.C. Roelofs, P. Piet, A.L. German, *Polym. Int.*, **33** (1993) 317.
62. E.T.W.M. Schipper, R.P.M. Pinckaers, P. Piet, A.L. German, *in preparation*.
63. E.T.W.M. Schipper, A.H.C. Roelofs, P. Piet, A.L. German, *in preparation*.
64. E.T.W.M. Schipper, H. Hopstaken, R.P.M. Pinckaers, P. Piet, A.L. German, *in preparation*.
65. J.P.A. Heuts, E.T.W.M. Schipper, P. Piet, A.L. German, *in preparation*.

## Chapter 2

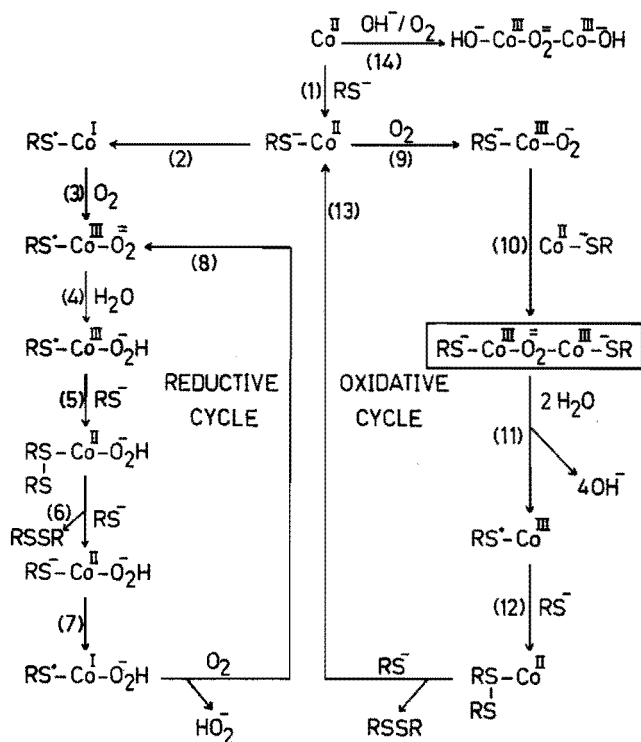
### Theoretical Background

#### 2.1 Mechanism of the Cobalt Phthalocyanine-Catalyzed Thiol Autoxidation

The first reaction mechanism of the cobalt phthalocyanine-catalyzed autoxidation of thiols to disulfides was postulated by Kundo and Keier<sup>1,2</sup>, who proposed that the thiol oxidation proceeds by free thiyl radicals, formed through electron transfer from the thiol to the cobalt(II) phthalocyanine species, followed by reoxidation of the catalyst by dioxygen. This mechanism was refuted based on kinetic results by Wagnerová *et al.*<sup>3-5</sup>, because the suggested liberation of free thiyl radicals in the absence of oxygen could not be demonstrated. They proposed the reaction proceeds by a ternary complex in which oxygen and thiol are simultaneously bound to the active catalytic centre. A similar ternary complex was suggested by Kozylak *et al.*<sup>6,7</sup>. Furthermore, it was observed that the mechanism obeys two-substrate Michaelis-Menten kinetics, which was also confirmed by Hoffmann *et al.*<sup>8</sup>.

The most elaborate study of the CoPc(NaSO<sub>3</sub>)<sub>4</sub>-catalyzed oxidation of 2-mercaptoethanol was performed by Zwart<sup>9</sup>. After combining kinetic and spectroscopic measurements with electrochemical data it was concluded that the reaction mechanism of the thiol oxidation consists of two parallel reaction paths, *i.e.* an oxidative cycle and a reductive cycle. As presented in Scheme 2.1, it can be seen that the oxidative cycle is initiated by the addition of the thiolate anion, which is the reactive species, to the Co(II) centre. The next step is a direct oxygenation of the metal, which eventually leads to the formation of a relatively stable dioxygen bridged  $\mu$ -peroxo complex, which is inactive in the thiol oxidation. The

existence of this catalytically inactive complex causes a negative kinetic order in dioxygen.



*Scheme 2.1 Schematic representation of the polymer-free homogeneous CoPc(NaSO<sub>3</sub>)<sub>4</sub>-catalyzed oxidation of thiols as proposed by Zwart<sup>9</sup> (Co denotes the cobalt phthalocyanine complex).*

By contrast, the reductive cycle proceeds much faster. Addition of the thiolate anion leads to a reduction of the Co(II) centre to Co(I), subsequently followed by formation of a ternary complex after addition of dioxygen. As a result a two-electron transfer transforms Co(I) into Co(III) and leads to the formation of peroxide. In the last step a second thiolate anion combines with the thiol radical to form disulfide, which is released together with the peroxide. The generated hydrogen peroxide is able to react further with thiol, forming disulfide in a non-catalytic step.

Also the thiol oxidation catalyzed by polymer-anchored cobalt(II) phthalocyanine complexes has been subject to kinetic and mechanistic studies. Wöhrle *et al.* found



similar reaction kinetics for the mercaptoethanol oxidation catalyzed by cobalt phthalocyanine covalently bound to polystyrene<sup>10)</sup> and to modified silica<sup>11)</sup>, as compared with their homogeneous counterparts. Moreover, the same authors also investigated the effects of metal type<sup>12)</sup>, substituents and ligands<sup>13)</sup> on the phthalocyanine-catalyzed mercaptan oxidation.

## 2.2 Polymeric Effects on the Mechanism of the Cobalt Phthalocyanine-Catalyzed Thiol Oxidation

It appeared that cationic polymers exhibit large effects on the cobalt(II) phthalocyanine-catalyzed thiol autoxidation: even rate increases up to 40-fold were observed as compared with the polymer-free system. Zwart was the first who observed high thiol oxidation rates by applying bifunctional polymer-attached cobalt(II) phthalocyanine catalysts<sup>14-16)</sup>. All systems contain catalytic oxidation sites in combination with basic sites. This concept was further developed by Schutten who concentrated his work mainly on studying poly(vinylamine) (PVAm) containing catalytic systems<sup>16-18)</sup>.

Visible light spectroscopy showed an increase in monomeric phthalocyanine species in the presence of PVAm, whereas the  $\mu$ -peroxo complex disappeared, caused by electrostatic interactions between the quaternary ammonium groups and the negatively charged catalyst<sup>17)</sup>. Additionally, ESR measurements indicated a coordinative interaction of the amine groups with the Co, leading to a 5-coordination of the Co(II) centre. On these grounds, the enhanced catalytic activity was attributed to prevention of the formation of the catalytically inactive dioxygen-bridged dimeric complexes of  $\text{CoPc}(\text{NaSO}_3)_4$ , resulting in site isolation of the monomeric cobalt species and to enrichment of the polymer coils with thiol anions, *i.e.* the reactive species.

For the particular  $\text{CoPc}(\text{NaSO}_3)_4/\text{PVAm}$  system Brouwer investigated in detail the effect of pH<sup>19)</sup>, ionic strength, substrate concentrations, oxygen pressure, temperature<sup>20)</sup>, and molecular weight of the ligand<sup>21)</sup>. In addition, it was shown that polymeric ligands like poly(ethylenimine), poly(L-lysine) and several poly(quaternary ammonium)salts have a considerable effect on the thiol oxidation rate in comparison with their monomeric

analogues<sup>22</sup>). Furthermore, Brouwer<sup>23</sup>) revealed the importance of the charge density of the polymers, by showing the linear dependency of the reaction rate on the charge density, using copolymers of vinylamine and vinylalcohol. It was demonstrated that poly(quaternary ammonium)salts (the so-called ionenes), due to their pH-independent permanent charge, were the most effective promoters of the CoPc(NaSO<sub>3</sub>)<sub>4</sub>-catalyzed autoxidation of thiols<sup>22</sup>).

Van Welzen<sup>24</sup>) provided further insight into the CoPc(NaSO<sub>3</sub>)<sub>4</sub>-catalyzed oxidation of thiols by combining kinetic investigations with structure-elucidating techniques. First of all, van Welzen investigated the effect of addition of 2,4-ionene on the structure of the catalyst by means of visible light spectroscopy. CoPc(NaSO<sub>3</sub>)<sub>4</sub> occurs in neutral aqueous solution in its monomeric as well as in its dimeric form, with absorption maxima in the visible light spectrum at 662 nm and 628 nm, respectively<sup>25,26</sup>). Under alkaline conditions, where catalytic reactions normally are performed, CoPc(NaSO<sub>3</sub>)<sub>4</sub> is mainly present as dioxygen-bridged  $\mu$ -peroxo dimers (674 nm)<sup>27</sup>).

However, on adding 2,4-ionene to the solution the catalytically inactive  $\mu$ -peroxo complex is strongly suppressed: the absorbance peak at 674 nm in the visible light spectrum disappears<sup>28</sup>) (Fig. 2.1). Further addition of 2,4-ionene dramatically affects the dimer-monomer equilibrium, the dimeric form is favoured over the monomeric form. This aggregation of the catalyst was attributed to the suppression of charge repulsion between the fourfold negatively charged CoPc(NaSO<sub>3</sub>)<sub>4</sub> in the presence of the cationic polymer.

Moreover, it appeared that starting at a certain polymer/catalyst ratio, expressed as N<sup>+</sup>/Co ratio, further addition of 2,4-ionene did not further affect the absorbance spectrum. Exactly at this N<sup>+</sup>/Co ratio of 4, all positive charges of the polyelectrolyte are just matching the fourfold negatively charged cobalt species. This stoichiometric complexation remains unaffected by further addition of 2,4-ionene, even up to N<sup>+</sup>/Co = 10<sup>4</sup>. Moreover, further aggregation has been demonstrated by a shift to shorter wavelength (620-622 nm), whereas no change in the dimer-monomer equilibrium occurred. Such a drastic influence could not be observed in simple salt-induced aggregation<sup>28</sup>): addition of salts give no rise to stoichiometric complexation. Introduction of a monomerizing organic solvent<sup>26,29</sup>), like *N,N*-dimethylformamide or alcohol, could not influence the ionene-induced aggregation<sup>30,31</sup>).

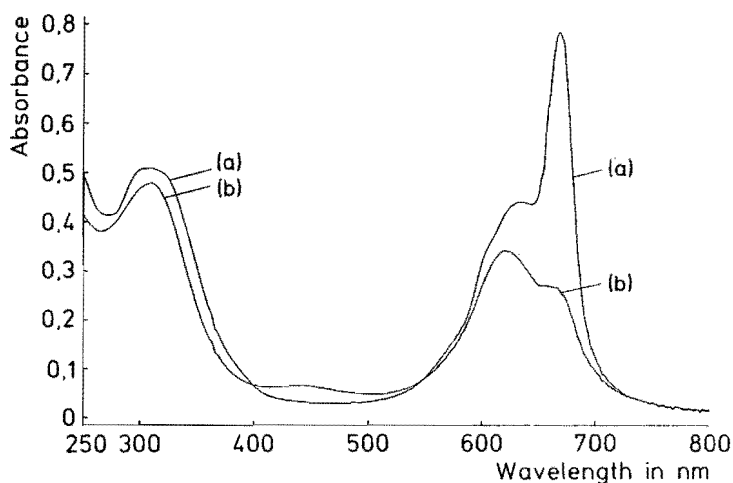


Figure 2.1 The effects of different amounts of 2,4-ionene on the visible light spectra of aqueous  $\text{CoPc}(\text{NaSO}_3)_4$  solutions<sup>28)</sup>.

(a)  $N^+/\text{Co} = 0$ , (b)  $N^+/\text{Co} = 0.1$ , (c)  $N^+/\text{Co} = 3$ , (d)  $N^+/\text{Co} = 4$ ,  
 (e)  $N^+/\text{Co} = 5$ , (f)  $N^+/\text{Co} = 100$ .  $[\text{CoPc}(\text{NaSO}_3)_4] = 2 \cdot 10^{-6}$   
 $\text{mol} \cdot \text{dm}^{-3}$ ,  $\bar{M}_n(2,4\text{-ionene}) = 22000 \text{ g} \cdot \text{mol}^{-1}$ .

Various types of ionenes (2,6-, 2,8- and 6,6-ionene) have been investigated with regard to their effect on the dimerization of the catalyst, leading to effects similar to those found with 2,4-ionene<sup>24,28)</sup>. In contrast to 6,6-ionene, for 2,10-ionene, with a similar linear charge density, a completely different behaviour has been observed. At low 2,10-ionene concentrations dimerization occurs, but at  $N^+/\text{Co}$  ratios higher than  $10^3$  the dimer/monomer equilibrium was shifted back to the monomer side: only monomers are present, which was confirmed by ESR spectroscopy<sup>24,31)</sup>. This site isolation can be explained by the hydrophobic character of the  $\text{C}_{10}$ -segments<sup>32)</sup> which allow formation of micelle-like structures. Also, for other polysoap-type of ionenes this typical behaviour was observed.

The dimerization of the catalyst, in combination with the suppression of the inactive  $\mu$ -peroxo complex in the presence of the polycation 2,4-ionene, and substrate enrichment, *i.e.* higher local concentrations in the polyelectrolyte domain, lead to a tremendous rate enhancement (40-fold) as compared with the polymer-free system<sup>31)</sup>.

The spectroscopic behaviour of the 2,10-ionene/ $\text{CoPc}(\text{NaSO}_3)_4$  system is also reflected in its catalytic properties<sup>31</sup>. Only at low 2,10-ionene concentration dimerization of the catalyst occurs, so in this region a maximum rate increase by only a factor of 2 is observed.

Van Welzen also extensively studied the influence of reaction conditions on kinetic parameters. The kinetics of the mercaptoethanol autoxidation catalyzed by 2,4-ionene/ $\text{CoPc}(\text{NaSO}_3)_4$  was found to obey the two-substrate Michaelis-Menten model<sup>33-35</sup>.

Most mechanistic studies are dealing with the oxidation of hydrophilic thiols and only few attempts have been made to investigate the autoxidation of water-insoluble thiols<sup>36-39</sup>. Brouwer studied the  $\text{CoPc}(\text{NaSO}_3)_4$ -catalyzed autoxidation of the hydrophobic 1-dodecanethiol in the presence of different surfactants<sup>36</sup>. Van Welzen proposed the catalytic reaction proceeds at the phase-boundary between the water-phase and the dodecanethiol phase<sup>39</sup>. At this interface the thiolate anions interact with the 2,4-ionene/catalyst complex. The influence of the ionene concentration on the thiol oxidation rate is depicted in Fig. 2.2. At low  $\text{N}^+$ -concentrations not all thiol droplets are interacting with the ionene. Increasing the ionene concentration leads to an increase in contact surface, which results in higher oxidation rates. After reaching a maximum, more ionene is unable to interact with the thiol droplets and will be present in the water-phase, where it will bind the cobalt complex. As a consequence, the reaction rate is lowered.

Further enhancement of the catalytic activity can be achieved by coupling a hydrophobic moiety to the ionene chain. Oleyl-3,3-ionene, an ionene end-capped with a hydrophobic alkyl chain, exhibited almost a two-fold higher activity as compared with the hydrophilic 2,4-ionene<sup>39</sup>. This effect was ascribed to the hydrophobic interaction between the polymer and the hydrophobic thiol.

In order to simplify continuous operation, various attempts have been made to immobilize the catalytic system on different polymeric supports. Cationic macroporous resin particles were used to immobilize  $\text{CoPc}(\text{NaSO}_3)_4$ , but low reactions rates were obtained comparable with the polymer-free system, mainly due to the absence of flexible cationic chains at the surface preventing effective dimerization of the cobalt species<sup>40,41</sup>. In order

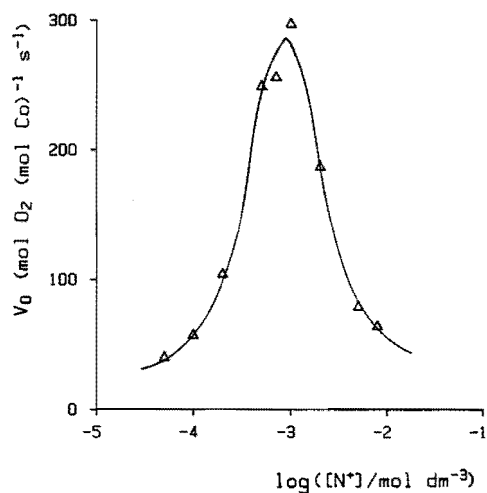


Figure 2.2 Effect of varying the 2,4-ionene concentration on the 1-dodecanethiol oxidation rate<sup>39</sup>.

Conditions:  $[\text{CoPc}(\text{NaSO}_3)_4] = 8 \cdot 10^{-7} \text{ M}$ ,  $\text{pH} = 13$ ,

$[\text{RSH}] = 2.1 \cdot 10^{-2} \text{ M}$  (reaction started by  $\text{CoPc}(\text{NaSO}_3)_4$  addition).

to overcome these problems small non-porous latex particles have been applied<sup>37,38,42-44</sup>. Only when flexible cationic tails of sufficient length are present at the particle surface high thiol oxidation rates could be achieved<sup>45,46</sup>.

## References

1. N.N. Kundo, N.P. Keier, *Russ. J. Phys. Chem.*, **42** (1968) 707.
2. A.D. Simonov, N.P. Keier, N.N. Kundo, E.K. Mamaeva, G.V. Glazneva, *Kinet. Catal.*, **14** (1973) 864.
3. D.M. Wagnerová, E. Schwertnerová, J. Vepřek-Šiška, *Coll. Czech. Chem. Commun.*, **38** (1973) 756.
4. D.M. Wagnerová, E. Schwertnerová, J. Vepřek-Šiška, *Coll. Czech. Chem. Commun.*, **39** (1974) 1980.
5. J. Dolanský, D.M. Wagnerová, J. Vepřek-Šiška, *Coll. Czech. Chem. Commun.*, **41** (1976) 2326.
6. E.I. Kozylak, A.S. Erokhin, A.K. Yatsimirskii, I.V. Berezin, *Bull. Acad. Sci. USSR, Div. Chem. Sci.*, **35** (1986) 741.
7. E.I. Kozylak, A.S. Erokhin, A.K. Yatsimirskii, *React. Kinet. Catal. Lett.*, **33** (1987) 113.
8. M.R. Hoffmann, B.C. Lim, *Environm. Sci. Technol.*, **13** (1979) 1406.
9. J. Zwart, Ph.D. Thesis, Eindhoven University of Technology, Eindhoven, 1978.
10. D. Wöhrle, T. Buck, G. Schneider, O. Schulz-Ekloff, H. Fischer, *J. Inorg. Organomet. Polym.*, **1** (1991) 115.
11. T. Buck, D. Wöhrle, G. Schulz-Ekloff, A. Andreev, *J. Mol. Catal.*, **70** (1991) 259.
12. T. Buck, E. Preussner, D. Wöhrle, G. Schulz-Ekloff, *J. Mol. Catal.*, **53** (1989) L17.
13. T. Buck, H. Bohlen, D. Wöhrle, G. Schulz-Ekloff, *J. Mol. Catal.*, **80** (1993) 253.
14. T.A.M.M. Maas, M. Kuijer, J. Zwart, *J. Chem. Soc., Chem. Commun.*, (1976) 86.
15. J. Zwart, H.C. van der Weide, N. Bröker, C. Rummens, G.C.A. Schuit, A.L. German, *J. Mol. Catal.*, **3** (1977/78) 151.
16. J.H. Schutten, J. Zwart, *J. Mol. Catal.*, **5** (1979) 109.
17. J.H. Schutten, P. Piet, A.L. German, *Makromol. Chem.*, **180** (1979) 2341.
18. J.H. Schutten, C.H. van Hastenberg, P. Piet, A.L. German, *Angew. Makromol. Chem.*, **89** (1980) 201.
19. W.M. Brouwer, P. Piet, A.L. German, *Polym. Bull.*, **8** (1982) 245.
20. W.M. Brouwer, P. Piet, A.L. German, *J. Mol. Catal.*, **22** (1984) 297.
21. W.M. Brouwer, P. Piet, A.L. German, *Makromol. Chem.*, **185** (1984) 363.
22. W.M. Brouwer, P. Piet, A.L. German, *J. Mol. Catal.*, **31** (1985) 169.
23. W.M. Brouwer, P. Piet, A.L. German, *J. Mol. Catal.*, **29** (1985) 335.
24. J. van Welzen, Ph.D. thesis, Eindhoven University of Technology, Eindhoven, 1989.
25. Z.A. Schelly, R.D. Farina, E.M. Eyring, *J. Phys. Chem.*, **74** (1970) 617.

26. Y.-C. Yang, J.R. Ward, R.P. Seiders, *Inorg. Chem.*, **24** (1985) 1765.
27. L.C. Gruen, R.J. Blagrove, *Aust. J. Chem.*, **26** (1973) 319.
28. J. van Welzen, A.M. van Herk, A.L. German, *Makromol. Chem.*, **188** (1987) 1923.
29. J.A. de Bolfo, T.D. Smith, J.F. Boas, J.R. Pilbrow, *J. Chem. Soc., Faraday Trans. II*, **72** (1976) 481.
30. J. van Welzen, A.M. van Herk, A.L. German, *Makromol. Chem.*, **189** (1988) 587.
31. J. van Welzen, A.M. van Herk, A.L. German, *Makromol. Chem.*, **190** (1989) 2477.
32. V. Soldi, N. de Magelhães Erismann, F.H. Quina, *J. Am. Chem. Soc.*, **110** (1988) 5137.
33. A.M. van Herk, A.H.J. Tullemans, J. van Welzen, A.L. German, *J. Mol. Catal.*, **44** (1988) 269.
34. J. van Welzen, A.M. van Herk, H. Kramer, A.L. German, *J. Mol. Catal.*, **59** (1990) 291.
35. J. van Welzen, A.M. van Herk, H. Kramer, T.G.L. Thijssen, A.L. German, *J. Mol. Catal.*, **59** (1990) 311.
36. W.M. Brouwer, P. Piet, A.L. German, *J. Mol. Catal.*, **29** (1985) 347.
37. M. Hassanein, W.T. Ford, *Macromolecules*, **21** (1988) 525.
38. M. Hassanein, W.T. Ford, *J. Org. Chem.*, **54** (1989) 3106.
39. J. van Welzen, A.M. van Herk, A.L. German, *J. Mol. Catal.*, **60** (1990) 351.
40. J.W. Hof, *Post-Graduate Research Training Program*, Eindhoven University of Technology, 1990.
41. M.T. Ratering, J. Meuldijk, P. Piet, A.L. German, *React. Polymers.*, **19** (1993) 233.
42. S. Hari Babu, W.T. Ford, *J. Polym. Sci. Polym. Chem.*, **30** (1992) 1917.
43. F. Twigt, P. Piet, A.L. German, *Eur. Polym. J.*, **27** (1991) 939.
44. K.H. van Streun, W.J. Belt, E.T.W.M. Schipper, P. Piet, A.L. German, *J. Mol. Catal.*, **71** (1992) 245.
45. F. Twigt, J. Broekman, P. Piet, A.L. German, *Eur. Polym. J.*, **29**, 745 (1993).
46. H. van Beek, J.-W. Leclercq, P. Piet, A.L. German, *Makromol. Chem., Rapid Commun.*, **14** (1993) 371.

## Chapter 3

### Experimental Section

#### 3.1 Materials

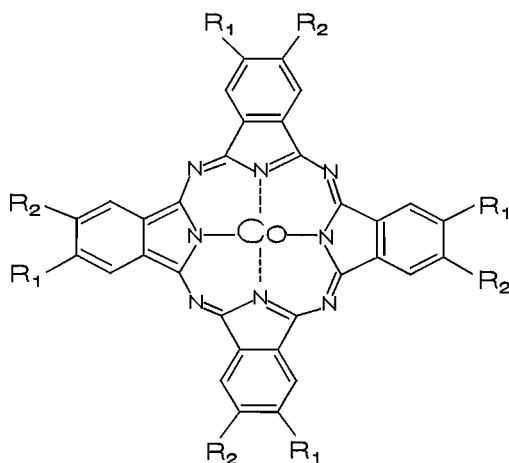
##### 3.1.1 Phthalocyanines

All cobalt phthalocyanines, that have been used throughout this thesis, are depicted in Fig. 3.1. Cobalt phthalocyaninetetrasodiumsulfonate ( $\text{CoPc}(\text{NaSO}_3)_4$ ) was kindly provided by dr.ir. T.P.M. Beelen (Eindhoven University of Technology) and had been prepared according to a slight adaption of the original method described by Weber and Busch<sup>1,2</sup>. Cobalt phthalocyaninetetra(trimethylammonium)iodide ( $\text{CoPc}[\text{N}(\text{CH}_3)_3\text{I}]_4$ ) was supplied as a  $2 \cdot 10^{-5} \text{ mol} \cdot \text{dm}^{-3}$  aqueous solution by dr.ir. T.P.M. Beelen and was prepared according to a literature procedure<sup>3</sup>. Cobalt phthalocyanineoctacarboxylic acid ( $\text{CoPc}(\text{COOH})_8$ ) was kindly provided by prof.dr. H. Shirai (Shinshu University, Ueda, Japan) and was synthesized according to a literature method<sup>4</sup>.

The synthesis of cobalt phthalocyaninetetracarboxylic acid ( $\text{CoPc}(\text{COOH})_4$ ) was carried out with a few modifications according to the procedure described by Shirai *et al.*<sup>5</sup>, and by Wöhrle *et al.*<sup>6</sup>. First, cobalt phthalocyaninetetracarboxamide ( $\text{CoPc}(\text{CONH}_2)_4$ ) was prepared: 10.0 g of trimellitic anhydride (1,2,4-benzenetricarboxylic anhydride) (Janssen Chimica, 97%), 30.0 g of urea (Merck, p.a.), 3.9 g of cobalt(II) chloride (Janssen Chimica, 97%) and 1.3 g of ammonium molybdate(VI)-tetrahydrate (Janssen Chimica, p.a.) were thoroughly mixed with 50 ml of nitrobenzene, and this mixture was added to 100 ml of nitrobenzene in a round-bottomed flask, equipped with a magnetic stirrer and a reflux condenser. The mixture was heated in an argon atmosphere for 3 h at 160 °C. After filtration over a glass funnel, the crude reaction product was washed with methanol,



followed by extraction with methanol for 48 h in a soxhlet apparatus in order to remove the remaining nitrobenzene. Subsequently, most of the inorganic contaminants were removed by extraction with water for 4 d. This product was acidified with 600 ml of 6 M HCl and stirred for 24 h, followed by filtration applying a glass funnel. Next, the product was extracted with an acetone/water mixture for 16 h. The blue-green solid obtained was dried at reduced pressure at 50-70 °C for 5 d. Yield of  $\text{CoPc}(\text{CONH}_2)_4$ : 8.08 g (87 %).



	$R_1, R_2$
$\text{CoPc}(\text{NaSO}_3)_4$	$\text{SO}_3\text{Na}, \text{H}$
$\text{CoPc}[\text{N}(\text{CH}_3)_3\text{I}]_4$	$\text{N}(\text{CH}_3)_3\text{I}, \text{H}$
$\text{CoPc}(\text{COOH})_4$	$\text{COOH}, \text{H}$
$\text{CoPc}(\text{COOH})_8$	$\text{COOH}, \text{COOH}$

Figure 3.1 Structures of  $\text{CoPc}(\text{NaSO}_3)_4$ ,  $\text{CoPc}[\text{N}(\text{CH}_3)_3\text{I}]_4$ ,  $\text{CoPc}(\text{COOH})_4$  and  $\text{CoPc}(\text{COOH})_8$ .

Subsequently, 2.0 g of  $\text{CoPc}(\text{CONH}_2)_4$ , 50 g of KOH and 50 ml of water were refluxed in a round-bottomed flask for 24 h. After this, the following purification procedure was carried out: first, the reaction mixture was acidified with 6 M HCl to pH 2. Then, the

blue precipitate was filtered off with a glass funnel and washed with 0.1 M HCl, acetone and ether. The obtained product was dissolved in 500 ml of water at pH 10. This solution was filtrated over a glass funnel and the filtrate was again acidified. After repeating this procedure three times, the product was washed with water, ethanol and ether, and dried at reduced pressure at 70 °C for 24 h. Yield of  $\text{Co}(\text{COOH})_4 \cdot 4\text{H}_2\text{O}^{7)}$ : 1.2 g (60 %). Anal. calcd. for  $\text{CoPc}(\text{COOH})_4 \cdot 4\text{H}_2\text{O}$ : C, 52.76; H, 2.95; N, 13.68. Found: C, 52.65; H, 2.93; N, 13.71.

### 3.1.2 Synthesis of Ionene Polymers

The polymeric 2,4-ionenes (Fig. 3.2) were prepared according to the method developed by Rembaum *et al.*<sup>8)</sup> with a few modifications. In most cases, 2,4-ionene was synthesized by dissolving equimolar amounts of 1,4-dibromobutane (Janssen Chimica, 99 %) and *N,N,N',N'*-tetramethylethylenediamine (TMEDA) (Janssen Chimica, 99 %) in a 1:1 mixture of *N,N*-dimethylformamide (DMF) (Janssen Chimica, p.a.) and methanol (Merck, p.a.). After reaction (1-30 d) at room temperature without stirring, the polymer was precipitated in a large excess of acetone, filtered off using a glass funnel and washed with acetone. Next, the product was dried for 24 h at reduced pressure at 50 °C. All yields were in the order of 90 % or higher.

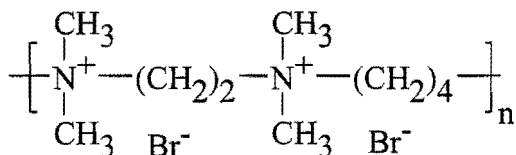


Figure 3.2 Structure of 2,4-ionene

The number average molecular weight ( $\bar{M}_n$ ) of the ionenes was determined by a general procedure, consisting of titration of the dimethylamino end-group with hydrochloric acid. Thus, the ionenes were end-capped with dimethylamino groups by reacting with a large excess of TMEDA in water for 24 h at 25 °C. The number average molecular weights of the 2,4-ionenes obtained will be specified in each chapter.

Average molecular weights of the 2,4-ionenes obtained ranged from 1000 to 23000  $\text{g} \cdot \text{mol}^{-1}$ . These were obtained by varying either the reaction stoichiometry or the

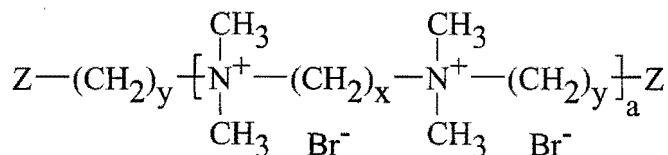
polymerization times. The high molar mass ionenes were obtained, when experimental conditions were chosen as reported by Brouwer *et al.*<sup>9)</sup> (concentrated solutions ( $1.5 \text{ mol} \cdot \text{dm}^{-3}$ ) of TMEDA and 1,4-dibromobutane in DMF/methanol at room temperature combined with long reaction times).

### 3.1.3 Preparation of Monodisperse Ionene Oligomers

The monodisperse ionene oligomers synthesized are represented in Fig. 3.3. The reagents used, TMEDA and 1,4-dibromobutane, were purified before use by distillation and were stored under argon. A typical experiment to prepare the dimethylamino-terminated 2,4-ionene trimer (N-trimer): 18.2 g ( $8.43 \cdot 10^{-2} \text{ mol}$ ) of 1,4-dibromobutane and 146.9 g (1.26 mol, 15 equiv.) of TMEDA were dissolved in 250 ml of a 1:1 mixture of methanol/DMF and were reacted for 48 h at 50 °C. The same purification method followed for all oligomers, consisted of precipitation in a large excess of acetone and washing with acetone. The product was dried at reduced pressure for 24 h at 50 °C.

The Br-terminated 2,4-ionene trimer (Br-trimer), with two quaternary ammonium groups and bromo end-groups, was prepared in a similar way using the same reaction conditions: 11.4 g ( $9.8 \cdot 10^{-2} \text{ mol}$ ) of TMEDA and 317.5 g (1.47 mol, 15 equiv.) of 1,4-dibromobutane. The Br-terminated 2,4-ionene pentamer (Br-pentamer) was synthesized by dissolving 10.5 g ( $2.34 \cdot 10^{-2} \text{ mol}$ ) of N-trimer and 100.9 g (0.467 mol, 20 equiv.) of 1,4-dibromobutane in 40 ml of methanol, 20 ml of DMF and 2 ml of water. After a reaction time of 3 d at 40 °C the product was treated the same way as the other oligomeric ionenes. The N-pentamer was prepared by reacting the Br-trimer with a twentyfive-fold excess of TMEDA in a mixture of DMF, methanol and water. In a similar way after consecutive steps, always using a twenty-fold excess of one of the monomers, the other monodisperse oligomers of 2,4-ionene, reported in Fig. 3.3, have been obtained.

Likewise, three trimers were synthesized with two, three and six methylene groups between the positive charges, respectively. H-trimer-2C was prepared by reacting 1.7 g ( $1.46 \cdot 10^{-2} \text{ mol}$ ) of TMEDA and 12.7 g ( $9.27 \cdot 10^{-2} \text{ mol}$ , 6 equiv.) of 1-monobromobutane (Janssen Chimica, 99 %) in 25 ml of methanol/DMF (1/1, v/v) during 3 d at 50 °C. Following a similar procedure, H-trimer-3C was synthesized using the same reaction



(name)	a	x	y	Z
Br-trimer	1	2	4	Br
N-trimer	1	4	2	N-(CH <sub>3</sub> ) <sub>2</sub>
Br-pentamer	2	2	4	Br
N-pentamer	2	4	2	N-(CH <sub>3</sub> ) <sub>2</sub>
N-heptamer	3	4	2	N-(CH <sub>3</sub> ) <sub>2</sub>
Br-nonamer	4	2	4	Br
H-trimer-2C	1	2	4	H
H-trimer-3C	1	3	4	H
N-trimer-6C	1	6	2	N-(CH <sub>3</sub> ) <sub>2</sub>

Figure 3.3 Structures of the different monodisperse ionene oligomers.

conditions: 1.9 g ( $1.46 \cdot 10^{-2}$  mol) of *N,N,N',N'*-tetramethylpropanediamine (Janssen Chimica, 99%) and 11.0 g ( $8.03 \cdot 10^{-2}$  mol) of 1-monobromobutane. N-trimer-6C was prepared by reacting 3.4 g ( $1.39 \cdot 10^{-2}$  mol) of 1,6-dibromohexane (Fluka, 97%) and 17.1 g (0.147 mol, 10 equiv.) of TMEDA according to the same method.

All molecular weights of the oligomers were determined by titration of the tertiary amino end-groups in an identical approach as described earlier for the polymeric ionenes. The obtained molecular weights of the oligomers (see Tab. 3.1) were in close agreement with their theoretical values. Despite many reaction steps small differences between the experimental and theoretical molecular weights of the oligomeric ionenes were found.

Table 3.1 Molecular weights of the different oligomeric ionenes prepared

	end-group	$\bar{M}_n$ (theoretical) (g·mol <sup>-1</sup> )	$\bar{M}_n$ (experimental) (g·mol <sup>-1</sup> )
Br-trimer	Br	548	589
N-trimer	N	448	459
Br-pentamer	Br	880	954
N-pentamer	N	780	865
N-heptamer	N	1113	1196
Br-nonamer	Br	1544	1645
H-trimer-2C	H	390	a)
H-trimer-3C	H	404	a)
N-trimer-6C	N	476	492

a) Titration showed the absence of dimethyl-amino groups.

## 3.2 Experimental Techniques

### 3.2.1 Catalytic Activity Measurements

The catalytic thiol autoxidations were carried out batchwise, in an all-glass double-walled Warburg apparatus (250 ml) with a flat bottom (diameter  $6.5 \cdot 10^{-2}$  m) and supplied with four symmetrically located baffles (diameter  $1.0 \cdot 10^{-2}$  m). The temperature was kept constant at  $25.0 \pm 0.1$  °C with a thermostated bath. The reactor was equipped with a fourbladed turbine glass stirrer with a diameter of  $2.5 \cdot 10^{-2}$  m and a blade width of  $1.1 \cdot 10^{-2}$  m. The shaft and blades of the impeller were hollow to achieve a very effective gas dispersion. The stirring rate was always 2600 r.p.m., at which no transport limitations have been found to occur for the homogeneous 2,4-ionene/CoPc(NaSO<sub>3</sub>)<sub>4</sub> system<sup>10</sup>.

The catalyst solution consisting of the cobalt phthalocyanine derivatives, polymers and doubly distilled water, was added to the reactor, followed by adjustment of the pH by the addition of a concentrated KOH or NaOH (Merck, p.a.) solution (total reaction volume was always 0.10 dm<sup>3</sup>). The reaction vessel was degassed by vacuum evacuation, followed by saturation of the solution with oxygen. After repeating this procedure twice, the mixture was stirred vigorously for 5 minutes. The reaction was started by addition of 2-mercaptoethanol (ME) by means of a syringe into the reactor. Prior to use ME (Janssen Chimica, 98 %) was distilled in an argon atmosphere, stored in the dark and kept under argon in sealed flasks at 5 °C. Using 1-dodecanethiol (dodecylmercaptan, DM) (Janssen Chimica, 98 %) a different order of addition was followed: the reaction was started by introducing a concentrated CoPc(NaSO<sub>3</sub>)<sub>4</sub> solution to the oxygen-saturated reactor, already containing dodecanethiol, polymer and base. DM was vacuum distilled prior to use and further treated the same as ME.

Reaction rates were monitored by measuring the oxygen uptake with a digital mass flow controller (Inacom, Veenendaal), having a maximal capacity of 10 or 50 cm<sup>3</sup>/min, at constant oxygen pressure at 100 ± 0.05 kPa. The pressure was kept constant with a Micro Switch 142PC01D pressure meter. The initial reaction rate (experimental error ± 5 %), determined as the maximum in the oxygen flow, was measured immediately after ME, or CoPc(NaSO<sub>3</sub>)<sub>4</sub> in case of DM oxidations, was added. During the reaction, the pH was monitored by a GK 2401B pH electrode (Radiometer), connected to a pHM 62 pH-meter. After every catalytic run the reactor was extensively cleaned with water and after some consecutive runs washed with a soap solution (Hellma).

### 3.2.2 UV-Vis Spectroscopy

All VIS spectra were recorded on a Hewlett-Packard diode array 8451 A spectrophotometer at 25 °C, using a 1-cm cell of quartz.

## References

1. J.H. Weber, D.H. Busch, *Inorg. Chem.*, **4** (1965) 469.
2. J. Zwart, H.C. van der Weide, N. Bröker, C. Rummens, G.C.A. Schuit, A.L. German, *J. Mol. Catal.*, **3** (1977-78) 151.
3. R.T.L. Martis, Internal report, Eindhoven University of Technology, Eindhoven, 1985.
4. D.R. Boston, J.C. Bailar, Jr., *Inorg. Chem.*, **11** (1972) 1578.
5. H. Shirai, A. Maruyama, K. Kobayashi, N. Hojo, K. Urushido, *Makromol. Chem.*, **181** (1980) 575.
6. D. Wöhrle, T. Buck, G. Schneider, G. Schulz-Ekloff, H. Fischer, *J. Inorg. Organomet. Pol.*, **1** (1991) 115.
7. J. Zwart, Ph.D. Thesis, Eindhoven University of Technology, Eindhoven, 1978, p. 65.
8. A. Rembaum, W. Baumgartner, E. Eisenberg, *J. Polym. Sci. Polym. Lett. Ed.*, **6** (1968) 159.
9. W.M. Brouwer, P. Piet, A.L. German, *J. Mol. Catal.*, **31** (1985) 169.
10. J. van Welzen, A.M. van Herk, A.L. German, *J. Mol. Catal.*, **60** (1990) 351.

## Chapter 4

# Influence of the Molecular Weight of Ionenes on the Cobalt Phthalocyanine-Catalyzed Autoxidation of Mercaptoethanol

**SUMMARY:** In order to study the promoting effects of polycations on the cobalt(II) phthalocyaninetetrasodiumsulfonate- ( $\text{CoPc}(\text{NaSO}_3)_4$ ) catalyzed autoxidation of thiols, it is imperative to know the molecular weight dependence of the polymer. For this reason monodisperse oligomers can often supply a lot of information. To elucidate the mechanism of the promoting effect of 2,4-ionene on the  $\text{CoPc}(\text{NaSO}_3)_4$ -catalyzed autoxidation of 2-mercaptoethanol a series of monodisperse 2,4-ionene oligomers were prepared. Trimeric 2,4-ionenes, containing two quaternary ammonium groups separated by four methylene groups, already showed a high co-catalytic activity and active Co-aggregates were detected with visible light spectroscopy. The spectroscopic behaviour was in close agreement with that of high molecular 2,4-ionene/ $\text{CoPc}(\text{NaSO}_3)_4$  complexes. In order to achieve this aggregation several oligomeric ionenes have to act concertedly. If the distance between the ionic sites is short, the trimer acts as a simple salt in stabilizing the aggregates. With respect to the catalytic activity the optimal polycation/catalyst ratio, expressed as the  $\text{N}^+/\text{Co}$  ratio, decreased with increasing chain length and reached a constant level of 50 at a 2,4-ionene nonamer. For the trimers and pentamers this ratio is affected by the type of end-group. All synthesized 2,4-ionene oligomers exhibited excellent co-catalytic properties at the optimal  $\text{N}^+/\text{Co}$  ratio with maximal turnover frequencies of 1150 mol  $\text{O}_2/(\text{mol Co}\cdot\text{s})$ , *i.e.* forty times higher than those obtained for the polymer-free system. In the case of monodisperse 2,4-ionene pentamer with bromo end-groups Michaelis-Menten kinetics were observed, as also was exhibited by high molecular weight ionene.



## 4.1 Introduction

Several cationic polymers appeared to have large promoting effects on the  $\text{CoPc}(\text{NaSO}_3)_4^-$  (Fig. 3.1) catalyzed autoxidation of thiols to disulfides, as pointed out before in Chapter 2. The most effective promoters for the thiol autoxidation proved to be poly(quaternary ammonium)salts, the so-called ionenes<sup>1)</sup>. The highest rate enhancement, an increase by a factor of fourty, has been reported for 2,4-ionene<sup>2)</sup>.

So far various types of ionenes have been investigated with regard to their influence on the dimerization of the catalyst as well as on the catalytic activity<sup>2-4)</sup>. Till now, little attention has been paid to the effect of the length of the ionene chain at the formation of the cobalt aggregates and the catalytic oxidation rates, because monodisperse 2,4-ionene oligomers were not available. Earlier attempts have been made to determine the influence of the chain length of poly(vinylamine) as co-catalyst on the activity of the thiol autoxidation. Brouwer *et al.*<sup>5)</sup> observed a molecular weight dependence on the catalytic activity in the case of poly(vinylamine). Van Streun *et al.*<sup>6)</sup> attempted to study the effects of two different molecular weight 2,4-ionenes on the kinetics, but due to the small variation in the molecular weights, no significant difference could be observed.

Since we are able to prepare monodisperse oligomers of 2,4-ionene (Chapter 3), which primarily have been used to obtain amphiphilic polystyrene-ionene diblock copolymers (see Chapter 7), these well-defined oligomers can perfectly be used to study the influence of the molecular weight of 2,4-ionene on the thiol oxidation. Some types of low molecular weight ionene oligomers also have been used as model compounds in the X-ray analysis of crystal structures<sup>7,8)</sup> and in studies on the formation of ionene polymers<sup>9)</sup> and their surface tension properties<sup>10)</sup>.

From a mechanistic point of view it is very important to know the minimum length of 2,4-ionene necessary to obtain the active aggregates of  $\text{CoPc}(\text{NaSO}_3)_4^-$ . In this chapter we will discuss the influence of the length of monodisperse 2,4-ionene oligomers and of 2,4-ionene polymers, prepared by step condensation polymerization, on the dimerization of the catalyst. Also the resulting effects on the catalytic activity and the kinetics of these ionene-promoted reactions will be discussed.

## 4.2 Influence of the Molecular Weight of 2,4-Ionene on Cobalt Phthalocyanine Dimerization

The addition of 2,4-ionene to an aqueous  $\text{CoPc}(\text{NaSO}_3)_4$  catalyst solution dramatically affects the dimer-monomer equilibrium in the visible light spectrum<sup>3)</sup> (Fig. 2.1). Besides suppression of the  $\mu$ -peroxo complex formation, the dimeric form (628 nm) of the catalyst is drastically favoured over its monomeric form (662 nm). This shift has been attributed to be one of the polymeric promoting effects of ionenes, resulting in a tremendous increase in the reaction rate<sup>2)</sup>. These visible light experiments were all performed with a high molecular weight 2,4-ionene ( $\bar{M}_n = 22000 \text{ g} \cdot \text{mol}^{-1}$ )<sup>3)</sup>, which therefore provides no information about a possible molecular weight dependence. The new method of preparing monodisperse oligomeric 2,4-ionenes described in Chapter 3, enables us to determine the minimal chain length of 2,4-ionene required for the formation of dimers of the catalyst.

In order to study the molecular weight dependence on the aggregation phenomenon we measured the absorbances at 628 nm and 662 nm of several monodisperse oligomers of 2,4-ionene (Fig. 3.3) by varying the ionene/ $\text{CoPc}(\text{NaSO}_3)_4$  ratio, expressed as the  $\text{N}^+/\text{Co}$  ratio. The effect of varying the  $\text{N}^+/\text{Co}$  ratio for the Br-trimer (Fig. 3.3) on the ratio of both absorbances, which is a measure of the relative amount of aggregated cobalt species<sup>2)</sup>, is given in Fig. 4.1. An increase in the dimer over monomer ratio can be seen, but no sharp increase, characteristic of a high molecular weight 2,4-ionene at a  $\text{N}^+/\text{Co}$  ratio of 4, can be detected. The only effect which can be observed is increasing aggregation of the cobalt complex due to increasing Br-trimer concentration. Obviously, the Br-trimer is unable to stabilize the dimers as effectively as does the polymeric 2,4-ionene. The spectroscopic behaviour looks more or less like the earlier reported<sup>3,11)</sup> effect of adding a simple salt.

Additionally, we measured both absorbances for the other 2,4-ionene trimer, *i.e.* the N-trimer (Fig. 3.3). Looking at the results in Fig. 4.1, a quite different behaviour can be observed. These results are quite similar to those found for the high molecular weight 2,4-ionene<sup>3)</sup>. As  $\text{N}^+/\text{Co}$  increases from 0 to 4, it appears that the dimer/monomer ratio increases. At about  $\text{N}^+/\text{Co} = 4$  a discontinuity in the plot arises, which suggests the formation of an ionene/ $\text{CoPc}(\text{NaSO}_3)_4$  complex with fixed stoichiometry. Above a  $\text{N}^+/\text{Co}$

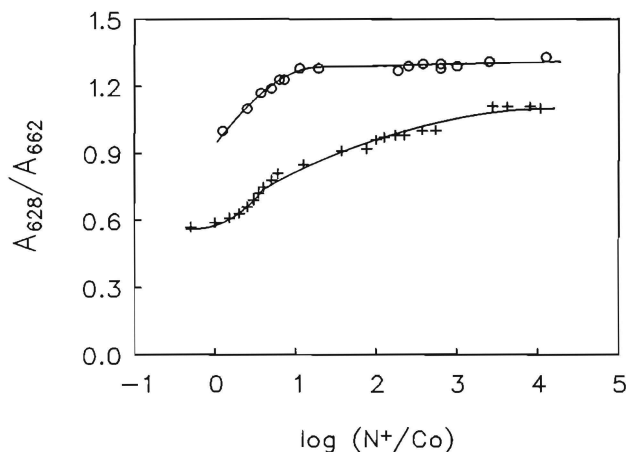


Figure 4.1 Ratio of absorbances at 628 nm and 662 nm as a function of the  $N^+/Co$  ratio for Br-trimer (+) and N-trimer (o).  $[CoPc(NaSO_3)_4] = 2 \cdot 10^{-6} \text{ mol} \cdot \text{dm}^{-3}$ .

ratio of 4 a relatively high  $A_{628}/A_{662}$  ratio is found, which remains constant even after increasing the N-trimer concentration: the existing complex is not further affected. This implies that apparently the N-trimer stabilizes the dimeric form better than does the Br-trimer, which can be ascribed to the difference in the distance between the quaternary ammonium groups in both trimers, *i.e.* approximately 4.1 Å and 6.1 Å for the Br-trimer and N-trimer, respectively.

In order to elucidate the role of the distance between the two quaternary ammonium groups, we synthesized trimeric oligomeric ionenes with two, three, and six methylene groups between the ionic sites, respectively. A similar structure of the H-trimer-2C (Fig. 3.3) as compared with the Br-trimer, explains the analogous spectroscopic behaviour (Fig. 4.2). In addition, the H-trimer-3C where the positive charges are separated by three methylene groups (distance  $\sim 5.3$  Å), is also unable to induce aggregation. By contrast, the N-trimer-6C stimulates the aggregation of  $CoPc(NaSO_3)_4$ . Therefore, it is interesting to notice a critical distance of minimal four methylene groups between the positive charges in an ionene trimer is required, in order to obtain a spectroscopic behaviour closely resembling that of the high molecular weight 2,4-ionenes. Apparently, a trimer

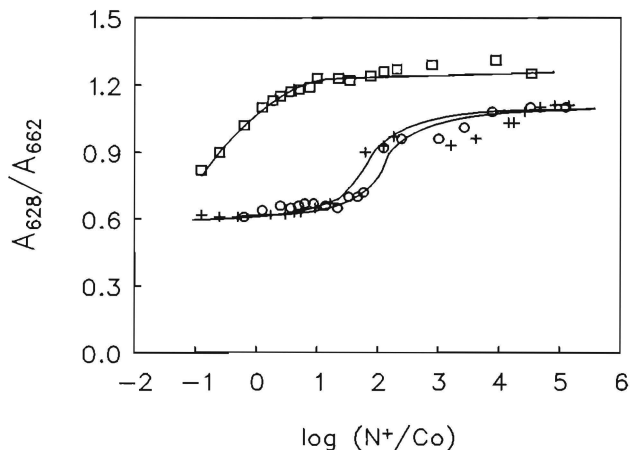


Figure 4.2 Ratio of absorbances at 628 nm and 662 nm as a function of the  $N^+/Co$  ratio for H-trimer-2C (o), H-trimer-3C (+) and N-trimer-6C ( $\square$ ).  $[CoPc(NaSO_3)_4] = 2 \cdot 10^{-6} \text{ mol} \cdot \text{dm}^{-3}$ .

where the distance between the quaternary ammonium groups is shorter than approximately  $6.1 \text{ \AA}$ , cannot stabilize a dimer of  $CoPc(NaSO_3)_4$  because only one of the two positive charges per trimer chain is capable to interact with one negative charge of the catalyst. On the other hand, in the case of the N-trimers, due to a larger distance between the ionic sites, the two quaternary ammonium groups can compensate the charges of two  $CoPc(NaSO_3)_4$  molecules, and hence a dimer can be formed.

Looking at the results for the N-pentamer and Br-pentamer (Fig. 4.3), both containing four quaternary ammonium groups, the spectroscopic behaviour is in agreement with that of high molecular weight 2,4-ionenes. The ratio of absorbances at 628 nm and 662 nm increases until a discontinuity arises at a  $N^+/Co$  ratio of 4, after which further addition of 2,4-ionene does not affect this ratio. A similar spectroscopic behaviour has also been determined for the N-heptamer and Br-nonamer.

With respect to the formation of a Co-dimer in principle 8 positive charges are required to counterbalance the negative charges of the dimer. At a  $N^+/Co$  ratio of 4, 8 positive charges of the ionene are just matching the opposite charge on the dimeric complex. Until now this was thought to be characteristic of ionene polymers only<sup>3)</sup>. Hence, it can be

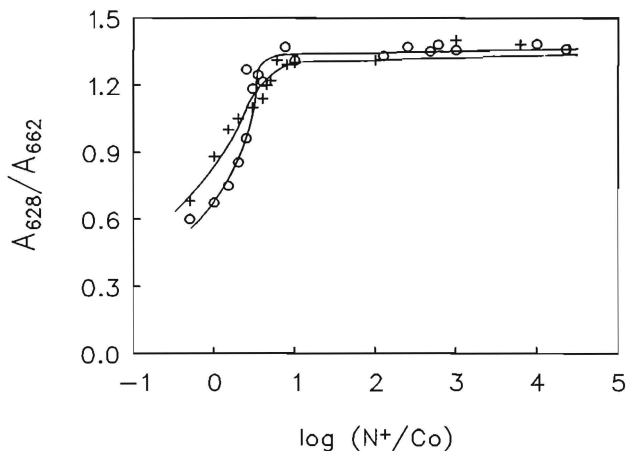


Figure 4.3 Ratio of absorbances at 628 nm and 662 nm as a function of the  $N^+/\text{Co}$  ratio for Br-pentamer (+) and N-pentamer (o).  $[\text{CoPc}(\text{NaSO}_3)_4] = 2 \cdot 10^{-6} \text{ mol} \cdot \text{dm}^{-3}$ .

inferred that in the case of trimers, where the relevant distance is at least four methylene groups, and both pentamers, several oligomeric ionene chains collectively contribute to an effective stabilization of dimers of  $\text{CoPc}(\text{NaSO}_3)_4$ .

The same effect of ionenes acting concertedly also has been observed in the catalyzed oxidation of 1-dodecanethiol, applying the identical oligomeric ionenes or amphiphilic polystyrene-ionene diblock copolymers as co-catalyst (see Chapter 9). In the latter system several 2,4-ionene segments, with a block length of only 4 quaternary ammonium groups extending in the water-phase, have been found to cooperatively stabilize the  $\text{CoPc}(\text{NaSO}_3)_4$ -aggregates.

### 4.3 Effects of the Molecular Weight of 2,4-Ionene on the Mercaptoethanol Oxidation Rate

As reported before, the 2-mercaptoethanol (ME) oxidation rate is a function of the co-catalyst concentration<sup>2)</sup>. When the catalyst concentration is kept constant and the ionene concentration is varied, a maximum in the activity arises at about  $N^+/\text{Co} = 200$  for a high

molecular weight 2,4-ionene<sup>2</sup>). Van Streun *et al.* examined two different 2,4-ionenes of molecular weights of  $1740 \text{ g}\cdot\text{mol}^{-1}$  and  $6600 \text{ g}\cdot\text{mol}^{-1}$ , respectively, and found not only similar maximal catalytic activities, but also identical optimal  $\text{N}^+/\text{Co}$  ratios for both polymers<sup>6</sup>).

The question arises now if the monodisperse oligomers of 2,4-ionene will exhibit a similar characteristic behaviour with respect to the optimal  $\text{N}^+/\text{Co}$  ratio and corresponding catalytic activities. It is already known that the monomeric analogue of 2,4-ionene, tetramethylammoniumhydroxide, shows no increase in reaction rate as compared with the polymer-free system<sup>12</sup>). In addition, Schutten found enhanced catalytic activities at extremely high salt concentrations, where only dimerization occurs and no substrate enrichment takes place, and as a consequence low reaction rates as compared with those when using ionenes were observed<sup>13</sup>).

We measured the oxidation rate as a function of the concentrations of Br-trimer and N-trimer (Fig. 4.4). At very high  $\text{N}^+$ -concentrations an optimum is reached for both trimers and the same high reaction rates are achieved. This high reaction rate is attributed to aggregation of the catalyst induced by high trimer concentrations, leading to the same

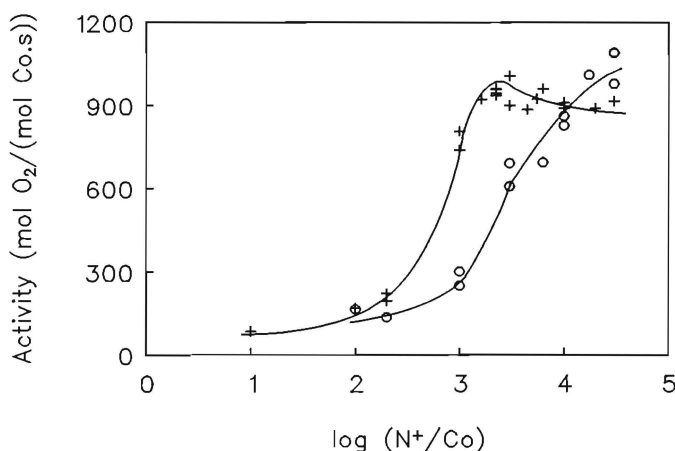
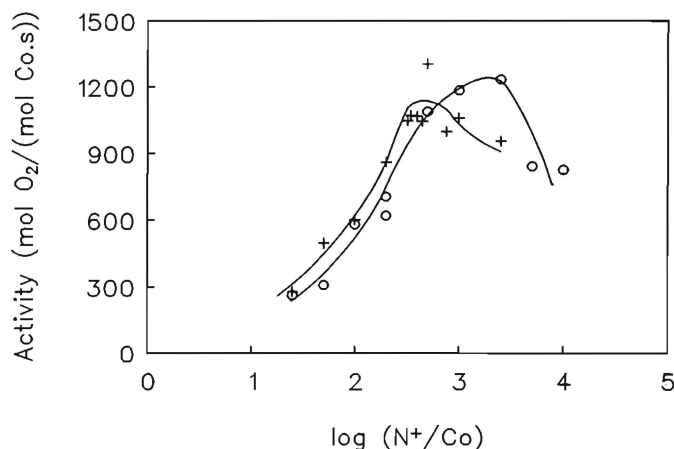


Figure 4.4 Effect of  $\text{N}^+/\text{Co}$  ratio on the ME oxidation rate.  
[CoPc(NaSO<sub>3</sub>)<sub>4</sub>] =  $2 \cdot 10^{-7} \text{ mol}\cdot\text{dm}^{-3}$ , pH = 9.0,  
[ME] =  $7.1 \cdot 10^{-2} \text{ mol}\cdot\text{dm}^{-3}$ ; (+) Br-trimer, (o) N-trimer.

relative amount of  $\text{CoPc}(\text{NaSO}_3)_4$ -dimers for both trimers. Furthermore, it appears that these high  $\text{N}^+$ -concentrations are necessary to achieve substrate enrichment of the thiolate anions in the positively charged oligomer domain (see also Chapter 5).

The effect of variation of the  $\text{N}^+$ -concentrations in the Br-pentamer and N-pentamer promoted mercaptoethanol autoxidation is depicted in Fig. 4.5. The low activities, at low pentamer concentrations, are caused by the absence of substrate enrichment, an effect that disappears upon raising the co-catalyst concentration. After an optimal  $\text{N}^+/\text{Co}$  has been reached, further increase in the pentamer concentration leads to a decrease in activity as a result of a decrease in the local thiolate anion concentration at the catalytically active site and simultaneous competition between bromide counterions on the one hand, and thiolate anions on the other. It can be concluded that apart from a higher optimal  $\text{N}^+/\text{Co}$  ratio, the pentamers behave like high molecular weight 2,4-ionene.



**Figure 4.5** Effect of the  $\text{N}^+/\text{Co}$  ratio on the thiol oxidation rate.  
 $[\text{CoPc}(\text{NaSO}_3)_4] = 2 \cdot 10^{-7} \text{ mol} \cdot \text{dm}^{-3}$ ,  $\text{pH} = 9.0$ ,  
 $[\text{ME}] = 7.1 \cdot 10^{-2} \text{ mol} \cdot \text{dm}^{-3}$ ; (+) Br-pentamer, (o) N-pentamer.

Additionally, we have determined the oxidation rates as a function of the concentration of N-heptamer, Br-nonamer and other polymeric 2,4-ionenes, comprising the whole range of molecular weights. A typical dependence of the amount of a polymeric 2,4-ionene on the catalytic ME oxidation rate is illustrated in Fig. 4.6. This figure clearly shows that

the maximal catalytic activity is comparable with those measured for the small oligomeric 2,4-ionenes. Only the corresponding  $N^+/Co$  ratio is shifted to a lower value.

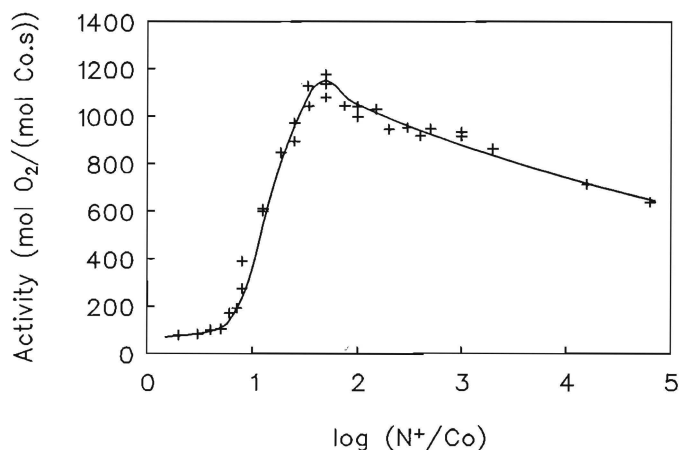


Figure 4.6 Effect of the 2,4-ionene concentration on the ME oxidation rate.  
 $[CoPc(NaSO_3)_4] = 2 \cdot 10^{-7} \text{ mol} \cdot \text{dm}^{-3}$ ,  $pH = 9.0$ ,  
 $[ME] = 7.1 \cdot 10^{-2} \text{ mol} \cdot \text{dm}^{-3}$ ,  $\bar{M}_n(2,4\text{-ionene}) = 6200 \text{ g} \cdot \text{mol}^{-1}$ .

The optimal  $N^+/Co$  ratios of the various polyelectrolytes as function of the number of quaternary ammonium groups per chain are presented in Fig. 4.7. Two important conclusions can be drawn from this figure. First, the optimal  $N^+/Co$  ratio is a function of the chain length of 2,4-ionene. This ratio decreases with the increase in the polycation length until a value of 50 is reached, this value is already reached for the Br-nonamer, with 8 positive charges. The higher optimal  $N^+/Co$  ratio for smaller oligomer lengths have to be attributed to the higher  $N^+$ -concentrations necessary to achieve an effective substrate enrichment. Moreover, the tertiary amino terminated oligomers show higher optimal  $N^+/Co$  ratios as compared with the Br-terminated oligomers with an equal number of quaternary ammonium groups.

Presumably, in solution the more hydrophobic butylbromide end-groups form hydrophobic domains, resulting in higher local oligomer concentrations: hence, more effective substrate enrichment is reached at a lower overall  $N^+$ -concentration. A similar influence of the hydrophobicity of the end-group of the Br-terminated oligomers has also been ob-



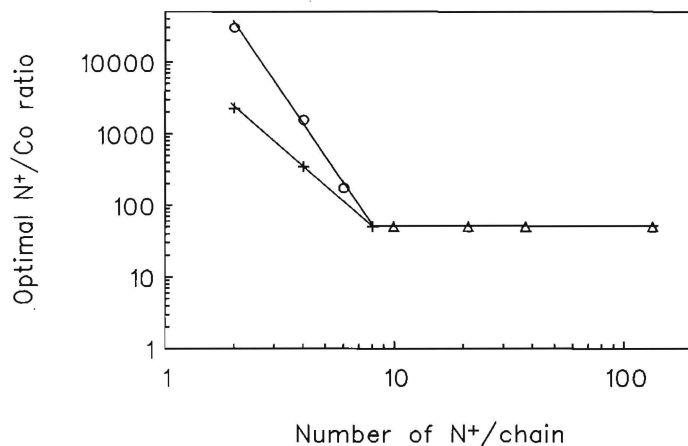


Figure 4.7 The optimal  $N^+/\text{Co}$  ratio as a function of the number of quaternary ammonium groups per chain.

$[\text{CoPc}(\text{NaSO}_3)_4] = 2 \cdot 10^{-7} \text{ mol} \cdot \text{dm}^{-3}$ ,  $\text{pH} = 9.0$ ,

$[\text{ME}] = 7.1 \cdot 10^{-2} \text{ mol} \cdot \text{dm}^{-3}$ ; (+) Br-terminated and (o)

N-terminated monodisperse oligomers, ( $\Delta$ ) polymeric 2,4-ionenes.

served in the 1-dodecanethiol oxidation. In that case the Br-terminated trimers and pentamers, in contrast to the N-terminated oligomers, showed a promoting effect as a result of their hydrophobic interaction with the hydrophobic thiol. The effects of these end-groups will be further discussed in Chapter 5 and 9.

The catalytic activities at these optimal  $N^+/\text{Co}$  ratios are depicted in Fig. 4.8. It clearly shows that the maximum reaction rates are nearly independent of the molecular weights of 2,4-ionene oligomers and polymers, and remain practically constant around  $1150 \text{ mol O}_2/(\text{mol CoPc}(\text{NaSO}_3)_4 \cdot \text{s})$ . It should be emphasized, however, that this value is forty times higher than that for the polymer-free system.

The  $\text{CoPc}(\text{NaSO}_3)_4$ -catalyzed oxidative coupling of ME gives rise to an enzyme-like kinetic behaviour. Double-substrate Michaelis-Menten kinetics have been observed earlier when using cationic polymers as co-catalysts<sup>14,15</sup>. In the present investigation we have compared the kinetic behaviour of a Br-pentamer with that of a high molecular weight 2,4-ionene.

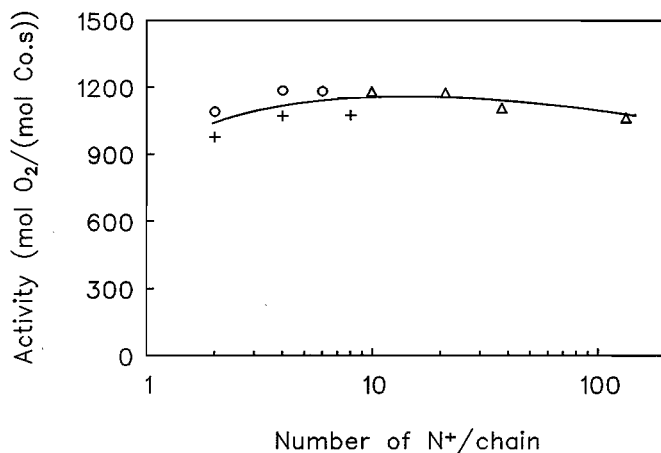


**Figure 4.8** The maximum catalytic activities at the optimal  $N^+/Co$  ratios as a function of the number of quaternary ammonium groups per chain.  $[CoPc(NaSO_3)_4] = 2 \cdot 10^{-7} \text{ mol} \cdot \text{dm}^{-3}$ ,  $\text{pH} = 9.0$ ,  $[ME] = 7.1 \cdot 10^{-2} \text{ mol} \cdot \text{dm}^{-3}$ ; (+) Br-terminated and (o) N-terminated monodisperse oligomers, ( $\Delta$ ) polymeric 2,4-ionenes.

First of all, in Fig. 4.9 the pH dependence of the thiol oxidation rate at the optimal  $N^+/Co$  ratio is depicted. From this figure it becomes evident that the oxidation rate increases on increasing pH, because the reactive species is the thiolate anion and not 2-mercaptoethanol ( $\text{pK}_a = 9.6$ ) itself. However, after reaching an optimum the catalytic activity decreases: a simultaneous increase in ionic strength and hydroxide concentration leads to a competitive ion effect. Comparison of the results of the Br-pentamer with those of a high molecular weight 2,4-ionene, which have been described earlier<sup>12)</sup>, demonstrates that the bell-shaped pH-curves for both polycations are quite similar.

In order to study intrinsic kinetics mass transfer limitations have to be ruled out. The linear dependence of the catalytic activity on the catalyst concentration ( $N^+/Co$  ratio is constant for the Br-pentamer) (Fig. 4.10) clearly indicates the absence of mass transfer limitations in the present case.

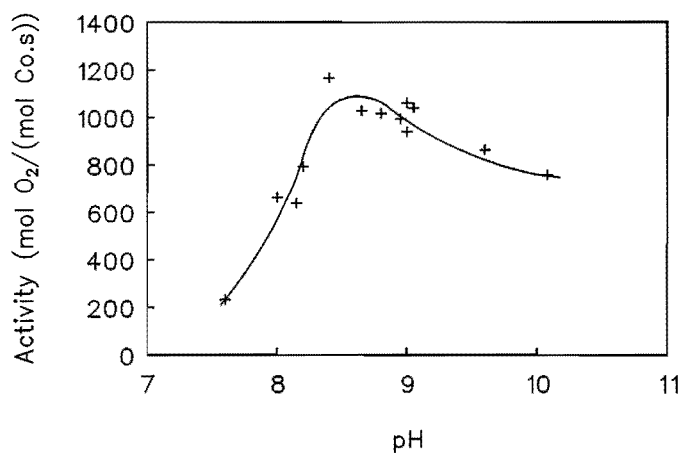


**Figure 4.9** Catalytic ME oxidation rate as a function of pH.  
 $[CoPc(NaSO_3)_4] = 2 \cdot 10^{-7} \text{ mol} \cdot \text{dm}^{-3}$ ,  $[N^+] = 7 \cdot 10^{-5} \text{ mol} \cdot \text{dm}^{-3}$ ,  
 $[ME] = 7.1 \cdot 10^{-2} \text{ mol} \cdot \text{dm}^{-3}$ ; (+) Br-pentamer.

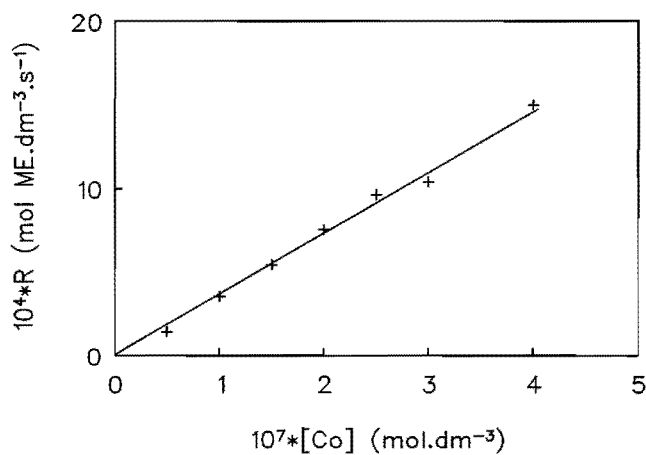


**Figure 4.10** Reaction rate as a function of the catalyst concentration at constant  $N^+/Co$ .  $N^+/Co = 350$ ,  $pH = 9.0$ ,  $[ME] = 7.1 \cdot 10^{-2} \text{ mol} \cdot \text{dm}^{-3}$ ;  
 (+) Br-pentamer.

The kinetics of the oxidative coupling of ME can be described as a Michaelis-Menten kinetic model<sup>16</sup>. At a constant oxygen concentration the rate of thiol oxidation ( $R$ ) is given by

$$R = \frac{k' [\text{CoPc}(\text{NaSO}_3)_4][\text{ME}]}{K'_M + [\text{ME}]} \quad (4.1)$$

with  $k'$ , the minimum turnover frequency for thiol conversion, at 0.1 MPa  $\text{O}_2$  and saturation in thiol, and  $K'_M$ , the apparent Michaelis constant. The dependence of reaction rate on the thiol concentration at optimal pH and  $[\text{N}^+]$  conditions are depicted in Fig. 4.11 for the Br-pentamer and two 2,4-ionenes with number average molecular weights of 6200 and 22000  $\text{g}\cdot\text{mol}^{-1}$ , respectively. Saturation behaviour typical of enzyme-like kinetics can be observed. Both, minimum turnover frequencies and apparent Michaelis constants were determined from Lineweaver-Burk plots. These constants, indicative of

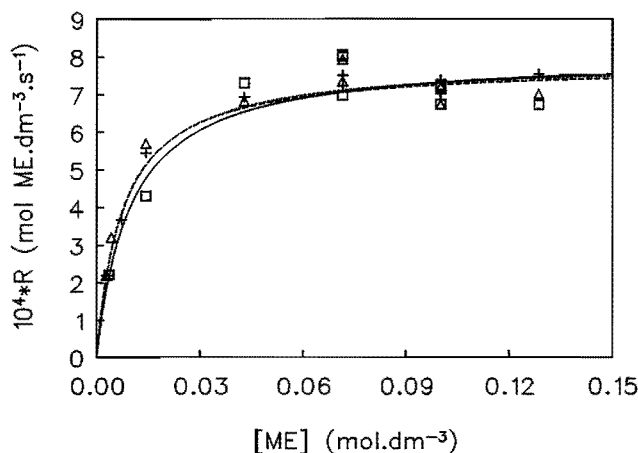


Figure 4.11 Catalytic activity as a function of substrate (ME) concentration.  
 $[\text{CoPc}(\text{NaSO}_3)_4] = 2 \cdot 10^{-7} \text{ mol}\cdot\text{dm}^{-3}$ ,  $\text{pH} = 9.0$ ,  
 $[\text{ME}] = 7.1 \cdot 10^{-2} \text{ mol}\cdot\text{dm}^{-3}$ ;  
 (+) (—) Br-pentamer  $[\text{N}^+] = 7 \cdot 10^{-5} \text{ mol}\cdot\text{dm}^{-3}$ ,  
 ( $\Delta$ ) (···) 2,4-ionene ( $\bar{M}_n = 6200 \text{ g}\cdot\text{mol}^{-1}$ )  $[\text{N}^+] = 10^{-5} \text{ mol}\cdot\text{dm}^{-3}$ ,  
 ( $\square$ ) (---) 2,4-ionene ( $\bar{M}_n = 22000 \text{ g}\cdot\text{mol}^{-1}$ )  $[\text{N}^+] = 10^{-5} \text{ mol}\cdot\text{dm}^{-3}$ .

the activity of the catalytic system, are listed in Table 4.1. As can be seen, no significant discrepancies can be detected between the kinetics of the different ionenes, so it can be concluded that the mechanism of the 2,4-ionene promoted catalytic oxidation of ME is independent of the polymer chain length.

*Table 4.1 Minimum turnover frequencies and apparent Michaelis constants of the catalytic systems under study.*

*Experimental conditions as in Fig. 4.11.*

	$\bar{M}_n$ (g · mol <sup>-1</sup> )	$k'_2$ (mol ME · (mol CoPc · s) <sup>-1</sup> )	$10^3 \cdot K'_M$ (mol ME · dm <sup>-3</sup> )
Br-pentamer	880	3900 ± 200	7.4 ± 1.0
2,4-ionene	6200	3940 ± 200	7.1 ± 1.4
2,4-ionene	22000	4020 ± 200	9.8 ± 2.0

The insights acquired on the minimal critical chain length provides the basis for the preparation of ideal diblock copolymers (Chapter 9), with well-defined block lengths, that will act as effective promoters in the phase-transfer catalyzed oxidation of 1-dodecane-thiol. Until now it was assumed that it was essential to apply long and flexible ionene chains in order to stabilize the active aggregates of the catalyst. This concept has to be amended in the case of the mercaptoethanol oxidation, since a number of short oligomeric ionene chains is also capable of stabilizing the CoPc(NaSO<sub>3</sub>)<sub>4</sub>-aggregates. On the other hand in immobilized systems, for example latices carrying catalytic groups, it might still be required to have long cationic tails. In those cases it will be more difficult for fixed short chains to contribute collectively to the stabilization of catalytically active aggregates. Therefore, in Chapter 8 we will discuss the effect of the ionene chain length at the latex surface on the mercaptoethanol oxidation rate.

#### **4.4 Conclusions**

Visible light spectroscopy experiments showed aggregation of  $\text{CoPc}(\text{NaSO}_3)_4$  already when using relatively low molecular weight 2,4-ionene. Trimeric oligomers, in which the two positive charges are separated by at least four methylene groups, induced aggregation in a way similar to that occurring in high molecular weight 2,4-ionene.

The optimal  $\text{N}^+/\text{Co}$  ratio is very high for the smaller oligomers, because only at those high values effective substrate enrichment can be achieved. Besides, the hydrophobicity of the end-groups of the oligomers plays an important role in attaining the optimal co-catalytic activity. It may be inferred, that the formation of hydrophobic domains, consisting of butylbromide end-groups, shifts the optimal  $\text{N}^+/\text{Co}$  ratio of the Br-terminated oligomers to lower values. The final co-catalytic activity at optimal  $\text{N}^+/\text{Co}$  ratio is very high for all 2,4-ionenes and is independent of molecular weight and type of end-group.

## References

1. W.M. Brouwer, P. Piet, A.L. German, *J. Mol. Catal.*, **31** (1985) 169.
2. J. van Welzen, A.M. van Herk, A.L. German, *Makromol. Chem.*, **190** (1989) 2477.
3. J. van Welzen, A.M. van Herk, A.L. German, *Makromol. Chem.*, **188** (1987) 1923.
4. J. van Welzen, Ph.D. Thesis, Eindhoven University of Technology, Eindhoven, 1989.
5. W.M. Brouwer, P. Piet, A.L. German, *Makromol. Chem.*, **185** (1984) 363.
6. K.H. van Streun, P. Piet, A.L. German, *Eur. Polym. J.*, **23** (1987) 941.
7. L. Dominguez, W.H. Meyer, G. Wegner, *Makromol. Chem. Rapid. Commun.*, **8** (1987) 151.
8. L. Dominguez, V. Enkelmann, W.H. Meyer, G. Wegner, *Polymer*, **30** (1989) 2030.
9. N. Noguchi, *Makromol. Chem. Rapid. Commun.*, **13** (1992) 185.
10. T. Okubo, *J. Coll. Interf. Sci.*, **125** (1988) 386.
11. L.C. Gruen, R.J. Blagrove, *Aust. J. Chem.*, **26** (1973) 319.
12. W.M. Brouwer, P. Piet, A.L. German, *J. Mol. Catal.*, **31** (1985) 169.
13. J.H. Schutten, Ph.D. Thesis, Eindhoven University of Technology, Eindhoven, 1981.
14. A.M. van Herk, A.H.J. Tullemaans, J. van Welzen, A.L. German, *J. Mol. Catal.*, **44** (1988) 269.
15. J. van Welzen, A.M. van Herk, T.G.L. Thijssen, A.L. German, *J. Mol. Catal.*, **59** (1990) 311.
16. A.M. van Herk, K.H. van Streun, J. van Welzen, A.L. German, *Br. Polym. J.*, **21** (1989) 125.

## Chapter 5

### Role of Polycation Promoters in the Cobalt(II) Phthalocyaninetetracarboxylic and -Octacarboxylic Acid-Catalyzed Autoxidation of 2-Mercaptoethanol

**SUMMARY:** The promoting effects of 2,4-ionene on the cobalt(II) phthalocyanine-tetracarboxylic acid- ( $\text{CoPc}(\text{COOH})_4$ ) and cobalt(II) phthalocyanineoctacarboxylic acid- ( $\text{CoPc}(\text{COOH})_8$ ) catalyzed autoxidation of 2-mercaptoethanol were studied. Dimerization of the  $\text{CoPc}(\text{COOH})_4$  catalyst combined with the disappearance of the catalytically inactive  $\mu$ -peroxo complex and the appearance of substrate enrichment in the presence of 2,4-ionene, results in a 40-fold oxidation rate enhancement as compared with the polymer-free system.

UV-VIS spectroscopy indicates that  $\text{CoPc}(\text{COOH})_8$  is incapable of forming  $\mu$ -peroxo complexes or 2,4-ionene-induced dimeric catalyst species under normal reaction conditions. Hence, it was possible to study exclusively the ionene-induced effect of substrate enrichment. Addition of 2,4-ionene to an aqueous  $\text{CoPc}(\text{COOH})_8$  solution results in an activity enhancement by a factor of 2-3, which can entirely be ascribed to substrate enrichment.

Additionally, applying monodisperse ionene oligomers showed a molecular weight dependence of 2,4-ionene on the catalytic activity of  $\text{CoPc}(\text{COOH})_8$ , similar as was observed for the conventional 2,4-ionene/ $\text{CoPc}(\text{NaSO}_3)_4$  system. The optimal polycation/catalyst ratios of both systems decreases with increasing chain length of 2,4-ionene, till a constant value is reached. This leads to the conclusion that the optimal polymer/catalyst ratios are predominantly determined by substrate enrichment.



## 5.1 Introduction

One of the most important polymeric promoting effects on catalytic reactions is substrate enrichment caused by electrostatic or hydrophobic interactions, resulting in higher local substrate concentrations and therefore leading to higher reaction rates<sup>1-3</sup>). Substrate enrichment is also one of the three promoting effects polycations exhibit on the CoPc(NaSO<sub>3</sub>)<sub>4</sub>-catalyzed autoxidation of thiols to disulfides<sup>4-7</sup>). Since the catalytic active species, *i.e.* the thiolate anions, and the catalyst are both negatively charged, the presence of polycations, especially ionenes (poly(quaternary ammonium)salts)<sup>4</sup>), results in higher local concentrations of the reactive species near the catalytically active sites in the polyelectrolyte domain. Besides, the formation of the catalytically inactive dioxygen bridged  $\mu$ -peroxo complex is suppressed and simultaneously aggregates of CoPc(NaSO<sub>3</sub>)<sub>4</sub> are formed due to the presence of ionenes<sup>8</sup>). These three effects collectively contribute to an increase in the catalytic activity. In order to elucidate which polycationic promoting effect has the largest contribution to this rate enhancement we will focus in this chapter on one of the effects, *i.e.* substrate enrichment.

It appears that cobalt(II) phthalocyanineoctacarboxylic acid (CoPc(COOH)<sub>8</sub>) (Fig. 3.1), a catalyst which has been used before to study H<sub>2</sub>O<sub>2</sub> decomposition<sup>9</sup>, the thiol oxidation<sup>10</sup> and after immobilization on cellulose fibers for the application of odour-removers<sup>11</sup>, provides valuable insight into this ionene promoting effect. A study of the spectroscopic properties of CoPc(COOH)<sub>8</sub>, revealed that this catalyst is incapable of forming ionene-induced aggregates. Therefore, CoPc(COOH)<sub>8</sub> offers the possibility to study exclusively the effect of substrate enrichment on the mercaptoethanol oxidation in the presence of a positively charged polymer domain. Moreover, we investigated the influence of the chain length of 2,4-ionene on the process of substrate enrichment, which was found to have a large influence on the conventional 2,4-ionene/CoPc(NaSO<sub>3</sub>)<sub>4</sub> system as discussed in Chapter 4. Furthermore, the catalytic properties of CoPc(COOH)<sub>8</sub> were compared with those of cobalt(II) phthalocyaninetetracarboxylic acid (CoPc(COOH)<sub>4</sub>) (Fig. 3.1), containing four negative charges.

## 5.2 Effects of 2,4-Ionene on the Spectroscopic Behaviour of CoPc(COOH)<sub>4</sub> and CoPc(COOH)<sub>8</sub>

The fact that ionenes showed a large influence on the aggregation behaviour of CoPc(NaSO<sub>3</sub>)<sub>4</sub><sup>8,12</sup>, it was necessary, before performing catalytic experiments, to study the spectroscopic properties of CoPc(COOH)<sub>8</sub> in the presence of ionene. The visible light absorption spectra of CoPc(COOH)<sub>8</sub> under different conditions are depicted in Fig. 5.1. Under neutral conditions (pH = 7, ionic strength (I) = 0.1 M) two main absorption bands can be detected, *i.e.* at 618 nm and at 682 nm, the latter one has been assigned to the monomeric species of CoPc(COOH)<sub>8</sub><sup>13</sup>. Varying the conditions (pH = 13, O<sub>2</sub>-atmosphere) a spectrum was obtained comparable with the spectrum at pH = 7. No formation of a dioxygen bridged dimeric  $\mu$ -peroxo complex was detected, which in the case of CoPc(NaSO<sub>3</sub>)<sub>4</sub> normally appears at high pH under aerobic conditions<sup>14</sup>. Presumably, it may be stated that CoPc(COOH)<sub>8</sub> is unable to form  $\mu$ -peroxo complexes.

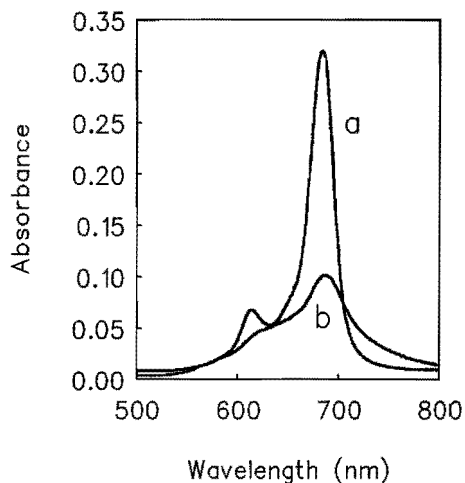


Figure 5.1 Absorption spectra of aqueous solutions of CoPc(COOH)<sub>8</sub> at constant ionic strength (I = 0.1 M).

(a) pH = 7, (b) pH = 5 + 2,4-ionene ( $\bar{M}_n = 6200 \text{ g}\cdot\text{mol}^{-1}$ ,  $[N^+] = 1.5 \cdot 10^{-2} \text{ mol}\cdot\text{dm}^{-3}$ );  $[\text{CoPc(COOH)}_8] = 5 \cdot 10^{-6} \text{ mol}\cdot\text{dm}^{-3}$ .

Additionally, dissolving CoPc(COOH)<sub>8</sub> in *N,N*-dimethylformamide under anaerobic conditions (argon atmosphere), a solvent in which phthalocyanine aggregates are known

to dissociate into monomeric species upon addition<sup>15</sup>), did not lead to any shift in the VIS spectrum.

The question arises if the highly charged  $\text{CoPc}(\text{COOH})_8$  is capable of forming dimeric complexes. Aggregation of charged phthalocyanine complexes normally can be achieved in the presence of high electrolyte concentration<sup>16-18</sup> or induced by polyelectrolytes<sup>8</sup>. No dimerization of the catalyst was observed after addition of KCl or 2,4-ionene to an aqueous  $\text{CoPc}(\text{COOH})_8$  solution ( $\text{pH} > 7$ ): the absorption spectrum was unaffected. Obviously, the neutralizing of the negative charges by cations or ionene proceeds inefficiently, so the repulsive forces between two  $\text{CoPc}(\text{COOH})_8$  molecules remain too large to form a dimeric complex. Thus, it can be stated that in an alkaline solution no aggregation of  $\text{CoPc}(\text{COOH})_8$  can be attained upon addition of salts or polysalts.

However, we observed aggregation of  $\text{CoPc}(\text{COOH})_8$  in the presence of 2,4-ionene when the pH was lowered to 5. As can be seen in Fig. 5.1 the absorbance band at 682 nm decreases as a result of polymer-induced aggregation of the Co-species. At this low pH value only a fraction of the carboxylic acid groups is deprotonated ( $\text{pK}_a$  values of carboxylic acid groups in *o*-phthalic acid are 2.9 and 5.5, respectively)<sup>19</sup>, which results in less charged phthalocyanine complexes able to dimerize. Shirai *et al.* showed that the carboxyl groups in the peripheral site of the phthalocyanine ring dissociate into carboxylate at  $\text{pH} 7.0$ <sup>10</sup>. Hence, we may conclude that no aggregation of  $\text{CoPc}(\text{COOH})_8$  will occur during the catalytic experiments, because they are always performed under alkaline conditions.

In addition, we studied the spectroscopic behaviour of  $\text{CoPc}(\text{COOH})_4$  in the presence of 2,4-ionene. It should be expected that the spectral properties of  $\text{CoPc}(\text{COOH})_4$  in the presence of 2,4-ionene would not differ from those of  $\text{CoPc}(\text{NaSO}_3)_4$ , because only electrostatic interactions are determining the aggregation behaviour. In Fig. 5.2 the ratio of the absorbances at 620 nm and 672 nm of the  $\text{CoPc}(\text{COOH})_4$ , which is a measure of the relative amount of aggregated cobalt species<sup>8</sup>, is depicted, as a function of the 2,4-ionene/ $\text{CoPc}(\text{COOH})_4$  ratio, expressed as the  $\text{N}^+/\text{Co}$  ratio. As  $\text{N}^+/\text{Co}$  increases from 0 to 4, it appears that the  $A_{620}/A_{672}$  ratio increases. At  $\text{N}^+/\text{Co} = 4$ , where no  $\mu$ -peroxo complexes could be detected, a discontinuity in the plot arises, indicating the formation of an ionene/ $\text{CoPc}(\text{COOH})_4$  complex with fixed stoichiometry. Above a  $\text{N}^+/\text{Co}$  ratio of

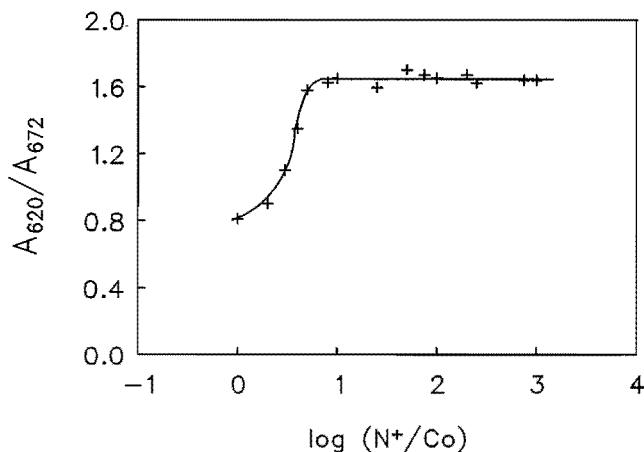


**Figure 5.2** Ratio of absorbances at 620 nm and 672 nm as a function of the  $N^+/Co$  ratio for a 2,4-ionene/ $CoPc(COOH)_4$  system.  $[CoPc(COOH)_4] = 2 \cdot 10^{-6} \text{ mol} \cdot \text{dm}^{-3}$ ,  $pH = 9$  (buffer,  $I = 0.1 \text{ M}$ ),  $\bar{M}_n(2,4\text{-ionene}) = 6200 \text{ g} \cdot \text{mol}^{-1}$ .

4 a relatively high  $A_{620}/A_{672}$  ratio is found, which is unaffected even after raising the amount of ionene. An analogous aggregation phenomenon has been observed for the conventional 2,4-ionene/ $CoPc(NaSO_3)_4$  system<sup>8)</sup>.

These results clearly show that replacement of the peripheral sulfonate group by a carboxylic acid group, has no influence on the aggregation behaviour of the cobalt complex, because purely electrostatic shielding of charges is involved. In a similar way, it has been demonstrated before that complexation is also independent on the type of metal centre of the phthalocyanine<sup>20)</sup>.

### 5.3 Influence of 2,4-Ionene on the Catalytic Properties of $CoPc(COOH)_4$ and $CoPc(COOH)_8$

The incapability of  $CoPc(COOH)_8$  to form ionene-induced aggregates under catalytic conditions gives us the opportunity to study solely the effect of substrate enrichment in the  $CoPc(COOH)_8$ -catalyzed thiol autoxidations. The effect of varying the

$N^+$ -concentrations on the 2,4-ionene promoted mercaptoethanol oxidation catalyzed by  $\text{CoPc}(\text{COOH})_8$  is depicted in Fig. 5.3. At low ionene concentrations low oxidation rates are observed, similar to the activities obtained for a polymer-free system. Exactly at a  $N^+/\text{Co}$  ratio of 8, where an electrostatic neutral complex is formed, the oxidation rate increases. A further increase of the  $N^+$ -concentration leads to higher reaction rates till the highest catalytic activity is reached at an optimal  $N^+/\text{Co}$  ratio of 50, a value which has also been found for the 2,4-ionene/ $\text{CoPc}(\text{NaSO}_3)_4$  system (see Chapter 4).

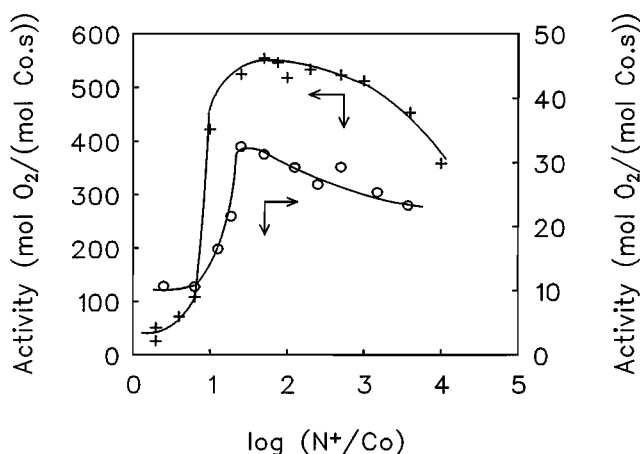


**Figure 5.3** Effect of  $N^+/\text{Co}$  ratio on the mercaptoethanol oxidation rate.  
 (+)  $\text{CoPc}(\text{COOH})_4$ ,  $[\text{CoPc}(\text{COOH})_4] = 2 \cdot 10^{-7} \text{ mol} \cdot \text{dm}^{-3}$ ,  
 (o)  $\text{CoPc}(\text{COOH})_8$ ,  $[\text{CoPc}(\text{COOH})_8] = 2 \cdot 10^{-6} \text{ mol} \cdot \text{dm}^{-3}$ ;  
 $\text{pH} = 9.0$ ,  $[\text{ME}] = 7.1 \cdot 10^{-2} \text{ mol} \cdot \text{dm}^{-3}$ ,  
 $\bar{M}_n(2,4\text{-ionene}) = 6200 \text{ g} \cdot \text{mol}^{-1}$ .

Responsible for this rate increase is only substrate enrichment, *i.e.* higher concentrations of the reactive species, the thiolate anions, near the active catalytic sites. Subsequently, a further increase of the polycation concentration leads to a small decrease in the catalytic activity, because at these high concentrations the local thiolate anion concentration diminishes around the catalytic active centre.

The rate enhancement after addition of 2,4-ionene to  $\text{CoPc}(\text{COOH})_8$ , only caused by substrate enrichment, is a factor of 2-3. Similar rate enhancements as compared with

ionene-free systems have been observed in other phthalocyanine containing systems. Addition of 2,4-ionene to a dimeric  $\text{CoPc}(\text{N}(\text{CH}_3)_3\text{I})_4/\text{CoPc}(\text{NaSO}_3)_4$  complex, also raised the reaction rate (see following chapter). Despite a net zero charge of this complex, an acceleration factor of 2-3 was obtained, indicating that this dimeric complex is totally present in the polyelectrolyte domain, and addition of 2,4-ionene only results in substrate enrichment. Additionally, a similar rate increase by a factor of 2 was noticed for a dimeric  $\text{CoPc}(\text{N}(\text{CH}_3)_3\text{I})_4/\text{CoPc}(\text{COOH})_8$  complex in the presence of 2,4-ionene. An analogous acceleration factor for substrate enrichment, also purely caused by electrostatic interactions, has been regarded earlier for the interionic reaction between phenolate and glyoxylic acid to  $\alpha$ ,4-dihydroxybenzene-acetic acid in the presence of 3,3-ionene<sup>21)</sup>.

In comparison, the dependence of the catalytic activity of  $\text{CoPc}(\text{COOH})_4$  as a function of the 2,4-ionene concentration is also depicted in Fig. 5.3. This figure clearly shows that the influence of polycation addition on the catalytic activity of  $\text{CoPc}(\text{COOH})_4$  is a result of the three 2,4-ionene promoting effects<sup>5)</sup>. At low ionene concentrations, the low catalytic activity is comparable with a polymer-free system. At a  $\text{N}^+/\text{Co}$  ratio of 4 higher reaction rates are achieved due to suppression of the catalytically inactive  $\mu$ -peroxo complexes and simultaneously formation of  $\text{CoPc}(\text{COOH})_4$  dimers. Upon raising the co-catalyst amount the oxidation rate further increases which was ascribed to substrate enrichment and mainly to enhanced aggregation of the catalyst, *i.e.* higher aggregates of dimeric  $\text{CoPc}(\text{COOH})_4$  species<sup>5,8)</sup>. The optimal catalytic conditions, where the highest reaction rates are observed, are reached at a  $\text{N}^+/\text{Co}$  ratio of 50. After an optimal  $\text{N}^+/\text{Co}$  has been realized, the decrease in activity is a result of a decrease in the local thiolate anion concentration at the catalytically active site.

Moreover, two other important aspects should be remarked. First, when comparing the catalytic properties of  $\text{CoPc}(\text{COOH})_4$  and  $\text{CoPc}(\text{COOH})_8$  both in the presence of 2,4-ionene, it can be observed that despite the expected higher activities for  $\text{CoPc}(\text{COOH})_4$  than for  $\text{CoPc}(\text{COOH})_8$ , the shapes of both curves are quite similar and the maximal catalytic activities are reached at  $\text{N}^+/\text{Co}$  ratios of 50 (Fig. 5.3). Secondly, similar rate enhancements are observed upon addition of 2,4-ionene to  $\text{CoPc}(\text{COOH})_4$  as well as to the conventional  $\text{CoPc}(\text{NaSO}_3)_4$  system<sup>5)</sup>.

In Chapter 4 it was demonstrated that the molecular weight of 2,4-ionene plays a major role in achieving the optimal  $N^+/Co$  ratio at the highest oxidation rate. By using monodisperse oligomeric 2,4-ionenes it was found that the optimal  $N^+/Co$  ratio for a 2,4-ionene/ $CoPc(NaSO_3)_4$  system decreases while the chain length of the ionene increases till a constant value of 50 is reached at eight  $N^+$  per chain. From a mechanistic point of view these monodisperse ionene oligomers (Fig. 3.3) are excellent tools to provide insight into the molar mass dependence on the process of substrate enrichment in the case of the thiol oxidation catalyzed by  $CoPc(COOH)_8$ .

In Fig. 5.4 the mercaptoethanol oxidation rates are presented as a function of  $N^+/Co$  ratio for two monodisperse oligomers, containing two quaternary ammonium groups, *i.e.* the Br-trimer and N-trimer. A maximum in the catalytic activity at very high trimer concentrations can be noticed for the Br-trimer, indicating that substrate enrichment occurs only at these high oligomer concentrations. Compared with the polymer-free system addition of Br-trimer leads to a rate increase by a factor of 2. The very high optimal  $N^+/Co$  ratio, which is necessary to achieve effective substrate enrichment, is similar as revealed for the Br-trimer/ $CoPc(NaSO_3)_4$  combination (see Fig. 4.4).

Surprisingly, no rate enhancement can be observed upon addition of N-trimer to an aqueous  $CoPc(COOH)_8$  solution (Fig. 5.4). This implies that apparently the Br-trimer is capable of inducing substrate enrichment in contrast to the N-trimer, which probably can be ascribed to the difference in the distance between the two quaternary ammonium groups in both trimers, *i.e.* approximately 4.1 Å and 6.1 Å for the Br-trimer and N-trimer, respectively.

In order to elucidate the role of the distance between the two quaternary ammonium groups, we used other trimeric ionenes with three and six methylene groups between the two ionic sites (Fig. 3.3). The H-trimer-3C, where the distance between the charges is approximately 5.3 Å, is also unable to cause substrate enrichment: no raise in the activity can be observed while increasing the co-catalyst concentration (Fig. 5.4). Also for the N-trimer-6C, in which the positive charges are separated by six methylene groups an analogous behaviour can be observed. The fact that the end-group of a trimeric ionene plays no role was demonstrated by the H-trimer-2C, which achieved a similar rate

increase as the Br-trimer. The addition of  $N,N,N',N'$ -tetramethylethylenediamine to the Br-trimer promoted thiol oxidation neither affected the rate acceleration.

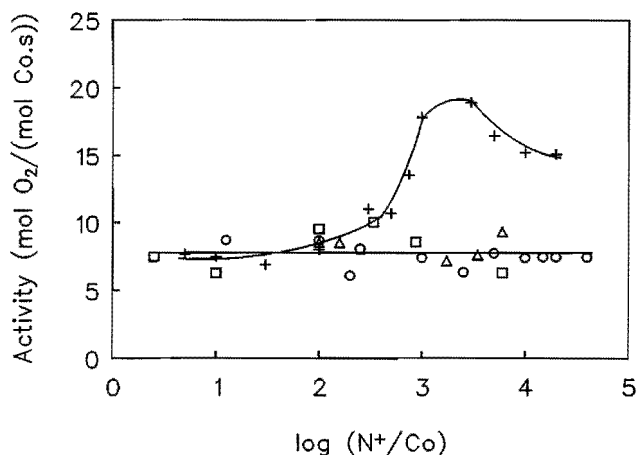


**Figure 5.4** Effect of  $N^+/Co$  ratio on the mercaptoethanol oxidation rate.  
 (+) Br-trimer, (o) N-trimer, ( $\Delta$ ) H-trimer-3C, ( $\square$ ) N-trimer-6C;  
 $[CoPc(COOH)_8] = 2 \cdot 10^{-6} \text{ mol} \cdot \text{dm}^{-3}$ ,  $pH = 9.0$ ,  
 $[ME] = 7.1 \cdot 10^{-2} \text{ mol} \cdot \text{dm}^{-3}$ .

Apparently, only trimeric ionene oligomers, where the distance between the two quaternary ammonium groups is less than about  $5.3 \text{ \AA}$ , are capable of inducing substrate enrichment. Considering the distance between the two carboxylic end-groups ( $\sim 4.2 \text{ \AA}$ ) attached to one phenyl ring, the reason of the incapability to induce substrate enrichment by trimeric oligomers, where the ionic sites are separated by more than three methylene groups, lies in the fact that both quaternary ammonium groups are able to neutralize the two carboxylate groups attached to one phenyl ring. In such a case no extra  $N^+$  is available for substrate enrichment. Obviously, the gap between the ionic sites in the Br-trimer ( $\sim 4.1 \text{ \AA}$ ) is too short to interact with both carboxylate groups, so one quaternary ammonium group is involved in binding the cobalt complex and the residual  $N^+$  is available for substrate enrichment.

The influence of the  $N^+/Co$  ratio of two other oligomers, *i.e.* Br-pentamer and N-heptamer (Fig. 3.3), with four and six  $N^+$ , respectively, on the mercaptoethanol



oxidation rate is shown in Fig. 5.5. For both oligomers rate increases by a factor of 2-3 are detectable upon addition of the ionene-oligomer. The optimal  $N^+/Co$  ratios for both Br-pentamer and N-heptamer are higher than those measured for high molecular weight 2,4-ionene and lower than determined for the Br-trimer. Furthermore, the optimal  $N^+/Co$  ratios and the shapes of both curves are identical to those obtained for the corresponding oligomer/ $CoPc(NaSO_3)_4$  systems (Chapter 4).

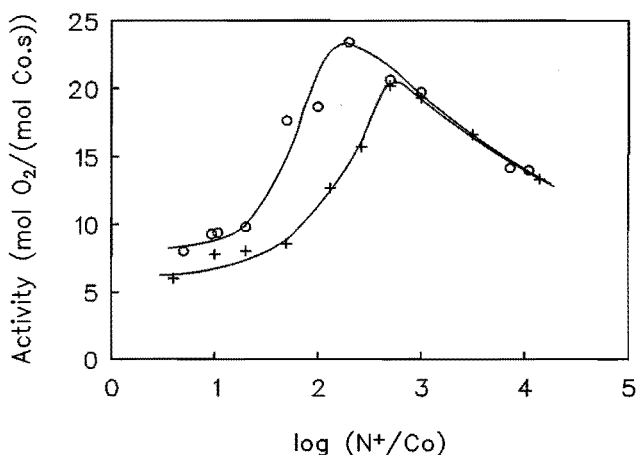
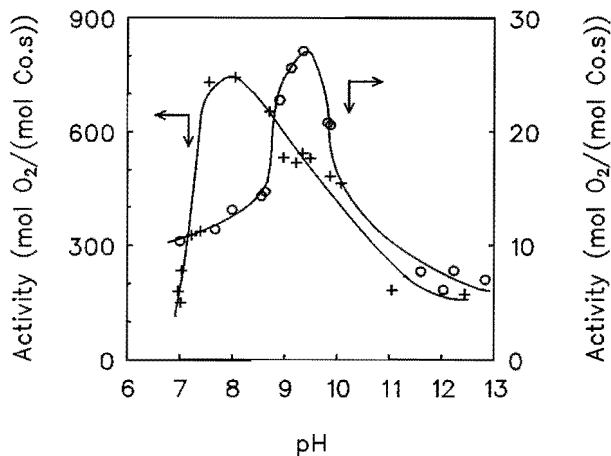


Figure 5.5 Effect of  $N^+/Co$  ratio on the mercaptoethanol oxidation rate. (+) Br-pentamer, (o) N-heptamer;  $[CoPc(COOH)_8] = 2 \cdot 10^{-6} \text{ mol} \cdot \text{dm}^{-3}$ ,  $pH = 9.0$ ,  $[ME] = 7.1 \cdot 10^{-2} \text{ mol} \cdot \text{dm}^{-3}$ .

Considering all results we have seen that the 2,4-ionene molecular weight dependence on the values of the  $N^+/Co$  optima for the  $CoPc(COOH)_8$  is similar as for the  $CoPc(NaSO_3)_4$  system. Despite lower catalytic activities, the shape of the curves are similar. Only the N-trimer deviates from this observation. Therefore, we may conclude that the values for the optimal  $N^+/Co$  ratio in a 2,4-ionene/ $CoPc(NaSO_3)_4$  system, where all three polycation promoting effects are involved, is exclusively determined by substrate enrichment and not by formation of higher aggregates of  $CoPc(NaSO_3)_4$ , which was thought before<sup>9)</sup>.

Furthermore, we investigated the pH dependence of the thiol oxidation rate at the optimal  $N^+/Co$  ratio for both 2,4-ionene containing  $CoPc(COOH)_4$  as well as  $CoPc(COOH)_8$  systems (Fig. 5.6). With respect to  $CoPc(COOH)_4$  a typical "bell-shaped" curve can be



**Figure 5.6** Catalytic activity as a function of pH.  
 (+)  $\text{CoPc}(\text{COOH})_4$ ,  $[\text{CoPc}(\text{COOH})_4] = 2 \cdot 10^{-7} \text{ mol} \cdot \text{dm}^{-3}$ ,  
 $[\text{N}^+] = 1.5 \cdot 10^5 \text{ mol} \cdot \text{dm}^{-3}$ ,  
 (o)  $\text{CoPc}(\text{COOH})_8$ ,  $[\text{CoPc}(\text{COOH})_8] = 2 \cdot 10^{-6} \text{ mol} \cdot \text{dm}^{-3}$ ,  
 $[\text{N}^+] = 2.5 \cdot 10^4 \text{ mol} \cdot \text{dm}^{-3}$ ;  $[\text{ME}] = 7.1 \cdot 10^{-2} \text{ mol} \cdot \text{dm}^{-3}$ .

observed, similar to the curve for the 2,4-ionene/ $\text{CoPc}(\text{NaSO}_3)_4$  system<sup>4)</sup>. The pH optimum of  $\text{CoPc}(\text{COOH})_8$  is shifted to a somewhat larger value, probably due to the larger repulsion between the phthalocyanine and the thiolate anions. From this figure it becomes evident that the oxidation rate increases on raising the pH, because the reactive species is the thiolate anion and not 2-mercaptoethanol ( $\text{pK}_a = 9.6$ )<sup>22)</sup> itself. However, after reaching an optimum the catalytic activity decreases: a simultaneous increase in ionic strength and hydroxide concentration leads to a competitive ion effect.

## 5.4 Conclusions

In the case of the 2,4-ionene/ $\text{CoPc}(\text{COOH})_4$  system the three polycation promoting effects result in a 40-fold rate enhancement as compared with the polymer-free system. UV-VIS spectroscopy experiments showed that  $\text{CoPc}(\text{COOH})_8$  was incapable of forming  $\mu$ -peroxo complexes, or ionene-induced dimeric catalyst complexes. Hence, it was possible to study exclusively the ionene promoting effect substrate enrichment. The addition of 2,4-ionene

to an aqueous  $\text{CoPc}(\text{COOH})_8$  solution therefore leads to a rate acceleration of a factor 2-3 ascribed completely to substrate enrichment, *i.e.* higher local concentrations of the reactive species, the thiolate anions.

Applying monodisperse ionene oligomers a molecular weight dependence was found, resulting in a shift of the optimal  $\text{N}^+/\text{Co}$  ratios to lower values with increasing chain length of the ionene. The results showed that similar molar mass dependent optimal polymer/catalyst ratios were realized for both 2,4-ionene containing  $\text{CoPc}(\text{COOH})_8$  and  $\text{CoPc}(\text{NaSO}_3)_4$  systems. Comparing both systems, we were able to conclude that substrate enrichment is the leading factor determining the optimal  $\text{N}^+/\text{Co}$  ratio.

## References

1. N. Ise, "Polyelectrolytes and Their Applications", A. Rembaum, E. Selegny, Eds., Reidel, Dordrecht, 1975.
2. J.H. Fendler, E.J. Fendler, "Catalysis in Micellar and Macromolecular Systems", Academic Press, New York, 1975.
3. D.C. Sherrington, P. Hodge, "Synthesis and Separations Using Functional Polymers", Wiley, Chichester, 1988.
4. W.M. Brouwer, P. Piet, A.L. German, *J. Mol. Catal.*, **31** (1985) 169.
5. J. van Welzen, A.M. van Herk, A.L. German, *Makromol. Chem.*, **190** (1989) 2477.
6. K.H. van Streun, W.J. Belt, E.T.W.M. Schipper, P. Piet, A.L. German, *J. Mol. Catal.*, **71** (1992) 245.
7. S. Hari Babu, W.T. Ford, *J. Polym. Sci. Polym. Chem.*, **30** (1992) 1917.
8. J. van Welzen, A.M. van Herk, A.L. German, *Makromol. Chem.*, **188** (1987) 1923.
9. H. Shirai, A. Maruyama, J. Takano, K. Kobayashi, N. Hojo, *Makromol. Chem.*, **180** (1979) 2073.
10. H. Shirai, H. Tsuiki, E. Masuda, T. Koyama, K. Hanabusa, N. Kobayashi, *J. Phys. Chem.*, **95** (1991) 417.
11. H. Shirai, K. Hanabusa, T. Koyama, H. Tsuiki, E. Masuda, *Makromol. Chem., Macromol. Symp.*, **59** (1992) 155.
12. Chapter 4 of this thesis.
13. H. Shirai, A. Maruyama, J. Takano, K. Kobayashi, N. Hojo, *Makromol. Chem.*, **181** (1980) 565.
14. L.C. Gruen, R.J. Blagrove, *Aust. J. Chem.*, **26** (1973) 319.
15. J.A. de Bolfo, T.D. Smith, J.F. Boas, J.R. Pilbrow, *J. Chem. Soc., Faraday Trans. II*, **72** (1976) 481.
16. Z.A Schelly, R.D. Farina, E.M. Eyring, *J. Phys. Chem.*, **74** (1970) 617.
17. N. Kobayashi, *J. Phys. Chem.*, **89** (1985) 1167.
18. Y.-C. Yang, J.R. Ward, R.P. Seiders, *Inorg. Chem.*, **24** (1985) 1765.
19. R.J. Fessenden, J.S. Fessenden, "Organic Chemistry", PWS publishers, Boston, 1982, Chapter 12.
20. J. van Welzen, A.M. van Herk, A.L. German, *Makromol. Chem.*, **189** (1988) 587.
21. M.-A. Schulten, *Post-Graduate Research Training Program Report*, Eindhoven University of Technology, Eindhoven, 1989.
22. J.P. Danchy, C.J. Noel, *J. Am. Chem. Soc.*, **82** (1960) 2511.

## Chapter 6

# Effects of Complexation of Oppositely Charged Water-Soluble Cobalt Phthalocyanines on the Catalytic Mercaptoethanol Autoxidation

**SUMMARY:** In order to elucidate the different promoting effects polycations have on the cobalt(II) phthalocyanine-catalyzed autoxidation of 2-mercaptoethanol, the properties of mixtures of oppositely charged water-soluble cobalt(II) phthalocyanines were studied. The contribution of polycation induced dimerization of the catalyst was investigated by means of combinations of cobalt(II) phthalocyanine-tetra(trimethylammonium)iodide ( $\text{CoPc}[\text{N}(\text{CH}_3)_3\text{I}]_4$ ) and  $\text{CoPc}(\text{NaSO}_3)_4$ . A mixture of equimolar amounts of both phthalocyanines shows an increase in reaction rate for the 2-mercaptoethanol autoxidation as compared with an equal amount of one of the catalyst species separately. The highest activities are achieved when the positive charges of the positive phthalocyanine just match the charges of the negative  $\text{CoPc}(\text{NaSO}_3)_4$ . A mixture of  $\text{CoPc}(\text{COOH})_8$  and  $\text{CoPc}[\text{N}(\text{CH}_3)_3\text{I}]_4$  exhibits its maximum activity at a ratio of 1:2, indicating the formation of a trimeric catalyst species. Visible light spectroscopy showed that these effects can be ascribed to the formation of aggregates of the phthalocyanines. These dimeric and trimeric catalyst complexes exhibit the highest catalytic activities measured so far for any phthalocyanine-catalyzed mercaptoethanol autoxidation in the absence of polycations. Addition of a poly(quaternary ammonium)salt, a so-called ionene, to a stoichiometric complex of oppositely charged phthalocyanines results in an increase in the catalytic activity due to substrate enrichment. The activities of an ionene containing equimolar  $\text{CoPc}[\text{N}(\text{CH}_3)_3\text{I}]_4/\text{CoPc}(\text{NaSO}_3)_4$  system were never as high as those achieved for a conventional  $\text{CoPc}(\text{NaSO}_3)_4/2,4\text{-ionene}$  system, probably as a result of the strong bonding between the two oppositely charged molecules, which prevents a break-up of the dimeric species. Conclusively, in order to achieve a high catalytic activity it is favourable to enhance the formation of aggregates of  $\text{CoPc}(\text{NaSO}_3)_4$ , which probably will break up during the catalytic cycle.

## 6.1 Introduction

Three polycationic promoting effects collectively are responsible for the rate enhancement in the oxidation of thiols catalyzed by  $\text{CoPc}(\text{NaSO}_3)_4$  in the presence of 2,4-ionene. The contribution of substrate enrichment in the polyelectrolyte domain has been extensively discussed in the former chapter. Moreover, in the presence of 2,4-ionene the formation of the catalytically inactive dioxygen bridged  $\mu$ -peroxo complex is strongly suppressed and simultaneously the dimeric form of the catalyst is drastically favoured over the monomeric form<sup>1</sup>. These dimers or aggregates of  $\text{CoPc}(\text{NaSO}_3)_4$  are assumed to be more active than the monomeric species, resulting in a tremendous increase in the reaction rate<sup>2</sup>.

This chapter is a further attempt to separate the different ionene promoting contributions to the observed rate enhancement. Therefore, we investigated the spectroscopic and catalytic properties of two mixtures of oppositely charged water-soluble cobalt(II) phthalocyanines, which offers us the possibility to study primarily the influence of dimerization of the catalyst in detail. In these cases, substrate enrichment due to a positively charged polymer domain does not occur. First, a combination of cobalt(II) phthalocyaninetetra(trimethylammonium)iodide ( $\text{CoPc}[\text{N}(\text{CH}_3)_3\text{I}]_4$ ) (Fig. 3.1) containing four positive charges and  $\text{CoPc}(\text{NaSO}_3)_4$  with four negative charges, was studied by visible light spectroscopy and catalytic activity measurements. Subsequently, a mixture consisting of  $\text{CoPc}[\text{N}(\text{CH}_3)_3\text{I}]_4$  and the eightfold negatively charged cobalt(II) phthalocyanineoctacarboxylic acid ( $\text{CoPc}(\text{COOH})_8$ ) (Fig. 3.1) was investigated.

In addition, the effects of introducing simple salts and two negatively charged polymers, *i.e.* poly(styrenesodiumsulfonate) (PNaSS) and poly(acrylic acid) (PAA), on the spectroscopic behaviour of  $\text{CoPc}[\text{N}(\text{CH}_3)_3\text{I}]_4$  were studied. Furthermore, we examined the effect of the addition of 2,4-ionene to the mixed phthalocyanine complexes and compared the catalytic activities with those observed for the conventional  $\text{CoPc}(\text{NaSO}_3)_4/2,4\text{-ionene}$  system. Finally, a reaction mechanism will be proposed based on the new insights.

## 6.2 Spectroscopic Properties of Mixtures of Oppositely Charged Cobalt Phthalocyanines

In order to elucidate which of the three 2,4-ionene induced promoting effects has the largest contribution, mixtures of oppositely charged water-soluble phthalocyanines can be used perfectly to study the effect of dimerization of the catalyst in the absence of ionene. As a consequence we investigated the spectroscopic behaviour of combinations of  $\text{CoPc}[\text{N}(\text{CH}_3)_3\text{I}]_4$  and  $\text{CoPc}(\text{NaSO}_3)_4$  in order to prove the existence of the dimeric form. Due to the fact that there is a lack of information about the spectral properties of  $\text{CoPc}[\text{N}(\text{CH}_3)_3\text{I}]_4$ , it was necessary to study the spectroscopic behaviour of the positively charged phthalocyanine in detail first.

Absorption spectra of  $\text{CoPc}[\text{N}(\text{CH}_3)_3\text{I}]_4$  at different pH values are depicted in Fig. 6.1. A broad absorption band in the visible light spectrum, consisting of a dimer peak at 626 nm and a monomer peak at 664 nm (Q-bands) can be observed. At high pH (*i. e.* > 12) the oxygen bridged  $\mu$ -peroxo complex at 670 nm is formed. The addition of a simple salt, in this case KCl, affects the absorption spectrum, by simultaneously suppressing  $\mu$ -peroxo complex formation and favouring the non-oxygen bridged dimeric form over the monomeric form at high ionic strengths (Fig. 6.1). Introducing simple salts to the positively charged phthalocyanine results in dimerization, which is caused by neutralization of the repulsive electrostatic forces of the peripheral quaternary ammonium groups by  $\text{Cl}^-$ , equivalent to  $\text{Na}^+$  in the case of  $\text{CoPc}(\text{NaSO}_3)_4$ <sup>3)</sup>. As in the case of  $\text{Na}^+$ , the induced aggregation of  $\text{CoPc}[\text{N}(\text{CH}_3)_3\text{I}]_4$  could be observed only at high salt concentrations.

It has been demonstrated before that positively charged polymers show a similar or an even more effective behaviour, as compared with simple salts, in enhancing aggregation of  $\text{CoPc}(\text{NaSO}_3)_4$ <sup>1)</sup> and negative porphyrins<sup>4)</sup>. Therefore, similar shielding effects should be expected in the case of addition of a negatively charged polymer, in fact a polysalt, to a  $\text{CoPc}[\text{N}(\text{CH}_3)_3\text{I}]_4$  solution. Addition of different amounts of poly(styrenesodium-sulfonate) (PNaSS) ( $\bar{M}_w = 70 \cdot 10^3 \text{ g} \cdot \text{mol}^{-1}$ ) to an aqueous  $\text{CoPc}[\text{N}(\text{CH}_3)_3\text{I}]_4$  solution has only a small effect on the visible light absorbance spectrum and a small decrease of the  $\mu$ -peroxo peak can be observed. Even at high concentrations PNaSS is not as effective

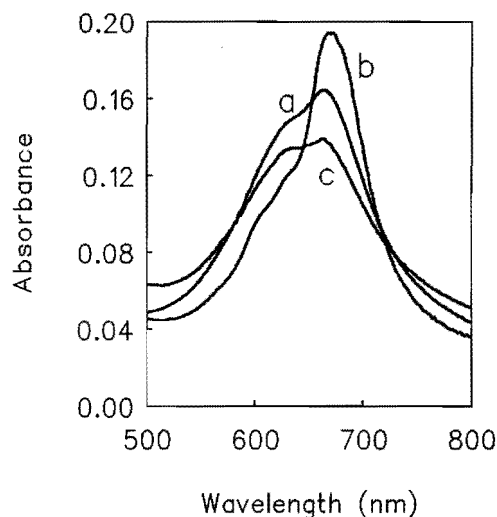


**Figure 6.1** Absorption spectra of aqueous  $\text{CoPc}[\text{N}(\text{CH}_3)_3\text{I}]_4$  solutions at different pH and effect of KCl addition.

(a)  $\text{pH} = 9$  (buffer, ionic strength  $I = 0.1 \text{ M}$ ), (b)  $\text{pH} = 13$  ( $I = 0.1 \text{ M}$ ), (c)  $M_{\text{KCl}} = 0.30 \text{ M}$  ( $\text{Cl}^-/\text{CoPc}^{4+} = 20000$ ) at  $\text{pH} = 12$  (buffer);  $[\text{CoPc}[\text{N}(\text{CH}_3)_3\text{I}]_4] = 1.5 \cdot 10^{-5} \text{ mol} \cdot \text{dm}^{-3}$ .

as simple salts in stabilizing the aggregates, probably as result of the less flexible backbone and the position of the negative charge in the bulky styrene side-groups.

In contrast poly(acrylic acid) (PAA) ( $\bar{M}_w = 500\text{-}1000 \cdot 10^3 \text{ g} \cdot \text{mol}^{-1}$ ), having a more flexible chain, induces aggregation of  $\text{CoPc}[\text{N}(\text{CH}_3)_3\text{I}]_4$  more effectively. Increasing the  $\text{COO}^-/\text{CoPc}[\text{N}(\text{CH}_3)_3\text{I}]_4$  ratio results in favouring the dimer absorbance band (626 nm) over the monomer band (664 nm). When the  $\text{COO}^-/\text{CoPc}[\text{N}(\text{CH}_3)_3\text{I}]_4$  ratio exceeds about 4, the ratio of the two absorbances remains constant (Fig. 6.2) almost similar to the 2,4-ionene/ $\text{CoPc}(\text{NaSO}_3)_4$  system<sup>1)</sup>. Further aggregation, which was observed for  $\text{CoPc}(\text{NaSO}_3)_4$  at high ionene concentrations, could not be detected in the PAA/ $\text{CoPc}[\text{N}(\text{CH}_3)_3\text{I}]_4$  system.



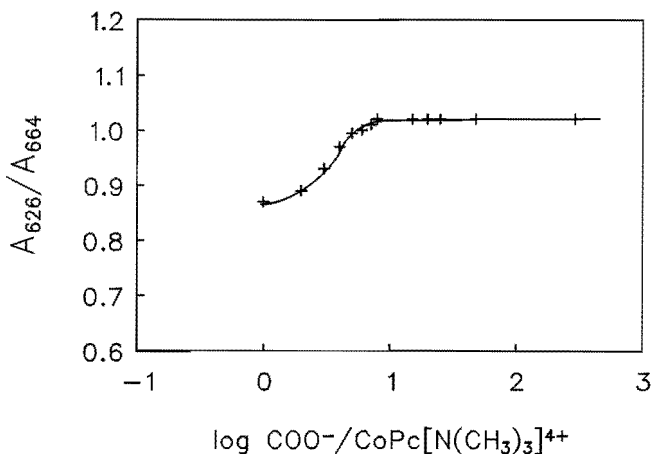
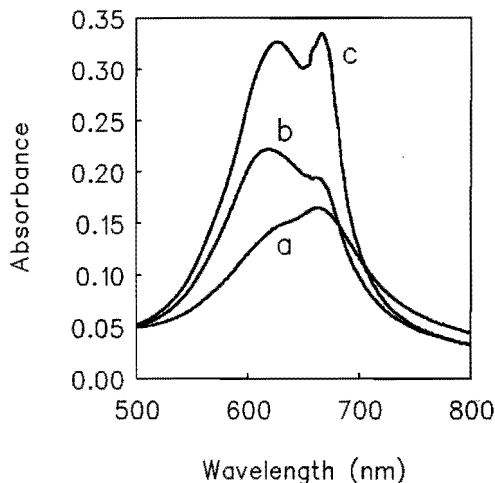


Figure 6.2 Ratio of absorbances at 626 nm and 664 nm as a function of the  $\text{COO}^-/\text{Co}$  ratio for a  $\text{CoPc}[\text{N}(\text{CH}_3)_3\text{I}]_4/\text{PAA}$  system.  $[\text{CoPc}[\text{N}(\text{CH}_3)_3\text{I}]_4] = 5 \cdot 10^{-6} \text{ mol} \cdot \text{dm}^{-3}$ ,  $\text{pH} = 12$  (buffer,  $I = 0.1 \text{ M}$ ).

It has been reported<sup>5,6)</sup> that positively charged phthalocyanines, such as copper and cobalt  $N,N',N'',N'''$ -tetramethyltetra-2,3-pyridinoporphyrazin derivatives did not aggregate in aqueous solution due to the fact that positive charges are located in the ring. After addition of salts, probably a less complete shielding of the positive charges is possible due to delocalization of the positive charge over the porphyrin ring. Obviously, in our case the positive charges of the ammonium groups of  $\text{CoPc}[\text{N}(\text{CH}_3)_3\text{I}]_4$  are not delocalized in the conjugated  $\pi$ -system and are similar to positively charged porphyrins where the positive charges were localized at a substituent pyridinium group<sup>7,8)</sup>, resulting in the formation of aggregates for both systems. Thus, upon addition of salt or PAA, the counterions can perfectly match the localized positive charges of  $\text{CoPc}[\text{N}(\text{CH}_3)_3\text{I}]_4$ .

Combinations of oppositely charged phthalocyanines should give us the opportunity to study their aggregation behaviour in the absence of polymers. Looking at the visible light spectroscopy results of mixtures of  $\text{CoPc}(\text{NaSO}_3)_4$  and  $\text{CoPc}[\text{N}(\text{CH}_3)_3\text{I}]_4$ , keeping the total amount of phthalocyanine constant, it can be seen that upon raising the  $\text{CoPc}(\text{NaSO}_3)_4$  concentration the dimer/monomer ratio increases (Fig. 6.3). Obviously, hetero-dimeric complexes of  $\text{CoPc}[\text{N}(\text{CH}_3)_3\text{I}]_4$  and  $\text{CoPc}(\text{NaSO}_3)_4$  are formed, which remain stable even



**Figure 6.3.** Absorption spectra of mixtures of  $\text{CoPc}[\text{N}(\text{CH}_3)_3\text{I}]_4$  and  $\text{CoPc}(\text{NaSO}_3)_4$ , keeping the total CoPc concentration constant at  $1.5 \cdot 10^{-5} \text{ M}$  and  $\text{pH} = 9$  (buffer,  $I = 0.1 \text{ M}$ ).  
 $\text{CoPc}(\text{NaSO}_3)_4 / \text{CoPc}[\text{N}(\text{CH}_3)_3\text{I}]_4 = 0$  (a); 0.5 (b); 1 (c).

after increasing the pH to 13, *i.e.* no formation of  $\mu$ -peroxo complexes could be observed. In contrast to  $\text{CoPc}(\text{NaSO}_3)_4$  dimers, the so-called homo-dimers, in the hetero-dimers the opposite charges of the phthalocyanines are additive to the Van der Waals attraction resulting in considerable stabilization. Neither precipitation was observed, so the hetero-dimeric complexes remain water-soluble.

Aggregation phenomena are also detectable in the case of mixtures of  $\text{CoPc}[\text{N}(\text{CH}_3)_3\text{I}]_4$  and the eightfold negatively charged  $\text{CoPc}(\text{COOH})_8$  (Fig. 6.4). Responsible for the high absorbance at 682 nm is not  $\mu$ -peroxo complex formation of  $\text{CoPc}(\text{COOH})_8$ , but the presence of monomeric species, because  $\text{CoPc}(\text{COOH})_8$  is unable to form  $\mu$ -peroxo complexes<sup>9</sup>. In Fig. 6.4 is shown that upon decreasing the  $\text{CoPc}[\text{N}(\text{CH}_3)_3\text{I}]_4$  concentration the dimer/monomer ratio increases. The spectra of several mixtures of  $\text{CoPc}[\text{N}(\text{CH}_3)_3\text{I}]_4$  and  $\text{CoPc}(\text{COOH})_8$  clearly indicate that aggregation of the two phthalocyanines occurs.

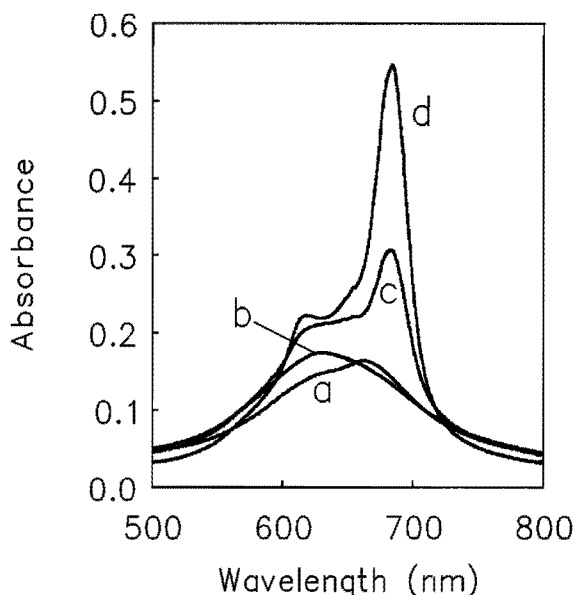
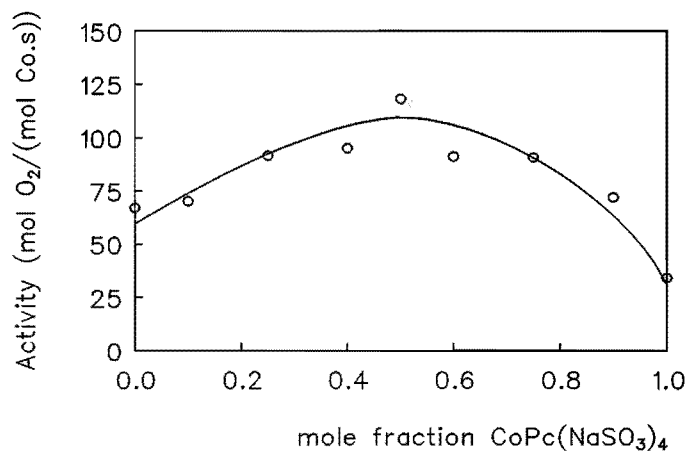


Figure 6.4 Absorption spectra of mixtures of  $\text{CoPc}[\text{N}(\text{CH}_3)_3\text{I}]_4$  and  $\text{CoPc}(\text{COOH})_8$ , keeping the total CoPc concentration constant at  $1.5 \cdot 10^{-5} \text{ M}$  and  $\text{pH} = 9$  (buffer,  $I = 0.1 \text{ M}$ ).  $\text{CoPc}(\text{COOH})_8 / \text{CoPc}[\text{N}(\text{CH}_3)_3\text{I}]_4 = 0$  (a); 0.2 (b); 0.5 (c); 1 (d).

### 6.3 Catalytic Properties of Different Mixtures of Cobalt Phthalocyanines with and without Polymers

In order to determine the effects of dimeric cobalt phthalocyanine complexes on the catalytic activity we varied the concentration ratios of the two phthalocyanine combinations. In Fig. 6.5 the mercaptoethanol oxidation rates of  $\text{CoPc}[\text{N}(\text{CH}_3)_3\text{I}]_4 / \text{CoPc}(\text{NaSO}_3)_4$  mixtures are depicted as a function of the mole fraction of  $\text{CoPc}(\text{NaSO}_3)_4$ , keeping the total amount of cobalt phthalocyanine constant. It clearly shows that at a  $\text{CoPc}[\text{N}(\text{CH}_3)_3\text{I}]_4 / \text{CoPc}(\text{NaSO}_3)_4$  ratio of 1 the highest reaction rate is reached, which is about three times higher than the activity measured for the same amount  $\text{CoPc}(\text{NaSO}_3)_4$ . At this ratio the opposite charges of  $\text{CoPc}[\text{N}(\text{CH}_3)_3\text{I}]_4$  are just matching the negative charges of  $\text{CoPc}(\text{NaSO}_3)_4$ , thus it may be concluded that dimeric complexes are responsible for the higher catalytic activity.



**Figure 6.5** The catalytic ME oxidation rate as function of the mole fraction of  $\text{CoPc}(\text{NaSO}_3)_4$  in  $\text{CoPc}[\text{N}(\text{CH}_3)_3\text{I}]_4/\text{CoPc}(\text{NaSO}_3)_4$  mixtures.  $[\text{CoPc}]_{\text{total}} = 4 \cdot 10^{-7} \text{ M}$ ,  $\text{pH} = 9$ ,  $[\text{ME}] = 7.1 \cdot 10^{-2} \text{ M}$ .

Moreover, it can be seen that the reaction rate of  $\text{CoPc}(\text{NaSO}_3)_4$  is lower as compared with  $\text{CoPc}[\text{N}(\text{CH}_3)_3\text{I}]_4$ , which is a result of electrostatic repulsion between the thiolate anion and the negative charges of  $\text{CoPc}(\text{NaSO}_3)_4$ . In order to compare the activity of the dimeric catalyst species with the activity of a  $\text{CoPc}(\text{NaSO}_3)_4$  monomer, one has to realize that a polymer-free  $\text{CoPc}(\text{NaSO}_3)_4$  system in fact can consist of monomers, dimers and  $\mu$ -peroxo complexes. However, Wöhrle *et al.*<sup>10</sup> showed that the activity of an aqueous  $\text{CoPc}(\text{NaSO}_3)_4$  solution exhibits a similar activity as cobalt phthalocyanine monomers covalently bonded to a silica surface. Therefore, it is a good model for a  $\text{CoPc}(\text{NaSO}_3)_4$  monomer in the catalytic system. Apparently, in an ionene-free  $\text{CoPc}(\text{NaSO}_3)_4$  solution the presence of the catalytically inactive  $\mu$ -peroxo complexes is compensated by the active dimeric cobalt species. Thus, the higher activity of the hetero-dimer compared with that of a  $\text{CoPc}(\text{NaSO}_3)_4$  monomer is presumably caused by suppression of the inactive  $\mu$ -peroxo complex.

In Fig. 6.6 the dependence of the mercaptoethanol oxidation rate on the concentration of mixtures of  $\text{CoPc}[\text{N}(\text{CH}_3)_3\text{I}]_4$  and  $\text{CoPc}(\text{COOH})_8$  is depicted. The results show the appearance of stoichiometric complexation of the  $\text{CoPc}[\text{N}(\text{CH}_3)_3\text{I}]_4/\text{CoPc}(\text{COOH})_8$  complex at a ratio of 2, where the highest activities are observed. At this point the eight

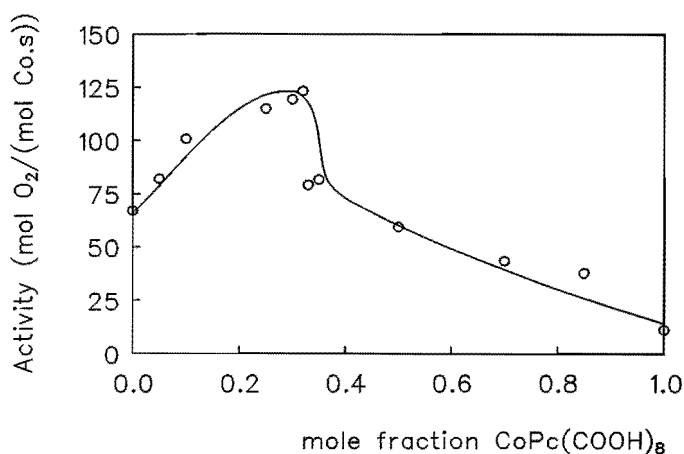


Figure 6.6 The catalytic ME oxidation rate as function of the mole fraction of  $\text{CoPc}(\text{COOH})_8$  in  $\text{CoPc}[\text{N}(\text{CH}_3)_3\text{I}]_4/\text{CoPc}(\text{COOH})_8$  mixtures.  $[\text{CoPc}]_{\text{total}} = 4 \cdot 10^{-7} \text{ M}$ ,  $\text{pH} = 9$ ,  $[\text{ME}] = 7.1 \cdot 10^{-2} \text{ M}$ .

negative charges of  $\text{CoPc}(\text{COOH})_8$  are matched by the eight positive charges of two  $\text{CoPc}[\text{N}(\text{CH}_3)_3\text{I}]_4$  molecules. Obviously, trimeric complexes are responsible for this rate enhancement. The higher oxidation rate of  $\text{CoPc}(\text{NaSO}_3)_4$  as compared with  $\text{CoPc}(\text{COOH})_8$  can be explained by the higher electrostatic repulsion between the phthalocyanine and the thiolate anion in the latter system.

The influence of substrate enrichment was investigated by studying the effects of polyelectrolytes on the activity of mixtures containing the different cobalt(II) phthalocyanines. First, the effects of introducing PNaSS and PAA on the oxidation rate of  $\text{CoPc}[\text{N}(\text{CH}_3)_3\text{I}]_4$  were studied. As presented in Tab. 6.1, it is demonstrated that after addition of PNaSS, the catalytic activity decreases as a result of the electrostatic repulsion between the negatively charged polymer domain and the thiolate anions. By contrast, the reaction rate for the  $\text{CoPc}[\text{N}(\text{CH}_3)_3\text{I}]_4/\text{PAA}$  system (Tab. 6.1) remains constant or even a small increase can be observed, due to two complementary effects. The reaction rate is again reduced by the above mentioned substrate repulsion, but this effect is compensated by the formation of the catalytically more active  $\text{CoPc}[\text{N}(\text{CH}_3)_3\text{I}]_4$  dimers on the flexible PAA.

Table 6.1 Dependence of ME oxidation rate for several PNaSS/CoPc[N(CH<sub>3</sub>)<sub>3</sub>I]<sub>4</sub> and PAA/CoPc[N(CH<sub>3</sub>)<sub>3</sub>I]<sub>4</sub> solutions

X/CoPc[N(CH <sub>3</sub> ) <sub>3</sub> I] <sub>4</sub>	activity (mol O <sub>2</sub> /(mol CoPc[N(CH <sub>3</sub> ) <sub>3</sub> I] <sub>4</sub> · s))	
	X = SO <sub>3</sub> <sup>-</sup>	X = COO <sup>-</sup>
0	67	67
3	47	73
5	42	70
10	40	82
150	35	86
1000	37	95

$$[\text{CoPc}[\text{N}(\text{CH}_3)_3\text{I}]_4] = 4 \cdot 10^{-7} \text{ M}, \text{ pH} = 9, [\text{ME}] = 7.1 \cdot 10^{-2} \text{ M}.$$

Likewise, we investigated the influence of the addition of ionene to a reaction mixture containing oppositely charged phthalocyanines. Primarily, we studied the effect of addition of 2,4-ionene to an equimolar solution of CoPc[N(CH<sub>3</sub>)<sub>3</sub>I]<sub>4</sub> and CoPc(NaSO<sub>3</sub>)<sub>4</sub>. After varying the procedure of addition, we were able to conclude that the binding between CoPc[N(CH<sub>3</sub>)<sub>3</sub>I]<sub>4</sub> and CoPc(NaSO<sub>3</sub>)<sub>4</sub> is stronger than between CoPc(NaSO<sub>3</sub>)<sub>4</sub> and 2,4-ionene, because similar activities were observed irrespective of the order of addition of the three compounds. In Tab. 6.2 the activities are presented for CoPc[N(CH<sub>3</sub>)<sub>3</sub>I]<sub>4</sub>/CoPc(NaSO<sub>3</sub>)<sub>4</sub> mixtures with and without 2,4-ionene. Keeping the total cobalt phthalocyanine concentration constant, one sees that addition of 2,4-ionene raises the absolute activity of the dimeric CoPc[N(CH<sub>3</sub>)<sub>3</sub>I]<sub>4</sub>/CoPc(NaSO<sub>3</sub>)<sub>4</sub> complex, but the reaction rates were much lower as compared with the conventional CoPc(NaSO<sub>3</sub>)<sub>4</sub>/2,4-ionene system. This difference in catalytic activities will be discussed later.

Addition of 2,4-ionene to several CoPc[N(CH<sub>3</sub>)<sub>3</sub>I]<sub>4</sub>/CoPc(COOH)<sub>8</sub> mixtures leads to a rate enhancement for all three investigated systems (Tab. 6.3) as compared with the ionene-free system. A similar rate increase by a factor of 2 can be noticed for both the CoPc(COOH)<sub>8</sub> and the dimeric CoPc[N(CH<sub>3</sub>)<sub>3</sub>I]<sub>4</sub>/CoPc(COOH)<sub>8</sub> complex. As reported in the previous chapter, this rate increase for a CoPc(COOH)<sub>8</sub>/2,4-ionene system as compared with the polymer-free system, is only caused by substrate enrichment. From

Table 6.2 Effect of 2,4-ionene on the catalytic ME oxidation rate of different mixtures of  $\text{CoPc}[\text{N}(\text{CH}_3)_3\text{I}]_4$  and  $\text{CoPc}(\text{NaSO}_3)_4$

mole fraction $\text{CoPc}(\text{NaSO}_3)_4$	mole fraction $\text{CoPc}[\text{N}(\text{CH}_3)_3\text{I}]_4$	activity (mol $\text{O}_2$ /(mol $\text{CoPc} \cdot \text{s}$ ))	+ 2,4-ionene activity (mol $\text{O}_2$ /(mol $\text{CoPc} \cdot \text{s}$ ))
1	0	34	1100
0.5	0.5	118	314
0	1	67	65

$[\text{CoPc}]_{\text{total}} = 4 \cdot 10^{-7} \text{ M}$ ,  $\text{pH} = 9$ ,  $[\text{ME}] = 7.1 \cdot 10^{-2} \text{ M}$ ,  $\text{N}^+/\text{Co} = 50$ ,  
 $\bar{M}_n(2,4\text{-ionene}) = 22 \cdot 10^3 \text{ g} \cdot \text{mol}^{-1}$ .

Table 6.3 Effect of 2,4-ionene on the catalytic ME oxidation rate of different mixtures of  $\text{CoPc}[\text{N}(\text{CH}_3)_3\text{I}]_4$  and  $\text{CoPc}(\text{COOH})_8$

mole fraction $\text{CoPc}(\text{COOH})_8$	mole fraction $\text{CoPc}[\text{N}(\text{CH}_3)_3\text{I}]_4$	activity (mol $\text{O}_2$ /(mol $\text{CoPc} \cdot \text{s}$ ))	+ 2,4-ionene activity (mol $\text{O}_2$ /(mol $\text{CoPc} \cdot \text{s}$ ))
1	0	10	25
0.5	0.5	56	109
0.33	0.67	121	165

$[\text{CoPc}]_{\text{total}} = 4 \cdot 10^{-7} \text{ M}$ ,  $\text{pH} = 9$ ,  $[\text{ME}] = 7.1 \cdot 10^{-2} \text{ M}$ ,  $\text{N}^+/\text{Co} = 50$ ,  
 $\bar{M}_n(2,4\text{-ionene}) = 22 \cdot 10^3 \text{ g} \cdot \text{mol}^{-1}$ .

the fact that a similar rate enhancement is observed for both the ionene containing dimeric  $\text{CoPc}[\text{N}(\text{CH}_3)_3\text{I}]_4/\text{CoPc}(\text{COOH})_8$  complex as well as the dimeric  $\text{CoPc}[\text{N}(\text{CH}_3)_3\text{I}]_4/\text{CoPc}(\text{NaSO}_3)_4$  complex in the presence of ionene, we are able to conclude that both dimeric complexes are fully contained within the polyelectrolyte domain, and addition of 2,4-ionene only results in substrate enrichment.

Only for the trimeric  $\text{CoPc}[\text{N}(\text{CH}_3)_3\text{I}]_4/\text{CoPc}(\text{COOH})_8$  complex a lower rate increase is observed in the presence of 2,4-ionene. The reason for this difference in relative rate enhancement, is the difference in electrostatic interactions with the positively charged

polymer domain. Presumably, in the case of trimeric complexes all negative charges are shielded by the positively charged phthalocyanines, which leads to a situation in which it is very likely that a large part of the trimeric species is not present in the polycation domain. In the case of the dimeric  $\text{CoPc}[\text{N}(\text{CH}_3)_3\text{I}]_4/\text{CoPc}(\text{NaSO}_3)_4$  complex there is also a shielding of the negative charges, but since there is only one positively charged phthalocyanine molecule involved in this shielding, one side of the negatively charged phthalocyanine will be accessible to electrostatic interaction with the positive polymer.

## 6.4 Discussion

The enhanced catalytic activity of the dimeric  $\text{CoPc}[\text{N}(\text{CH}_3)_3\text{I}]_4/\text{CoPc}(\text{NaSO}_3)_4$  complex as compared with the activity of a monomeric  $\text{CoPc}(\text{NaSO}_3)_4$  species by only a factor of 3, would imply an overestimation of the importance of the polymer-induced dimerization, which so far has been assumed to be responsible for the largest promoting contribution in a  $\text{CoPc}(\text{NaSO}_3)_4/2,4\text{-ionene}$  system<sup>2)</sup>.

It is only justified to compare the activity of a dimeric  $\text{CoPc}[\text{N}(\text{CH}_3)_3\text{I}]_4/\text{CoPc}(\text{NaSO}_3)_4$  complex with a  $\text{CoPc}(\text{NaSO}_3)_4$  dimer if the electronic structure of both dimeric species is identical. First, the interaction between two phthalocyanines molecules can be ascribed merely to Van der Waals interactions<sup>11-14)</sup>. Secondly, the peripheral groups have no significant influence on the electron distribution within the porphyrin ligand<sup>15)</sup>. Only a slight difference in molecular orbitals might occur if the inter-ring distance between the phthalocyanines in the hetero-dimer is shorter than in the homo-dimer, due to the extra electrostatic interaction. In Chapter 11 it will be demonstrated that the charge distribution of a cobalt phthalocyanine complex has no significant effect on the final geometry of a dimeric phthalocyanine species. Based on these grounds it is reasonable to assume that the catalytic activities of both dimeric species are comparable.

The question remains why the 2,4-ionene containing  $\text{CoPc}(\text{NaSO}_3)_4/\text{CoPc}[\text{N}(\text{CH}_3)_3\text{I}]_4$  system is less active than the conventional  $\text{CoPc}(\text{NaSO}_3)_4/2,4\text{-ionene}$  system. The contribution of the three polycation promoting effects appeared to be dependent of the polymer/catalyst ratio<sup>2)</sup>. If we look in more detail at the catalytic activity as a function of the 2,4-ionene/ $\text{CoPc}(\text{NaSO}_3)_4$  ratio, expressed as the  $\text{N}^+/\text{Co}$  ratio, the activity increases



at higher ionene concentrations (Fig. 4.6). At a  $N^+/Co$  ratio of 4 higher activities, as compared with the polymer-free system, are achieved due to suppression of the  $\mu$ -peroxo complex<sup>1</sup>. From that point on the rate increases, which is ascribed to substrate enrichment and aggregation of the catalyst<sup>2</sup>, eventually leading to an optimal  $N^+/Co$  ratio of 50 for polymeric 2,4-ionene<sup>16</sup>. So far, it was thought that this value of the optimal  $N^+/Co$  ratio was determined mainly to enhanced aggregation of the catalyst, *i.e.* higher aggregates of dimeric  $CoPc(NaSO_3)_4$  species<sup>1,2</sup>. However, in the previous two chapters it was concluded that this optimal  $N^+/Co$  ratio is predominantly determined by substrate enrichment and not by enhanced aggregation of the catalyst. Therefore, the difference in catalytic activities between homo-dimers and hetero-dimers in the presence of ionene can not be ascribed solely to the formation of higher  $CoPc(NaSO_3)_4$ -aggregates.

An acceptable explanation can be found in the fact that there is a difference between the intrinsic catalytic activities of a dimeric  $CoPc[N(CH_3)_3I]_4/CoPc(NaSO_3)_4$  species and a dimeric  $CoPc(NaSO_3)_4$  species. It is known for clamshell binuclear phthalocyanine complexes that these exhibit better redox properties as compared with monomeric species<sup>17,18</sup>. The same authors also suggested that in these covalently bonded binuclear phthalocyanine systems with a flexible linkage between the phthalocyanine rings which normally show cofacial dimerization, addition of a coordinating species, followed by reduction or oxidation, leads to a decrease in the coupling effects. These observations were explained by a possible dissociation of the dimeric species<sup>19-23</sup>.

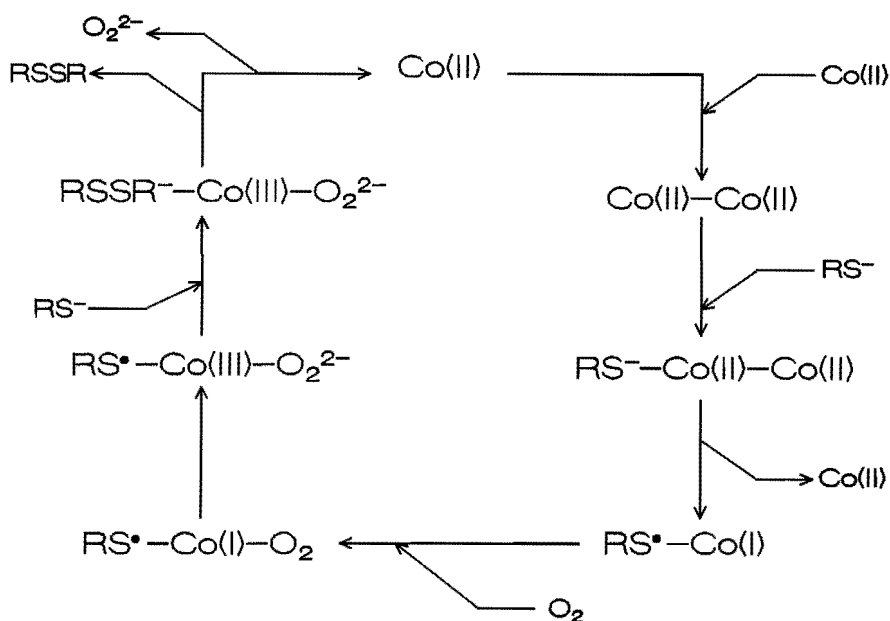
Additionally, Pasternack observed a similar break-up of homo-dimeric porphyrins after ligation<sup>24</sup>. The ligation step to the porphyrin dimer appeared faster than the break-up into a monomer and a ligated monomer. After breaking up, a very fast consecutive ligation of both the monomer and ligated monomer occurred.

Considering these data, we suggest in our case that the 2,4-ionene induced formation of dimers of  $CoPc(NaSO_3)_4$  improves the first step of addition of the thiolate anion, followed by oxidation of the thiolate and simultaneous reduction of  $Co(II)$  to  $Co(I)$ . This step is followed by break-up of the dimeric species, which also provides two extra catalytic sites. All effects result in a higher catalytic activity of a  $CoPc(NaSO_3)_4$  dimer as compared with a  $CoPc(NaSO_3)_4$  monomer. In the case of the  $CoPc[N(CH_3)_3I]_4/CoPc(NaSO_3)_4$  dimers it is very unlikely that these dimers will break up after the first reaction step due to the

strong electrostatic interaction, as was demonstrated by the catalytic experiments in which the procedure of the addition was varied. However, attempts failed<sup>2)</sup> to derive evidence about the existence of a Co(I)-RS\* species formed after break-up of CoPc(NaSO<sub>3</sub>)<sub>4</sub> dimers. On the other hand, it has not been established yet whether the dimeric species persists during the catalytic cycle. It has been demonstrated that aggregation is only little affected by addition of a second coordinating species: only at high thiolate anion concentrations the dimer will dissociate<sup>2)</sup>.

Other arguments supporting the mechanism of break-up of CoPc(NaSO<sub>3</sub>)<sub>4</sub> dimers after ligation can be based on earlier described experiments for a CoPc(NaSO<sub>3</sub>)<sub>4</sub> system with poly(vinylamine) (PVAm) as polymeric promoter<sup>25-27)</sup>. UV-VIS spectroscopy showed that the amount of dimers decreased upon raising the PVAm concentration, while enhanced catalytic activities were found. This effect is probably the result of the fact that a monomeric CoPc(NaSO<sub>3</sub>)<sub>4</sub> molecule is capable of interacting electrostatically with the quaternary ammonium groups as well as of coordinating with a nitrogen atom from PVAm. Such a situation is very similar to the supposed structure of a CoPc(NaSO<sub>3</sub>)<sub>4</sub> dimer, where a nitrogen atom from one CoPc(NaSO<sub>3</sub>)<sub>4</sub> molecule is axially positioned above the metal centre of the other phthalocyanine ring. Probably, a coordinative interaction of the CoPc(NaSO<sub>3</sub>)<sub>4</sub> molecule with the NH<sub>2</sub> group of PVAm has a similar effect on the thiol ligation as compared with a dimeric CoPc(NaSO<sub>3</sub>)<sub>4</sub> species.

Resuming, an adaptation of the reaction mechanism for a CoPc(NaSO<sub>3</sub>)<sub>4</sub>/2,4-ionene system, based on the reductive cycle of Zwart<sup>28)</sup> and further developed by van Herk *et al.*<sup>29)</sup>, is presented in Scheme 6.1. The catalyst is predominantly present in its dimeric form and leads to a faster ligation of thiolate anions, the subsequent reduction of Co(II) to Co(I), and the simultaneous oxidation of the thiolate anion to a thiol radical. After this step, the dimer breaks up and ligation of molecular oxygen occurs. Oxygen is reduced to peroxide by the oxidation of Co(I) to Co(III). Ligation of a second thiolate anion, followed by reduction of Co(III) leads to a release of the axially bonded reaction products. The free cobalt(II) phthalocyanine will now form a new dimer with a second phthalocyanine.



*Scheme 6.1* Reaction mechanism of the homogeneous  $\text{CoPc}(\text{NaSO}_3)_4/2,4\text{-ionene}$  catalyzed thiol oxidation.

*Co* denotes the  $\text{CoPc}(\text{NaSO}_3)_4$  complex.

## 6.5 Conclusions

The visible light spectroscopy experiments clearly showed interaction between oppositely charged phthalocyanines, resulting in aggregated species for both the  $\text{CoPc}[\text{N}(\text{CH}_3)_3\text{I}]_4/\text{CoPc}(\text{NaSO}_3)_4$  combination as well as  $\text{CoPc}[\text{N}(\text{CH}_3)_3\text{I}]_4/\text{CoPc}(\text{COOH})_8$  mixtures. Stoichiometric dimeric and trimeric catalyst complexes exhibited the highest catalytic activities measured so far for any phthalocyanine-catalyzed mercaptoethanol autoxidation in the absence of polycations. The addition of 2,4-ionene to these complexes leads to a further reaction rate increase, solely due to substrate enrichment of thiolate anions near the active sites. The difference in catalytic activity between a 2,4-ionene containing  $\text{CoPc}[\text{N}(\text{CH}_3)_3\text{I}]_4/\text{CoPc}(\text{NaSO}_3)_4$  system and the conventional  $\text{CoPc}(\text{NaSO}_3)_4/2,4\text{-ionene}$  system can probably be ascribed to a faster ligation of thiolate anions and the subsequent break-up of the homo-dimeric species.

## References

1. J. van Welzen, A.M. van Herk, A.L. German, *Makromol. Chem.*, **188** (1987) 1923.
2. J. van Welzen, A.M. van Herk, A.L. German, *Makromol. Chem.*, **190** (1989) 2477.
3. L.C. Gruen, R.J. Blagrove, *Aust. J. Chem.*, **26** (1973) 319.
4. G.S. Nahor, J. Rabani, *Macromolecules*, **22** (1989) 2516.
5. D. Wöhrle, J. Gitzel, I. Okuro, S. Aono, *J. Chem. Soc. Perkin Trans. II*, (1985) 1171.
6. T.D. Smith, H. Livorness, H. Taylor, J.R. Pilbrow, G.R. Sinclair, *J. Chem. Soc. Dalton Trans.*, (1983) 1391.
7. K. Kano, M. Takei, S. Hashimoto, *J. Phys. Chem.*, **94** (1990) 2181.
8. K. Kalyanasundaram, *J. Chem. Soc. Faraday Trans. II*, **79** (1983) 1365.
9. Chapter 5 of this thesis.
10. T. Buck, D. Wöhrle, G. Schulz-Ekloff, A. Andreev, *J. Mol. Catal.*, **70** (1991) 259.
11. K. Kano, M. Takei, S. Hashimoto, *J. Phys. Chem.*, **94** (1990) 2181.
12. K. Kano, T. Hayakawa, S. Hashimoto, *Bull. Chem. Soc. Jpn.*, **62** (1991) 778.
13. U. Hofstra, R.B.M. Koehorst, T.J. Schaafsma, *Chem. Phys. Lett.*, **130** (1986) 555.
14. Chapter 11 of this thesis.
15. K.M. Kadish, B.G. Maiya, C. Araullo-Adams, *J. Phys. Chem.*, **95** (1991) 427.
16. Chapter 4 of this thesis.
17. W.A. Nevin, W. Liu, S. Greenberg, M.R. Hempstead, S.M. Marcuccio, M. Melnik, C.C. Leznoff, A.B.P. Lever, *Inorg. Chem.*, **26** (1987) 891.
18. C.C. Leznoff, H. Lam, W.A. Nevin, N. Kobayashi, P. Janda, A.B.P. Lever, *Angew. Chem. Int. Ed., Engl.*, **26** (1987) 1021.
19. E.S. Dodsworth, A.B.P. Lever, P. Seymour, C.C. Leznoff, *J. Phys. Chem.*, **89** (1985) 5698.
20. A.B.P. Lever, M.R. Hempstead, C.C. Leznoff, W. Liu, M. Melnik, W.A. Nevin, P. Seymour, *Pure Appl. Chem.*, **58** (1986) 1467.
21. W. Liu, M.R. Hempstead, W.A. Nevin, M. Melnik, A.B.P. Lever, C.C. Leznoff, *J. Chem. Soc., Dalton Trans.*, (1987) 2511.
22. N. Kobayashi, H. Lam, W.A. Nevin, P. Janda, C.C. Leznoff, A.B.P. Lever, *Inorg. Chem.*, **29** (1990) 3415.
23. T.H. Tran-Thi, J.F. Lipskier, P. Maillard, M. Momenteau, J.-M. Lopez-Castillo, J.-P. Jay-Gerin, *J. Phys. Chem.*, **96** (1992) 1073.
24. R.F. Pasternack, G.R. Parr, *Inorg. Chem.*, **15** (1976) 3087.
25. J.H. Schutten, P. Piet, A.L. German, *Makromol. Chem.*, **180** (1979) 2341.

26. W.M. Brouwer, P. Piet, A.L. German, *Makromol. Chem.*, **185** (1984) 363.
27. W.M. Brouwer, P. Piet, A.L. German, *J. Mol. Catal.*, **31** (1985) 169.
28. J. Zwart, Ph.D. Thesis, Eindhoven University of Technology, Eindhoven, 1978.
29. A.M. van Herk, K.H. van Streun, J. van Welzen, A.L. German, *Br. Polym. J.*, **21** (1989) 125.

## Chapter 7

# Synthesis of Amphiphilic Polystyrene-Ionene Diblock Copolymers with Controlled Block Lengths

**SUMMARY:** Amphiphilic polystyrene-ionene diblock copolymers with blocks of controlled molecular weights were synthesized by a novel method. The preparation started with the anionic polymerization of styrene using 3-(dimethylamino)propyl-lithium as initiator, which yielded tertiary amino end-functionalized polystyrenes of molecular weights, which could be varied over a wide range (from 1 to 100 kg/mol), and of relatively low polydispersities ( $\overline{M}_w/\overline{M}_n = 1.1 - 1.4$ ). The crucial step in this method was the stepwise coupling of the reactive end-group of the polystyrene with bromo and tertiary amino terminated monodisperse oligomeric 2,4-ionenes, resulting in a monodisperse 2,4-ionene block. The amphiphilic polymers with well-defined block lengths were characterized by thin-layer chromatography, infrared spectroscopy, end-group titration and elemental analysis. Amphiphilic block copolymers with a monodisperse ionene block consisting of up to 10 quaternary ammonium groups, could be obtained.

### 7.1 Introduction

A growing interest exists in the synthesis of tailor-made well-defined ionic block copolymers, because they offer a wide variety of practical and potential applications<sup>1</sup>. Modified copolymers, containing quaternary ammonium groups or ionene block segments, exhibit unique properties. For example, incorporating quaternary ammonium groups in elastomeric materials often results in thermoplastic behaviour<sup>2</sup>. Also, elastomeric ionenes

of the polyurethane type<sup>3,4)</sup> and block copolymer ionenes with polytetrahydrofuran sequences<sup>5,6)</sup> have been reported. Furthermore, to obtain conducting elastomers Ikeno *et al.*<sup>7)</sup> synthesized ionene polymers containing poly(tetramethylene oxide) chain units, which, after addition of a doped salt to the ionene, exhibited electrical properties.

Apart from improvement of mechanical or electrical properties, we are interested in using these ionic block copolymers to study polymeric effects on catalytic reactions, especially when they contain a hydrophilic poly(quaternary ammonium) part, a so-called ionene, because of their promoting effect on the thiol oxidation. It has been shown before that with hydrophilic ionenes, high catalytic activities were achieved in the CoPc(NaSO<sub>3</sub>)<sub>4</sub>-catalyzed oxidation of mercaptoethanol<sup>8)</sup>, as well as of the water-insoluble, hydrophobic 1-dodecanethiol<sup>9)</sup>. In the latter system further enhancement of the catalytic reactivity can be achieved by coupling a hydrophobic moiety to the ionene chain. Oleyl-3,3-ionene, an ionene end-capped with a hydrophobic alkyl chain, exhibited almost a two-fold higher activity as compared with the hydrophilic 2,4-ionene<sup>9)</sup>. This effect was ascribed to the occurrence of hydrophobic interactions between the polymer and the hydrophobic thiol. In order to improve such polymer-substrate interactions and, thus, to increase the catalytic activity, block copolymers consisting of a hydrophobic and an ionene part should be preferred. Furthermore, these block copolymers can be perfectly utilized as an emulsifier during emulsion polymerization to obtain latices with ionene chains at their surface. After immobilizing the catalytic species these reactive latices can be applied as heterogeneous catalyst in the thiol oxidation. The present chapter deals with the synthesis of well-defined block copolymers, which is a prerequisite for the optimization of the dodecanethiol oxidation reactions and for the heterogenization of the catalytic system.

The general method that is mostly employed for the preparation of ionic block copolymers, is a sequential polymerization of different monomers, added successively. An alternative method to synthesize ionic block copolymers is by end-to-end linkage of preformed homopolymers, which has been used before to obtain ionene-*b*-poly(oxyethylene)-*b*-ionene and ionene-*b*-poly(oxytetramethylene)-*b*-ionene<sup>5,6)</sup>. These triblock polymers were prepared by quaternization of the amine end-group of the ionene with poly(oxyethylene) or poly(oxytetramethylene) having a reactive (brominated) end-group. In this chapter we will introduce a promising route for the synthesis of a new amphiphilic diblock copolymer by coupling polystyrene and ionene, both having reactive end-groups.

Due to the completely different mechanisms of ionene and polystyrene polymerization, the only route to such a polystyrene-ionene diblock copolymer is by reactive end-coupling.

Different techniques can be used to prepare monofunctionalized polystyrene. One of the routes best suited for synthesizing monofunctionalized polystyrene with an amine end-group is living anionic polymerization, especially when the amine group can be introduced by a functional initiator. By introducing the amine group in the initiation step, incomplete functionalization will be circumvented. This approach was first followed and further developed by Eisenbach and co-workers<sup>10,11</sup>, who synthesized a tertiary amino functionalized polymer, utilizing 3-(dimethylamino)propyllithium (DMAP-Li) as initiator. More recently, Stewart *et al.*<sup>12</sup> improved this concept and obtained polybutadiene with tertiary amino end-groups. In addition, DMAP-Li has also been applied to prepare tertiary amino terminated polyisoprene<sup>13</sup> and polystyrene<sup>14,15</sup>.

The complete synthesis of ionic diblock copolymers consisting of polystyrene and ionene by anionic polymerization is not possible, since ionene can only be prepared by step reaction polymerization. Therefore, other techniques have to be applied. Earlier attempts to prepare these types of block copolymers have been made by Van Streun<sup>16</sup>, who synthesized low molecular weight polystyrene by anionic polymerization, followed by termination with 1,4-dibromobutane. After purification, the product was reacted with aminated 2,4-ionenes in various solvent combinations and at various temperatures. One of the major problems encountered was the insolubility of the hydrophobic polystyrene in polar solvents, and the vice versa of 2,4-ionene in apolar solvents.

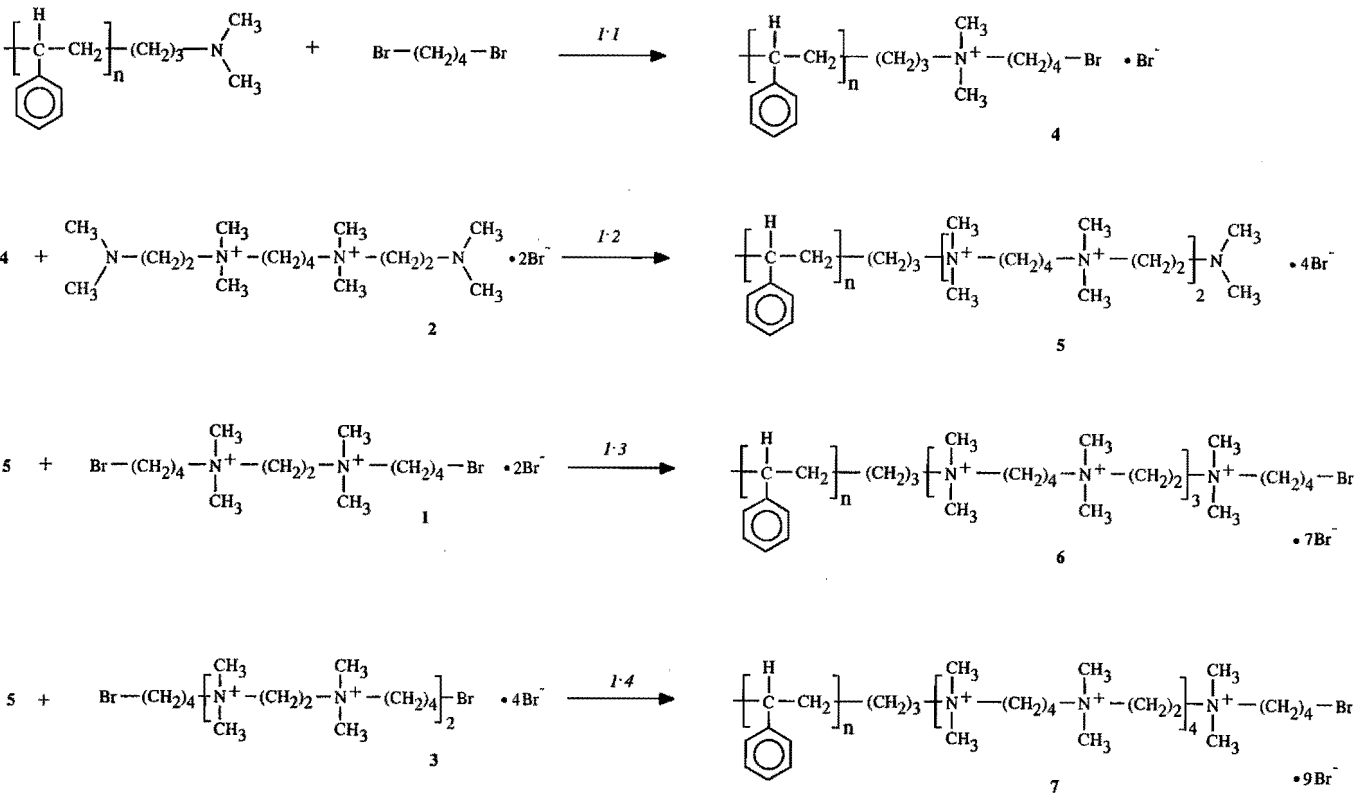
Another approach followed by Van Streun<sup>16</sup> was the polymerization of DMAP-Cl (a monomer for 3,3-ionene) in the presence of functionalized polystyrene under different experimental conditions. No coupling between DMAP-Cl and the polystyrene could be detected, due to the high homopolymerization rate of DMAP-Cl, as compared with the low reactivity of the polystyrene end-group. Since none of the outlined routes above turned out to be successful, a new strategy had to be developed.

Our idea was that if a monomer or an oligomeric ionene is soluble in the same solvent as the polystyrene, good solubilities of both reactants and, thus, high concentrations of



reactive end-groups would be achieved. In the applied step-growth process, each extension of the polymer chain with a neutral monomer molecule or a charged oligomer of 2,4-ionene occurs via a quaternization reaction and leads to a substituted ammonium ionic site in the polymer backbone. Eventually, one obtains a diblock copolymer consisting of an ionene and a polystyrene block. The different approaches to synthesize these ionic diblock copolymers are outlined in Scheme 7.1. Theoretically it is possible to obtain the block copolymer by reacting the polystyrene first with 1,4-dibromobutane (*step 1.1* in Scheme 7.1), then with TMEDA, again with 1,4-dibromobutane, and so further on. However, this route appeared impractical -because of the large number of reaction steps-, when compared to the following alternative.

The new concept we developed starts with the quaternization of the polystyrene with 1,4-dibromobutane (*step 1.1*), followed by reaction with the N-terminated trimer (**2**) (*step 1.2*). The most important reason for choosing this method, rather than reacting the polystyrene first with the Br-trimer (**1**) is that the N-trimer (**2**) proved to dissolve to much higher concentrations in an appropriate quaternization solvent such as DMF than does the Br-trimer (**1**). Besides variations in the molecular weight, the differences in the hydrophilicity between the end-groups and the fact that the distance between the two ammonium groups in the N-trimer (**2**) is larger than in the Br-trimer (**1**) determine the discrepancy in solubility. But nevertheless the Br-terminated trimer dissolves to much higher concentrations than high molecular weight 2,4-ionene in DMF. Consequently, a better solubility of the reactants creates the possibility of reaction in more concentrated solutions. Another advantage of this procedure is that the reactive bromo end-group will be better accessible for further coupling. This is important because the chemical modification of linear polymers is usually more difficult than that of their monomeric constituent parts. For example, during the hydrolysis of poly(chloromethylstyrene), the macromolecule is present in solution in a tightly coiled conformation -the polymeric environment almost forms a separate phase-, which implies that no or hardly any hydrolysis can take place, in contrast with its monomeric analogue<sup>17</sup>. Similar effects may be operative in the present case, where the chain end is still too hydrophobic to react with ionene.



Scheme 7.1 Various routes of coupling polystyrene with monodisperse oligomers of 2,4-ionene.

We will present in this chapter the use of DMAP-Li as initiator for the preparation of monodisperse polystyrene, monofunctionalized with a reactive tertiary amino end-group. Also, the stepwise coupling of functionalized polystyrene with reactive oligomer units of 2,4-ionene and the difficulties arising during the preparation will be discussed. Furthermore, it will be demonstrated that the new method for extending the polystyrene block with ionene can even be applied to relatively high molecular weight polystyrenes, and it will be shown that, in principle, the monodisperse ionene blocks can be prepared at any desired chain length. This will allow the preparation of amphiphilic polystyrene-ionene diblock copolymers with a wide range of controlled block lengths.

These tailor-made block copolymers can then be used and optimized as promoters for the catalytic oxidation of hydrophobic thiols. This will be discussed in Chapter 9. Additionally, the use of amphiphilic polymers as surfactants in emulsion polymerization to prepare reactive latices is described in Chapter 8.

## 7.2 Experimental Section

### *Materials*

Styrene (Merck) was distilled in a reduced argon atmosphere, after which it was kept in the dark and stored over  $\text{CaH}_2$  at 2 °C. Tetrahydrofuran (THF) (Merck, p.a.) was collected on  $\text{CaH}_2$  upon distillation, after refluxing in an argon atmosphere in the presence of sodium benzophenone (sodium diphenylketyl), which generates a permanent violet colour. Lithium metal (Fluka) was supplied and used as a 30% dispersion in mineral oil. 3-(Dimethylamino)propyl chloride (DMAP-Cl) (Janssen Chimica) was isolated from its hydrochloric salt according to a literature method<sup>18</sup>. Toluene (p.a.), benzene (p.a.) and n-hexane (p.a.) (Merck) were stored over  $\text{CaH}_2$  in an argon atmosphere and used without further purification. 1,4-Dibromobutane (Janssen Chimica) was distilled and stored under argon before use.

### General Procedure

All reactions were carried out in an argon atmosphere under a complete exclusion of water. The glassware and equipment were cleaned with acetone. Until needed it was dried and stored in an oven at 200 °C. All additions and transfers were conducted using polyethylene syringes equipped with stainless steel needles or, else, by siphoning with stainless steel capillaries.

### Preparation of 3-(Dimethylamino)propyllithium

3-(Dimethylamino)propyllithium (DMAP-Li) was prepared according to a route quite similar to that developed by Stewart *et al.*<sup>12)</sup>. 9.5 g (0.41 mol of Li) of lithium slurry (ten-fold excess over DMAP-Cl) was placed in a 50 ml crimp top flask (equipped with a septum and a magnetic stirrer). The slurry was diluted with 20 ml of n-hexane over a period of 15 min. After settling for 2 h the n-hexane was removed with a syringe and replaced by another 20 ml of n-hexane. The final wash was allowed to stand overnight before removal, after which another 20 ml of n-hexane was introduced, which acted as reaction medium. To start the reaction, about 20% of the required total amount of DMAP-Cl was added dropwise with a syringe at 15 °C, which resulted in a temperature rise of 2 °C. Throughout the whole reaction the reaction mixture was magnetically stirred. Over a period of 2 h the remaining aliquots of DMAP-Cl were added dropwise, keeping the temperature below 20 °C. To guarantee complete reaction, the reaction mixture was stirred for a further 3 h. After reaction the n-hexane was removed with a steel capillary and the mixture was washed with 20 ml of n-hexane. Finally, toluene was added to dissolve the n-hexane-insoluble DMAP-Li, and the product mixture was allowed to stand overnight at 2 °C. Subsequently, the toluene solution was removed and maintained in the dark at -15 °C until required.

### Preparation of 3-(Dimethylamino)propyllithium-Initiated Polystyrene

In a 50 ml crimp top flask, 25 ml of toluene and 0.5 ml of THF were introduced at 40 °C. In order to remove last traces of water and other impurities a titration solution (0.8 ml of styrene, 2 ml of a 1.6 M solution of n-butyllithium in hexane (Merck) and 30 ml of toluene) was added, until a light yellow solution was obtained. If decolorization

resulted, more titration solution was added. When the colour remained constant for at least 30 min, the temperature was lowered to 4 °C, followed by the addition of the required quantity of styrene and again careful titration of the solution. If no decolorization had occurred after 15 min, polymerization was initiated by rapid addition of the amount of initiator needed. Next, the temperature was raised and maintained at 20 °C for 5 min, and subsequently raised to 40 °C and kept at that level for 1 h. The polymer was precipitated in 2-propanol, filtered off and dried at 50 °C at reduced pressure. The polymers prepared are collected in Tab. 7.1.

### *Reactive End-Coupling of Dimethylamino Functionalized Polystyrene with Ionene Oligomers*

The coupling of polystyrene with small oligomeric units of 2,4-ionene (the oligomers Br-trimer (1), N-trimer (2) and Br-pentamer (3) were all prepared according to the procedures reported in Chapter 3) was performed according to the following procedure. First the dimethylamino functionalized polystyrene was quaternized with 1,4-dibromobutane (*step 1.1*, Scheme 7.1): 3.0 g of polystyrene B ( $\bar{M}_n = 2.7$  kg/mol (Tab. 7.1)) and a forty-fold excess of 1,4-dibromobutane were dissolved in 40 ml of DMF. The reaction conditions were so chosen as to accomplish the complete solution of both reactants throughout all the reactions. After reacting for 24 h at 50 °C, the quaternized polystyrene (4) was precipitated in 2-propanol, filtered off and dried at reduced pressure at 50 °C.

The next step of extending low molecular weight quaternized polystyrene ( $\bar{M}_n$  smaller than 3 kg/mol) consisted of coupling of the quaternized polystyrene (4) with the N-terminated 2,4-ionene trimer (2) (*step 1.2*). Again the reaction medium was chosen so that both polymers were dissolved easily: 2.08 g of quaternized polystyrene (4), dissolved in 10 ml of DMF, was added to a solution of a twenty-fold excess (6.40 g) of 2 in 10 ml of DMF and 7 ml of methanol. After 48 h at 50 °C the reaction was complete. The purification procedure comprised of the following steps: precipitation of the block copolymer in water, filtering off, washing with water and drying at reduced pressure.

1.49 g of the resulting polymer (5) was dissolved in 15 ml of DMF and added to a solution of a sixteen-fold excess (6.24 g) of Br-terminated 2,4-ionene pentamer (3) (*step*

1.4) in 7 ml of water, 17 ml of methanol and 5 ml of DMF. In order to obtain a clear solution, an additional portion of 10 ml of DMF was added, followed by reacting for 7 d at 50 °C to complete the conversion. The polymer was isolated and purified according to the procedure mentioned above. The so obtained polystyrene-ionene block copolymer (7) included nine quaternary ammonium groups in the backbone.

A typical procedure for coupling quaternized polystyrene with a relatively high molecular weight started with dissolving 5.2 g of quaternized polystyrene F ( $\bar{M}_n = 12.6$  kg/mol) in 31 ml of DMF, followed by addition of a thirty-fold excess of N-terminated trimer (2) (5.6 g in 7 ml of CH<sub>3</sub>OH and 12 ml of DMF) (step 1.2). When mixing both solutions an additional 12 ml of DMF had to be added in order to obtain a clear solution. After 48 h at 50 °C the reaction was complete. The reaction mixture was purified according to the procedure mentioned above. The next step consisted of dissolving 5.0 g of the resulting polymer (5) in 31 ml of DMF, and adding this solution to a mixture of a twentyfive-fold excess of Br-trimer (1) (5.1 g) in 10 ml of CH<sub>3</sub>OH, 2.5 ml of H<sub>2</sub>O and 9 ml of DMF (step 1.3). An additional 40 ml of DMF was added to avoid any possible precipitation. After 7 d at 50 °C the block copolymer (6) was isolated according to the above mentioned purification procedure. Further extension of the ionene block was performed with 2 g of the polymer (6) and a twenty-fold excess of N-trimer (2) in 3 ml of CH<sub>3</sub>OH and 24 ml of DMF for 14 d at 50 °C. This resulted after precipitation in water and washing with water in an ionene block with ten quaternary ammonium groups.

### Characterization

The yield of the initiator preparation was determined by measuring the number-average molecular weight  $\bar{M}_n$  of the polystyrene, prepared by anionic polymerization with the initiator. The number average molecular weights of the dimethylamino functionalized polystyrenes, as well as of the block copolymers were determined by titration of the dimethylamino chain end in a 1/1 (v/v) mixture of glacial acetic acid and chloroform (both Merck, p.a.), using perchloric acid (0.1001 M in glacial acetic acid, Aldrich) as titrant and methyl violet as indicator<sup>19</sup>. Molecular weight distributions were determined by gel-permeation chromatography (GPC) on a linear  $\mu$ -Styragel HT column (Waters) using THF as eluent at 30 °C, and a flow rate of 1 ml/min. Detection occurred both with a UV (254 nm) and a refractive index detector. Thin layer chromatography (TLC) was

carried out on SiO<sub>2</sub> plates (Merck Art. 5554), using a mixture of chloroform and methanol (9/1, v/v) as eluent<sup>20</sup>. Fourier-transformed infrared spectra of quaternized polystyrene (KBr, film technique) were recorded with a Polaris<sup>TM</sup> (Mattson) spectrometer.

### 7.3 Preparation of 3-(Dimethylamino)propyllithium-Initiated Polystyrene

The anionic functional initiator 3-(dimethylamino)propyllithium, which has been used before by Stewart *et al.*<sup>12)</sup> and by Richards *et al.*<sup>21)</sup> for the anionic polymerization of butadiene, also proved to be successful in synthesizing polystyrenes with relatively narrow molecular weight distributions, as can be seen in Tab. 7.1. The initiator proved to be suitable for the preparation of polystyrenes of a broad range of molecular weights, varying from 1 to 100 kg/mol. Several observations are important in evaluating the presented results. First of all, the type of solvent used to store DMAP-Li, has a strong influence on the initiator stability. Comparison of the different solvents showed a remarkable decomposition behaviour of the initiator in toluene. After one day, 90 % of the initiator had decomposed, even in an inert argon atmosphere at -15 °C. This behaviour was not observed, when the initiator was stored in benzene before use: even after two days no decomposition had occurred. The decomposition could be caused by reaction of DMAP-Li with the methyl group of toluene. The low initial yields obtained (maximally 50 %) are in contrast with the results reported by Stewart *et al.*<sup>12)</sup>.

Also, one initiator preparation was carried out in benzene instead of n-hexane, but a low yield was obtained, probably due to the fact that more Wurtz-coupling between DMAP-Li and DMAP-Cl occurred, when both reactants dissolved. This result is in good agreement with those of Ikker<sup>14,15)</sup>, who prepared DMAP-Li in benzene by a sonochemical reaction and achieved yields of maximally 40 %. The latter author also reported that solutions of DMAP-Li in benzene did not degenerate over several months. Therefore, it can be concluded that the best solvent to prepare DMAP-Li in high yields is n-hexane and that the initiator should be stored in benzene.

Table 7.1 Molecular weights of the polystyrenes prepared with 3-(dimethylamino)propyllithium

Polystyrene	$\bar{M}_n$ (kg/mol)		$\bar{M}_w/\bar{M}_n$
	titration	GPC	GPC
A	1.1	1.2	1.3
B <sup>a)</sup>	2.7	2.1	1.4
C	4.3	5.8	1.2
D <sup>b)</sup>	5.2	2.6	1.3
E	7.8	11.2	1.1
F	8.4	12.6	1.4
G	9.2	9.3	1.4
H	-	15	1.3
I	14	19	1.4
J	17	12	1.2
K	43	35	1.1
L	50	36	1.2
M	84	82	1.1

<sup>a)</sup> Initiator stored in benzene instead of in toluene.

<sup>b)</sup> Initiator prepared and stored in benzene.

Additional evidence that the preparation of polystyrene with DMAP-Li had been successful, was derived from TLC, because only one spot could be detected.

In addition, it can be noticed that no large discrepancies were found between the molecular weights, as determined by end-group titration and by size exclusion chromatography. The range of molecular weight distributions found lies in between 1.1 and 1.4, which are relatively broad for anionic polymerizations. This implies that the initiation was significantly slower than that with other anionic alkyllithium initiators. All polystyrenes



obtained showed characteristics with respect to the molecular weight distributions similar to those found by Ikker<sup>14,15)</sup> who performed the polymerization under high-vacuum conditions.

A typical chromatogram of a dimethylamino functionalized polystyrene, prepared with DMAP-Li, is given in Fig. 7.1. It can be seen that the peak is symmetrical. This phenomenon was not only observed for polystyrene C, but also for all other polystyrenes.

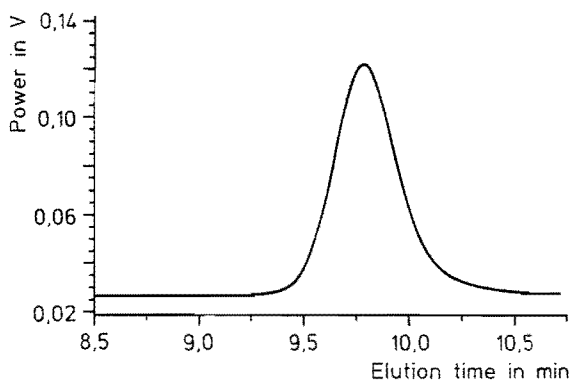


Figure 7.1 *Size exclusion chromatogram of the dimethylamino functionalized polystyrene C.*

Apparently, polystyrenes with tertiary amino end-groups give less problems in GPC analysis than those with primary amine end-groups. Ueda *et al.*<sup>20)</sup> encountered problems in characterizing their amine-functionalized polystyrenes, which, in contrast to our polymers, were equipped with a primary amine group. Their chromatograms always showed broad molecular weight distributions with low molecular weight tails, prohibiting the determination of the number-average molecular weight. Quirk and Cheng<sup>22)</sup> suggested that physical adsorption effects are complicating the size exclusion process for this type of amine-functionalized polymer. After benzylation of the aminated polymers, Ueda and Quirk managed to perfectly characterize their polymers by GPC. In our case we may conclude that polystyrenes carrying a dimethylamino end-group exhibit no adsorption or repulsion characteristics towards the packing material in GPC analysis.

## 7.4 End-Coupling of Dimethylamino Functionalized Polystyrene with Ionene Oligomers

Before extending the polystyrene obtained with an ionene chain, one has to realize that a direct coupling between the reactive end-groups of polystyrene and a 2,4-ionene polymer is not straightforward, because of the large differences in solubility<sup>16</sup>. Polystyrene dissolves only in very low concentrations in a solvent for ionene and vice versa. As a first attempt, we tried to couple a dimethylamino terminated polystyrene with Br-terminated 2,4-ionene in a  $\text{CHCl}_3/\text{CH}_3\text{OH}$  mixture, in which both polymers dissolve. However, this approach raised a problem: the concentrations of the reactive end-groups were so low that even after a long reaction period no conversion could be detected.

The new strategy started with the quaternization of aminated polystyrene with 1,4-dibromobutane (*step 1.1*, Scheme 7.1). Different techniques can be applied to characterize the quaternized polystyrene. FTIR turned out to be a suitable technique, because the quaternized polystyrene (**4**) has a characteristic absorption<sup>23</sup> at  $1260\text{ cm}^{-1}$  (Fig. 7.2), which is absent in the starting material. Another method for determining the extent of coupling 1,4-dibromobutane to the aminated polystyrene proved to be thin-layer chromatography. It has been reported before that aminated polystyrene can be readily

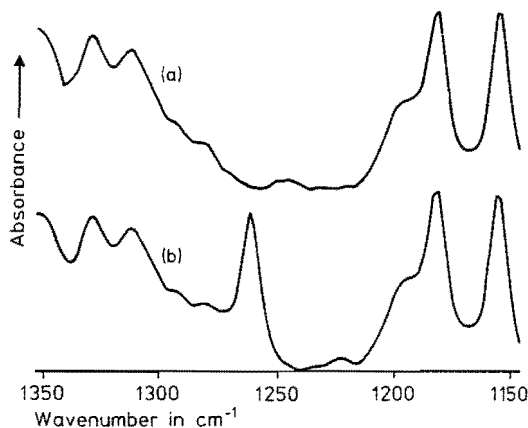


Figure 7.2 FTIR spectrum of polystyrene H (a) before and (b) after reaction with 1,4-dibromobutane.

observed and separated from unfunctionalized polystyrene by thin-layer chromatography with different eluents using  $\text{SiO}_2$  or  $\text{Al}_2\text{O}_3$  as solid phase<sup>20</sup>. With a proper solvent system ( $\text{CHCl}_3/\text{CH}_3\text{OH} = 9/1$ , v/v), well-separated spots can be obtained, because the amino group has a strong interaction with  $\text{Al}_2\text{O}_3$  or  $\text{SiO}_2$ . These TLC experiments showed that the quaternization of the polystyrene with 1,4-dibromobutane in a proper solvent like DMF occurred quantitatively in 24 h.

It also became clear that polystyrenes ( $\bar{M}_n$  smaller than 10 kg/mol) extended with one or more quaternary ammonium groups can easily be separated from the non-quaternized polystyrene by TLC. The separation between polystyrenes with more than two quaternized nitrogens could not be established. Also, no difference in  $R_f$ -value was found between non-quaternized and quaternized polystyrenes of molecular weights exceeding 10 kg/mol.

TLC was also applied in the analysis of the coupling between the quaternized polystyrene (4) with the N-terminated trimer (2) (*step 1.2*). Quantitative quaternization was observed after two days. Supporting evidence for the completeness of the coupling reactions was derived from titration of the tertiary amino terminated amphiphilic polymers with perchloric acid, which showed molecular weights comparable with the theoretical values (Tab. 7.2).

Further extension of the polymers proceeded as indicated in Scheme 7.1. Polystyrene F and G (see Tab. 7.1) could be coupled further with a Br-trimer (1) (*step 1.3*) and polystyrene B and D with a Br-pentamer (3) (*step 1.4*). Via *step 1.4* it was possible to extend the ionene chain, by coupling 3 with 5. In order to dissolve both reactants completely a mixture of DMF/ $\text{CH}_3\text{OH}$ /water was the most effective solvent combination.

During the reaction gelation of the mixture was observed, indicating that conversion had taken place. From *step 1.3* onwards, TLC analysis had become useless in determining conversions, so other characterization techniques had to be used. To elucidate the success of the coupling, first elemental analysis was utilized. As can be seen in Tab. 7.2, the experimental values were somewhat lower than the corresponding theoretical values, indicating that incomplete conversion had taken place. Unfortunately, the experimental values showed large deviations. Similar problems have been encountered before in the

Table 7.2 Data characterizing the amphiphilic polystyrene-ionene diblock copolymers

polystyrene block	end- group	N <sup>+</sup> /block	nitrogen content		$\bar{M}_n$ (titration) (kg/mol)
			theor.	exp.	
A	N	4	3.86	2.79	-
A	Br	7	4.29	3.27	<sup>a)</sup>
B	N	4	2.08	1.65	1.6
B	Br	9	2.94	1.99	<sup>a)</sup>
D	N	4	2.08	1.95	6.2
D	Br	9	2.94	2.27	-
F	N	4	0.53	-	6.5
F	Br	7	0.71	0.70	<sup>a)</sup>
F	N	10	1.08	0.78	60
G	N	4	0.71	0.57	10.7
G	Br	7	0.94	0.96	<sup>a)</sup>

<sup>a)</sup> Direct change of colour in the titration, indicating a bromo end-group.

elemental analysis of ionenes<sup>24</sup>). The discrepancies we observed, could have resulted from the tendency of ionenes to absorb water, especially when bromine is the counterion<sup>25</sup>). This highly hygroscopic behaviour should be reflected in a higher hydrogen content, which was indeed detected in some cases.

Nevertheless, despite the low accuracy of elemental analysis, the increasing nitrogen content proved that a high degree of conversion was reached after coupling with the Br-terminated oligomers. In addition, the resulting amphiphilic polymers were titrated with perchloric acid, to confirm the absence of amino end-groups. These titration experiments instantly gave a change in colour, showing the absence of amino end-groups and indicating that coupling had been completed in very high conversions.

Because of the good solubility of the N-trimer (2) in DMF, the obtained polystyrene F (7) can even be further extended, resulting in ten quaternary ammonium groups. Titration, followed by elemental analysis confirmed the formation of this type of polystyrene-ionene block copolymer.

Besides, reacting aminated polystyrene with the Br-terminated trimer (1) was also successful in a CH<sub>3</sub>OH/DMF mixture within three days. Additionally, a direct coupling between the Br-terminated pentamer (3) and the amino-functionalized polystyrene was accomplished within twelve days. The conversions could be monitored perfectly well with TLC and by titration of the block copolymer formed. Thus, this extra information is another verification that we are able to prepare an ionic diblock copolymer with nine positive charges.

In order to determine the scope of this novel method, the influence of the polystyrene molecular weight on the extension reaction was examined. This was studied by performing the extension reaction of Br-trimer (1) with two different tertiary amino functionalized polystyrenes ( $\bar{M}_n = 43$  kg/mol and 84 kg/mol). No conversion could be detected after the coupling of the longest polystyrene and only very low conversion was observed for the smaller one. No problems showed up during the coupling of polystyrene G ( $\bar{M}_n = 9.3$  kg/mol). Thus, if the molecular weight of the polystyrene exceeds about 20 kg/mol, coupling with Br-trimer (1) becomes very difficult, as a result of its lower solubility in DMF.

As was already mentioned before, a direct coupling of a Br-pentamer (3) ( $\bar{M}_n = 0.88$  kg/mol) with polystyrene was feasible. Thus, the question arose whether it was possible to combine polystyrene D ( $\bar{M}_n = 2.6$  kg/mol) with an even higher molecular weight Br-terminated 2,4-ionene ( $\bar{M}_n = 1.65$  kg/mol), under the same conditions, as this would reduce the number of reaction steps in preparing this type of amphiphilic block copolymer. After a reaction time of 30 days a conversion of less than 10% was detected, which has to be attributed to the low concentrations of reactive end-groups.

Variations in reaction periods, noticed between a direct coupling of quaternized polystyrene with Br-pentamer (3) and the corresponding *step 1.4*, are probably due to the better solubility of the polystyrene with 4 positive charges and, consequently, an

improved accessibility for the ionene pentamer (3) to react. Based on these findings we tried to couple a polystyrene which already possessed two quaternary ammonium groups, with 2,4-ionene with bromo end-groups ( $\bar{M}_n = 1.65$  kg/mol). Despite the better solubility and accessibility no block copolymer could be detected. Hence, it can be concluded that the most important parameters in the present synthesis are the solubilities of the polymers and the concentrations of the reactive end-groups in a suitable quaternization solvent. Therefore, the only route to couple both polymers seems to be the reaction of high concentrations of small 2,4-ionene units with the polystyrene. Of course, the polystyrene can be extended by reacting with 1,4-dibromobutane and TMEDA, the two monomers of 2,4-ionene, successively, but this is inconvenient due to the many reaction steps involved.

It has been shown that it is possible to synthesize block copolymers consisting of polystyrene with different monodisperse ionene blocks, having different numbers of quaternary ammonium groups (between 1 and 10). As the final objective is the use of the amphiphilic polymer as a promoter in the  $\text{CoPc}(\text{NaSO}_3)_4$ -catalyzed autoxidation of hydrophobic thiols and as surfactant during emulsion polymerizations, it is not necessary to obtain polystyrene-ionene block copolymers with high ionene block lengths. As was shown in Chapter 4 monodisperse 2,4-ionenes with four or six quaternary ammonium groups already provide the aggregated form of  $\text{CoPc}(\text{NaSO}_3)_4$  with perfect stabilization, and, hence, exhibit excellent promoting activities in the  $\text{CoPc}(\text{NaSO}_3)_4$ -catalyzed oxidation of thiols.

## 7.5 Conclusions

3-(Dimethylamino)propyllithium proves to be a good initiator for the preparation of amino end-functionalized polystyrenes over a wide range of molecular weights with fairly narrow molecular weight distributions. The preparation of well-defined block copolymers by reactive end-coupling of the polystyrene with ionene oligomers proved to be a successful new route. Reactive end coupling with ionene appears to be dependent on the solubilities of the reactants and the concentrations of the reactive groups. According to the present method, polystyrenes even when possessing a relatively high molecular weight (up to about 20 kg/mol), can be extended with an ionene block. Furthermore, thin layer

---

chromatography and end-group titration of the block copolymers appeared to be good characterization techniques for this block copolymer synthesis route. Amphiphilic polystyrene-ionene diblock copolymers can be prepared with a monodisperse ionene block, containing between one and ten quaternary ammonium groups.

## References

1. Y. Selb, Y. Gallot, in "Developments in Blockcopolymers-2", I. Goodman, Ed., Elsevier Applied Science Publishers, London, 1985.
2. C. Roberts, W. Edward Lindsell, I. Soutar, *Br. Polym. J.*, **23** (1990) 55.
3. M. Watanabe, T. Kamiya, K. Goto, N. Matsubara, *Makromol. Chem.*, **182** (1981) 2659.
4. M. Watanabe, N. Toneaki, I. Shinohara, *Polym. J.*, **14** (1982) 189.
5. M. Kawaguchi, M. Oohira, M. Tajima, A. Takahashi, *Polym. J.*, **12** (1980) 849.
6. A. Takahashi, M. Kawaguchi, T. Kato, M. Kuno, S. Matsumoto, *J. Macromol. Sci.-Phys.*, **B17** (1980) 747.
7. S. Ikeno, M. Yokoyama, H. Mikawa, *J. Polym. Sci. Phys. Ed.*, **16** (1978) 717.
8. J. van Welzen, A.M. van Herk, A.L. German, *Makromol. Chem.*, **190** (1989) 2477.
9. J. van Welzen, A.M. van Herk, A.L. German, *J. Mol. Catal.*, **60** (1990) 351.
10. C.D. Eisenbach, H. Schnecko, W. Kern, *Eur. Polym. J.*, **11** (1975) 699.
11. H. Schnecko, C.D. Eisenbach, W. Kern, *J. Chromatogr. Sci.*, **14** (1976) 219.
12. M.J. Stewart, N. Shepherd, D.M. Service, *Br. Polym. J.*, **22** (1990) 319.
13. N.S. Davidson, L.J. Fetters, W.G. Funk, W.W. Graessley, N. Hadjichristidis, *Macromolecules*, **21** (1988) 112.
14. A. Ikker, Ph.D. Thesis, University of Technology Twente, Enschede, 1992.
15. A. Ikker, M. Möller, in "Proceedings of Sympol 90", Paris, 1990.
16. K.H. van Streun, Ph.D. Thesis, Eindhoven University of Technology, Eindhoven, 1990, pp. 109-120.
17. P. Hodge, D.C. Sherrington, "Polymer-Supported Reactions in Organic Synthesis", Wiley, New York, 1980, p. 38.
18. S.P.S. Yen, D. Casson, A. Rembaum, in "Water-Soluble Polymers", N.M. Bikalis, Ed., Plenum, New York, 1973.
19. J.S. Fritz, G.H. Schenk, "Quantitative Analytische Chemie", Vieweg, Braunschweig, 1989.
20. K. Ueda, A. Hirao, S. Nakahama, *Macromolecules*, **23** (1990) 939.
21. D.H. Richards, D.M. Service, M.J. Stewart, *Br. Polym. J.*, **16** (1984) 117.
22. R.P. Quirk, P.L. Cheng, *Macromolecules*, **19** (1986) 1291.
23. W.W. Simons, "The Sadtler Handbook of Infrared Spectra", Sadtler, Philadelphia, 1978.
24. L. Dominguez, W.H. Meyer, G. Wegner, *Makromol. Chem. Rapid Commun.*, **8** (1987) 151.
25. T. Tsutsui, R. Tanaka, T. Tanaka, *J. Polym. Sci. Polym. Phys. Ed.*, **14** (1976) 2273.



## Chapter 8

# Synthesis and Co-Catalytic Properties of Polystyrene-Ionene Stabilized Latices

**SUMMARY:** Cationic latices with excellent co-catalytic properties were designed by emulsion polymerization of styrene using monodisperse amphiphilic polystyrene-ionene diblock copolymers as surfactant. The amphiphilic block copolymers built in during the emulsion polymerization of styrene, with the water-soluble initiator 2,2'-azobis(2-amidinopropane) dihydrochloride, possess electrostatic as well as steric stabilization properties. Increasing the block copolymer concentration leads to latices with smaller particle sizes. A major advantage of the preparative procedure used is that no extensive cleaning procedures need to be applied. After immobilization of the  $\text{CoPc}(\text{NaSO}_3)_4$  catalyst onto the latex, reactive latices were obtained which show very high catalytic oxidation rates towards the mercaptoethanol autoxidation. The highest catalytic activity ( $500 \text{ mol O}_2/(\text{mol Co}\cdot\text{s})$ ), fifteen times higher as compared with the polymer-free system, was achieved with latices with relatively short ionene blocks with 7 quaternary ammonium groups at their particle surface. Despite relatively low surface charge densities, apparently enough ionene chains of sufficient length are present at the particle surface to stabilize the highly active  $\text{CoPc}(\text{NaSO}_3)_4$  dimers and to achieve substrate enrichment. Furthermore, the thiol oxidation with reactive latices obeys Michaelis-Menten kinetics.

### 8.1 Introduction

The excellent catalytic  $\text{CoPc}(\text{NaSO}_3)_4/2,4$ -ionene combination for the autoxidation of thiols to disulfides does not allow continuous operation because of the homogeneity of the

system. The disadvantages of this method for industrial applications are the recovery and the reuse of the catalyst. Therefore, it is necessary to apply a support in order to immobilize the highly active system. Several methods have been used before to immobilize the  $\text{CoPc}(\text{NaSO}_3)_4$  catalyst onto polymeric macroporous resins. For example,  $\text{CoPc}(\text{NaSO}_3)_4$  has been covalently bound to polystyrene beads in several ways<sup>1-6</sup>. Also, the catalyst was electrostatically immobilized to polyvinylamine grafted onto macroporous particles<sup>7</sup>, to cross-linked polyvinylamine<sup>8</sup> and to cationic resin particles and was subsequently tested in the mercaptoethanol autoxidation<sup>9,10</sup>. The disadvantages of these systems which are sometimes encountered are transport limitations and the absence of long flexible cationic tails at the particle surface, resulting in lower catalytic activities.

In order to overcome these difficulties polymer colloids proved to be more successful as support for catalysts, due to their higher specific surface areas and their non-porous character. Mass transport limitations are therefore unlikely because of the better accessibility of the latex surface. More and more attention is being focused on these latex particles which can easily be prepared by emulsion polymerization. Latex-supported catalysts have been successfully applied in hydrolysis reactions<sup>11-18</sup>, inversion of sucrose<sup>19,20</sup>, phase-transfer catalysis<sup>21-23</sup>, oxidation<sup>24,25</sup> and epoxidation<sup>26,27</sup> reactions.  $\text{CoPc}(\text{NaSO}_3)_4$  electrostatically bound to latex particles showed a rate enhancement in the autoxidation of 2,6-di-*tert*-butylphenol as compared with its soluble analogue<sup>28</sup>. Furthermore, immobilization of enzymes onto polymer colloids has been reported<sup>29</sup>.

Earlier attempts with  $\text{CoPc}(\text{NaSO}_3)_4$  electrostatically attached to the particle surface of cationic latices have been reported. These latices were used as catalysts in thiol autoxidations. The main problem was that the several preparative procedures did not result in long and flexible cationic chains at the latex particle surface. Mostly, a cationic surfactant with a polymerizable group was used, which was built in during the emulsion polymerization<sup>30-32</sup>. A few efforts, applying cationic comonomers or poly(styrene-co-1-methyl 4-vinyl-pyridinium bromide) copolymers resulted in positively charged chains at the surface, but in all cases these were too short to stabilize the highly active Co-dimers, and as a consequence low thiol oxidation rates were observed as compared with the homogeneous  $\text{CoPc}(\text{NaSO}_3)_4/2,4\text{-ionene}$  system<sup>33-36</sup>. Application of shot-growth techniques improved the activity<sup>36</sup>, but only when vinylbenzyl-telechelic macromonomers of 2,4-ionene were used, very high catalytic thiol oxidation rates were achieved<sup>37</sup>.

Monodisperse amphiphilic polystyrene-ionene diblock copolymers, prepared according to procedures described in Chapter 7 of this thesis, should allow us to prepare latex particles with well-defined ionene chains at the particle surface extending into the water phase. During the emulsion polymerization of styrene the tailor-made block copolymers will act as surfactant, so by the end of the reaction the hydrophobic polystyrene block will extend into the interior of the latex particles and the ionene block will extend into the aqueous phase. In this chapter the preparation and properties of polystyrene-ionene stabilized latices will be presented. Subsequently, the application of these latices as co-catalyst in the  $\text{CoPc}(\text{NaSO}_3)_4$ -catalyzed oxidation of mercaptoethanol will be discussed.

## 8.2 Experimental Procedures

### *Materials*

Styrene (Merck, p.a.) was distilled at reduced pressure prior to use. The preparation procedure of the different polystyrene-ionene diblock copolymers has been described in Chapter 7. 2,2'-Azobis(2-amidinopropane) dihydrochloride ( $\text{AIBA}\cdot 2\text{HCl}$ ) (Polyscience), cetyltrimethylammonium bromide (CTAB) (Fluka, 99 %) and 2,2'-azobis(2-methylpropionitrile) (AIBN) (Merck, zur synthese) were used without purification. Deionized water was used throughout the experiments after purging with argon.

### *Polymerization Procedures*

The polymerizations were carried out in a thermostated stirred glass batch reactor (1 dm<sup>3</sup>, no baffles), equipped with a disc turbine impeller, under argon atmosphere. First, the polystyrene-ionene diblock copolymer was dissolved in 6 ml ( $7.8\cdot 10^{-2}$  mol) of *N,N*-dimethylformamide (DMF) (Janssen Chimica, p.a.), for reasons mentioned in Chapter 9. This block copolymer solution was poured into the reactor and, subsequently, the styrene and water were added, respectively. When the reaction temperature (70 °C) was reached, initiator ( $\text{AIBA}\cdot 2\text{HCl}$ ), dissolved in 5 ml of water, was introduced by means of a syringe. Unless stated otherwise, the emulsion polymerizations were carried out with 5 g ( $4.8\cdot 10^{-2}$  mol) of styrene, 0.1 g ( $3.7\cdot 10^{-4}$  mol) of  $\text{AIBA}\cdot 2\text{HCl}$  and  $2.1\cdot 10^{-4}$  mol N<sup>+</sup> of diblock copolymer or of CTAB. The total reaction volume was

always 0.5 dm<sup>3</sup>. For the kinetic measurements, samples were taken from the reactor, the polymerizations were stopped with hydroquinone (Janssen Chimica) and the conversions were determined gravimetrically. Finally, after a polymerization time of 15–24 h at 300 r.p.m., the product was filtrated in order to remove any coagulum. With respect to the catalytic experiments it was not necessary to purify the latex any further.

### *Characterization Procedures*

Particle size distributions were determined by dynamic light scattering (DLS) (Malvern Autosizer 2C) and transmission electron microscopy (TEM) (Jeol 2000 FX). The latices were further characterized by determining the N<sup>+</sup>-content, present at the surface of the latex particles, by conductometric titration. Before titration the latices ( $\pm$  250 ml) were washed with 6 dm<sup>3</sup> of 0.001 M NaOH solution in a serum replacement cell (Amicon) equipped with a 100 nm pore size polycarbonate membrane (Nuclepore) in order to replace all counterions by hydroxide anions. Next, after washing with 6 dm<sup>3</sup> of deionized water in order to remove excess of base, the latices were conductometrically titrated with 0.01 M HCl under argon atmosphere using a Radiometer CDM80. From the solids content, the particle diameter, determined by TEM, and the titration data the surface charge density was calculated.

### *Catalytic Activity Measurements*

First, the latex was charged into the reaction vessel and diluted with water. Next, the catalyst was prepared by addition of a CoPc(NaSO<sub>3</sub>)<sub>4</sub> solution to the diluted latex. Further, the reactions proceeded as described in Chapter 3.

### 8.3 Emulsion Polymerization of Polystyrene-Ionene Diblock Copolymer Stabilized Polystyrene Latices

#### 8.3.1 Mechanism of the Emulsion Polymerization

First, we studied the kinetics of the emulsion polymerization of styrene in the presence of the ionic diblock copolymer, in order to find the answer to the question whether these amphiphilic block copolymers really act as stabilizers in the emulsion polymerization. The characteristics of the monodisperse polystyrene-ionene diblock copolymers used during the emulsion polymerizations are presented in Tab. 8.1.

Table 8.1 Characteristics of the amphiphilic polystyrene-ionene diblock copolymers used

diblock copolymer	polystyrene block $\bar{M}_n$ ( $10^3$ g·mol <sup>-1</sup> )	ionene block $\bar{M}_n$ ( $10^3$ g·mol <sup>-1</sup> )	number of N <sup>+</sup> per ionene block
A-4	1.1	0.71	4
A-7	1.1	1.18	7
D-4	2.6	0.71	4
D-9	2.6	1.51	9
G-7	9.2	1.18	7

The initiation of the emulsion polymerization will most probably proceed according to a homogeneous nucleation mechanism. The water-soluble initiator AIBA·2HCl forms two radicals, which will initiate the polymerization of styrene in the aqueous phase. The oligomers grow until a critical length is reached, determined by the water solubility of the oligomer. These precursors will coagulate, resulting in the formation of primary particles, which will grow to latex particles. Initially, the amphiphilic block copolymer is most probably present in the monomer droplets, due to the extremely low solubility in the water phase, but during the growth of the latex particles the block copolymer will be incorporated into the latex particles. Consequently, the copolymer acts as a stabilizer as the ionene part will be located at the particle surface. In fact these block copolymers have

all the prerequisites to function as highly efficient stabilizers, because the nature of the polystyrene block is similar to that of the latex particle, and the ionene block is perfectly soluble in the continuous phase.

We have to keep in mind that a significant part of the electrostatic stabilization of the latex particles originates from the initiator. AIBA generates two cationic water-soluble radicals which will end as covalently bound charged initiator residues at the particle surface. In order to investigate this effect, we tried to prepare latices with only AIBA (R1) (see Tab. 8.2) and without surfactant. The conversion never exceeded 35 % and the latex particle size was significantly larger as compared with latex (R2) prepared with block copolymer D-9. As a consequence, we may conclude that a polystyrene-ionene diblock copolymer exhibits stabilizing properties in the emulsion polymerization of styrene.

Furthermore, in order to examine the stabilization efficiency we studied the effect of the concentration of block copolymer D-9 on the particle size distributions of the latices (E1, E2 and E3). As can be seen in Tab. 8.2, increasing the block copolymer concentration results in an increase in the number of particles leading to a decrease in the particle diameters. Only when a low block copolymer concentration was used a monodisperse latex was obtained with a large diameter.

Additionally, we performed an experiment (R4) with the cationic surfactant cetyltrimethylammonium bromide (CTAB) with an equal amount of charged groups ( $N^+$ -groups) as latex R2. A comparison between the two latices is only possible if the soap concentration is below the critical micelle concentration ( $CMC_{CTAB} = 9.2 \cdot 10^{-4} \text{ M}$ )<sup>36</sup>). Although at higher ionic strengths the CMC will be shifted to lower values, the CTAB concentration used here will still be lower than its CMC. By comparing the two latices it appears that using the ionic block copolymer results in a smaller diameter. Hence, it can be assumed that amphiphilic polystyrene-ionene diblock copolymers possess electrostatic as well as steric stabilization properties.

Table 8.2 Effects of stabilizer, initiator and co-solvent concentrations on the particle size distributions of polystyrene latices

latex	surfactant			$\bar{d}_n$ (TEM) (nm)	$\bar{d}_w/\bar{d}_n$	$\bar{d}_z$ (DLS) (nm)
	type	$10^4 \cdot [N^+]$ (mol · dm <sup>-3</sup> )	$10^4 \cdot [AIBA \cdot 2HCl]$ (mol · dm <sup>-3</sup> )			
R1 <sup>a)</sup>	-	-	7.4	117	1.04	112
R2	<b>D-9</b>	4.4	7.4	58	1.10	71
E1 <sup>b)</sup>	<b>D-9</b>	2.2	18.5	207	1.01	-
E2 <sup>b)</sup>	<b>D-9</b>	4.4	18.5	70	1.27	74
E3 <sup>b)</sup>	<b>D-9</b>	11	18.5	54	1.19	75
R3 <sup>c)</sup>	CTAB	4.4	7.4	85	1.18	-
R4	CTAB	4.4	7.4	92	1.02	102
R5 <sup>d)</sup>	CTAB	4.4	7.4	95	1.02	104
R6	<b>D-4</b>	4.4	7.4	- <sup>e)</sup>	-	32
R7	<b>A-4</b>	4.4	7.4	- <sup>e)</sup>	-	40
R8	<b>A-7</b>	4.4	7.4	- <sup>e)</sup>	-	45
J1 <sup>b)</sup>	<b>G-7</b>	16.2	18.5	- <sup>f)</sup>	-	-

Conditions: [Styrene] =  $9.6 \cdot 10^{-2}$  mol · dm<sup>-3</sup><sub>water</sub>, [DMF] =  $1.6 \cdot 10^{-1}$  mol · dm<sup>-3</sup><sub>water</sub>,  
70 °C.

<sup>a)</sup> Maximum conversion 35 %.

<sup>b)</sup> [Styrene] =  $9.6 \cdot 10^{-1}$  mol · dm<sup>-3</sup><sub>water</sub>.

<sup>c)</sup> No DMF.

<sup>d)</sup> [DMF] =  $7.8 \cdot 10^{-1}$  mol · dm<sup>-3</sup><sub>water</sub>.

<sup>e)</sup> No reliable diameters could be determined with TEM.

<sup>f)</sup> Maximum conversion 47%, no colloidally stable latex.

The fact that AIBA contributes to the stabilization of the latex to a considerable extent, gives reason to prepare latex particles of which the stabilization results purely from ionene chains, because AIBA residues at the interface are assumed to be unable to bind the cobalt catalyst in its catalytically active dimeric form. In order to overcome the problem of AIBA binding the monomeric form of  $\text{CoPc}(\text{NaSO}_3)_4$ , a non-charged water-soluble or an oil-soluble initiator should be used. Applying the water-insoluble initiator AIBN in the emulsion polymerization of styrene with block copolymer **D-9** resulted in a colloiddally unstable latex and in low maximal conversion (47 %).

It has been reported before that co-solvents added during an emulsion polymerization influence the nucleation of the polymerization<sup>39-41</sup>. In our case DMF is used as a co-solvent to dissolve the block copolymer, because the copolymer is only sparsely soluble in water<sup>42</sup>. In order to study the effect of DMF we performed three emulsion polymerizations with 0, 6 and 30 ml of DMF (R3, R4 and R5) using CTAB as surfactant. Slightly smaller particle diameters were obtained if the amount of DMF was decreased and the polydispersity decreased if DMF was added.

Several block copolymers were used to examine their influence on the properties of the latices. In the case of non-ionic diblock copolymers, the molecular weights of both blocks and the hydrophobic/hydrophilic ratio appeared to have large effects on their behaviour in emulsion polymerizations<sup>43,44</sup>. First of all, we investigated the influence of the ionene block length on the latex properties. By reducing the ionene block length from 9 to 4 quaternary ammonium groups, keeping the total concentration of quaternary ammonium groups constant in the polymerization reactions (R2 vs R6), latices were obtained with a smaller particle size. By comparing latices R7 and R8, prepared with an amphiphilic block copolymer with a smaller polystyrene block and with 4 and 7  $\text{N}^+$ , respectively, similar results were obtained. From these experiments it becomes evident that with increasing surfactant concentration, the amount of surfactant to contribute to the stabilization of the latex also increases. The fact that with CTAB with similar  $\text{N}^+$ -concentrations, no smaller diameters were obtained, again emphasizes the possibility of steric stabilization by the polystyrene-ionene diblock copolymers. However, it should be remarked that the latices, prepared with copolymers consisting of four quaternary ammonium groups, exhibited a lower colloidal stability with respect to the latices with



ionene chains with 7 and 9 N<sup>+</sup>. This resulted in partial coagulation during the catalytic experiments.

We also performed polymerizations with **G-7** which has a relatively high polystyrene content and contains 7 quaternary ammonium groups. Even with very high block copolymer concentrations no colloiddally stable latices (**J1**) could be derived. Due to the high molecular weight of the polystyrene block, difficulties arise in its solubility during the emulsion polymerization and a part of the block copolymer precipitates.

It can be concluded that the preparation of colloiddally stable latex particles requires the use of amphiphilic polystyrene-ionene diblock copolymers with a restricted polystyrene content and an ionene chain length of at least 7 N<sup>+</sup>. When block copolymers with 4 N<sup>+</sup> are utilized, relatively high emulsifier concentrations should be applied in order to obtain stable latices. Before examining whether these short ionene chains are of sufficient length to exhibit co-catalytic properties it is necessary to know the total positive charge at the particle surface which can bind the CoPc(NaSO<sub>3</sub>)<sub>4</sub> catalyst.

### **8.3.2 Surface Charge Density**

The concentration of the positive charges from AIBA initiator residues and ionene at the latex surfaces was determined by conductometric titration. In Tab. 8.3 the surface charge densities of four different latices are presented. Latex R1, where AIBA residues solely contribute to the stabilization, shows the highest surface charge density. After a polymerization time of 15–24 h nearly all AIBA ( $k_d$  of  $1.2 \cdot 10^{-4} \text{ s}^{-1}$  at 70 °C) has decomposed. Present at the particle surface is 23 % of the initial amount of AIBA. Also, a significant part of the initiator residues is buried into the latex particles during the emulsion polymerization.

By contrast, latex E3 has a low surface charge density, because a relatively high styrene/block copolymer ratio was used in the emulsion polymerization. A high surface charge density so far has been assumed to be a very important co-catalytic parameter in the catalytic thiol oxidation<sup>34</sup>. In order to prepare latex particles with high surface charge densities, we reduced the styrene/surfactant ratio, which will lead to higher ionene concentrations at the latex surface. As can be seen in Tab. 8.3, indeed higher surface

Table 8.3 Surface charge densities ( $\sigma$ ) of the latices used in the catalytic measurements

latex	surfactant	$\bar{d}_n$ (nm)	$\bar{d}_w/\bar{d}_n$	$\bar{d}_z$ (nm)	$\sigma$ ( $\mu\text{C}\cdot\text{cm}^{-2}$ )
R1	-	117	1.04	112	11.6
E3	<b>D-9</b>	54	1.19	75	1.1
R2	<b>D-9</b>	58	1.10	71	7.4
R8	<b>A-7</b>	-	-	45	5.0 <sup>a)</sup>

For experimental conditions see Tab. 8.2.

<sup>a)</sup> Surface charge density is based on  $\bar{d}_z$ .

charge densities were obtained with latices R2 and R8 as compared with latex E3. In general, the charge densities determined are low in comparison with systems using ionic comonomers<sup>33,36</sup>). Nevertheless, besides a high concentration of positive charges at the latex surface, the other prerequisite for an efficient co-catalytic system is the presence of cationic tails. The latter effect can be studied by performing catalytic experiments with latices with different ionene lengths at their surface.

#### 8.4 Catalytic Activities of Latex-Supported $\text{CoPc}(\text{NaSO}_3)_4$ Catalysts in the Mercaptoethanol Autoxidation

One of the major problems encountered when reactive latices are applied in the thiol oxidation is the presence of free polyelectrolyte, which is an inevitable side product<sup>35-37,45</sup>). Desorption of polyelectrolyte, formed during the preparation, from the latex drastically affects the thiol oxidation rate and should therefore be avoided. Extensive and elaborous cleaning techniques, like ultrafiltration, serum replacement and treatment with silica, are necessary before performing catalytic experiments<sup>35-37,45</sup>). In our case no ionene-containing block copolymer could be detected in the water-phase after polymerization, because of its extremely low water solubility. Hence, latices stabilized by polystyrene-ionene diblock

copolymers can be applied directly after preparation as co-catalysts in the thiol autoxidation.

After electrostatic immobilization of the  $\text{CoPc}(\text{NaSO}_3)_4$  catalyst we first examined the effect of  $\text{N}^+$ -concentration on the catalytic mercaptoethanol oxidation rate. In Fig. 8.1 the catalytic activity is plotted as a function of the  $\text{N}^+/\text{Co}$  ratio for latex R2, prepared with a block copolymer with 9 quaternary ammonium groups. The oxidation rate rises if the  $\text{N}^+$ -concentration is increased due to the fact that  $\text{CoPc}(\text{NaSO}_3)_4$  dimers are formed and simultaneously substrate enrichment occurs, leading to a maximum in the catalytic activity. After this point the activity decreases because the local  $\text{RS}^-$ -concentration near the catalytic sites is reduced. The fact that ionene chains at the latex surface are responsible for the co-catalytic properties is demonstrated by the activities measured for the cobalt catalyst bound to latex R1, where only AIBA residues are present at the surface. In the latter case only a slight increase by a factor of 2-3 in the oxidation rate was observed as compared with the polymer-free system. This enhancement can be ascribed to substrate enrichment of thiolate anions at the active sites.

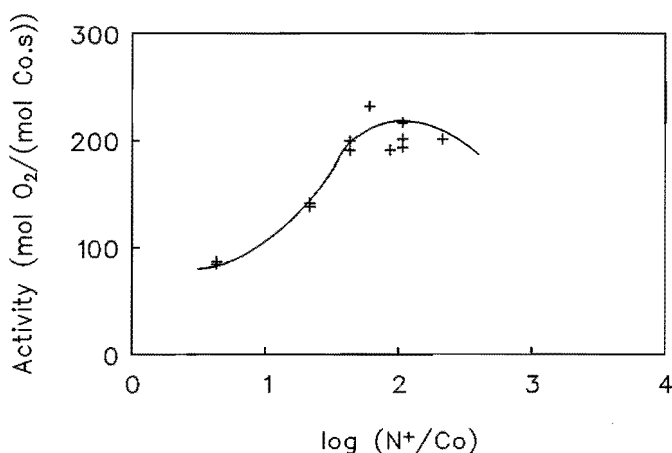


Figure 8.1 Catalytic mercaptoethanol oxidation rate as function of  $[\text{N}^+]$  (latex R2).

$[\text{CoPc}(\text{NaSO}_3)_4] = 4 \cdot 10^{-7} \text{ mol} \cdot \text{dm}^{-3}$ ,  $\text{pH} = 9.0$ ,

$[\text{ME}] = 7.1 \cdot 10^{-2} \text{ mol} \cdot \text{dm}^{-3}$ .

We also determined the pH dependence of the mercaptoethanol oxidation rate for the latex R2 (Fig. 8.2). As can be seen at low pH low activities are measured because of the absence of thiolate anions, the reactive species. After increasing the pH a maximum occurs, which is similar as observed for other polycation containing systems<sup>34-37,46</sup>. At higher pH lower activities are achieved due to a competitive ion effect between the thiolate and hydroxide anions.

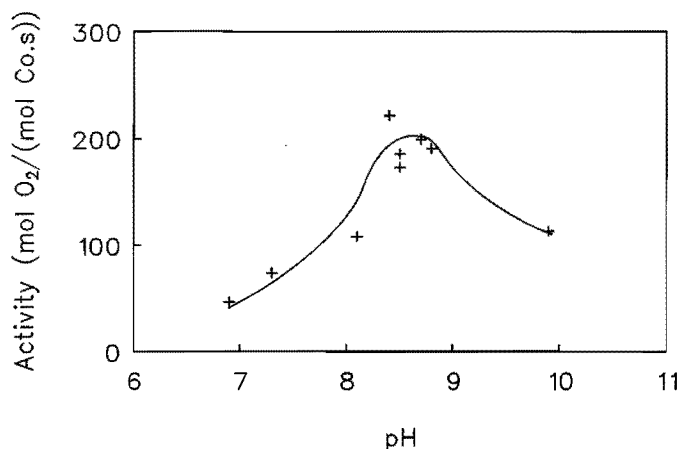


Figure 8.2 Catalytic mercaptoethanol oxidation rate as function of pH (latex R2).

$$[\text{CoPc}(\text{NaSO}_3)_4] = 4 \cdot 10^{-7} \text{ mol} \cdot \text{dm}^{-3}, \quad [\text{ME}] = 7.1 \cdot 10^{-2} \text{ mol} \cdot \text{dm}^{-3};$$

$$[\text{N}^+](\text{R2}) = 2 \cdot 10^{-5} \text{ mol} \cdot \text{dm}^{-3}.$$

An important parameter in the homogeneous  $\text{CoPc}(\text{NaSO}_3)_4/2,4$ -ionene system is the chain length of the ionene<sup>47</sup>. In immobilized systems the effects of ionene chains cooperating collectively are difficult to determine, because the ionene chains are linked to the surface. Nevertheless, we tried to investigate the effect of the length of ionene tails at the particle surface. In Fig. 8.3 the influence of the latex concentration on the oxidation rate is depicted for two latices R7 and R8 prepared with cationic tails consisting of 4  $\text{N}^+$  and 7  $\text{N}^+$ , respectively. It should be noted here that coagulation occurred on a small scale due to some colloidal instability of latex R7 during the catalytic experiments. Consequently, determination of the surface charge density was impossible.

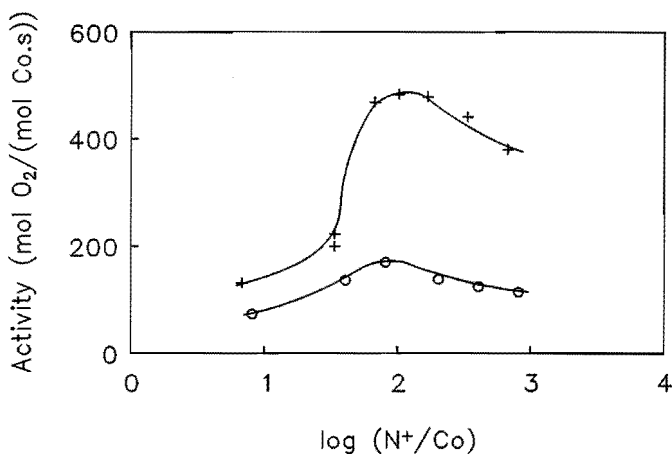


Figure 8.3 Catalytic mercaptoethanol oxidation rate as function of  $[N^+]$ .  
 $[CoPc(NaSO_3)_4] = 4 \cdot 10^{-7} \text{ mol} \cdot \text{dm}^{-3}$ ,  $pH = 9.0$ ,  
 $[ME] = 7.1 \cdot 10^{-2} \text{ mol} \cdot \text{dm}^{-3}$ ;  
 (o) R7, (+) R8.

Alternatively, we had to estimate the surface charge density of latex R7. Based on the measured surface charge density of latex R8 (Tab. 8.3) and the assumption that all block copolymer is present at the exterior of the particles, it is possible to calculate the amount of AIBA residues at the outside of the particle: 20 % of the initial amount of AIBA is present at the surface of latex R8. This value is comparable with the percentage AIBA (23 %) present at the particle surface of latex R1, prepared with only AIBA. Performing an analogous estimation for latex R2, a value of 28 % of the initial amount of AIBA was calculated. Next, the  $N^+$ -concentration at the surface of latices R7, E1 and E2 could be estimated, assuming an equivalent percentage AIBA present at the surface as of latex R1 and assuming all block copolymer is present at the surface of the latex particles.

The assumption, that all block copolymer will be built in at the particle surface, also implies that we are able to attribute the  $N^+$  at the particle surfaces to block copolymer or initiator residues. It appears that about 40 % of the  $N^+$  present at the surface of latex R8 can be ascribed to AIBA residues. In case of latex R2 this value is 45 %. These high percentages explain the fact that no colloiddally stable latices were obtained without AIBA

as initiator. This also means that about 60 % of the  $N^+$  at the particle surface can be ascribed to the ionene.

Despite a large amount of AIBA residues at the surface, very high oxidation rates (Fig. 8.3) are obtained applying latex R8 with ionene chains consisting of 7  $N^+$  at their surface. The maximum catalytic activity observed is a factor of 15 higher as compared with the polymer-free system. Even more important is that this heterogeneous catalytic system is able to compete with the highly active homogeneous  $CoPc(NaSO_3)_4/2,4$ -ionene system<sup>46</sup>. Furthermore, when shorter ionene chains are present at the surface (latex R7) catalytic activities are realized, which are a factor of 3 lower than measured for latex R8. With respect to latex R7, the cationic tails are fixed onto the particle surface and can not contribute collectively to the stabilization of the Co-dimers.

It should be noticed that higher maximal activities are achieved with latex R8 with ionene chains consisting of 7  $N^+$  than for latex R2 with ionene chains of 9  $N^+$  at the surface. The difference in activities could be explained by the length of polystyrene block of the copolymers used. Apparently, using copolymer **D-9** instead of **A-7**, more block copolymer should be embedded inside the particle, because of its higher polystyrene content and its higher hydrophobic/hydrophilic ratio. However, this should affect the surface charge density, which is similar in both cases. Therefore, the reason for this discrepancy is not yet clear.

Additionally, we investigated the co-catalytic properties of a series of latices prepared with different concentrations of the polystyrene-ionene block copolymer **D-9**. In Fig. 8.4 the effect of the  $N^+/Co$  ratio of latices E1, E2 and E3 on the mercaptoethanol oxidation rate is presented. It clearly shows that increasing the amount of block copolymer present during the emulsion polymerization leads to a higher concentration of ionene tails at the surface and as a result higher oxidation rates are observed. It can be noticed further that the use of latex R2, with a higher surface charge density than E3, did not result in better co-catalytic properties (see also Fig. 8.1). Apparently, in both cases the cationic tails sticking into the water phase are capable of achieving aggregation of the cobalt species.

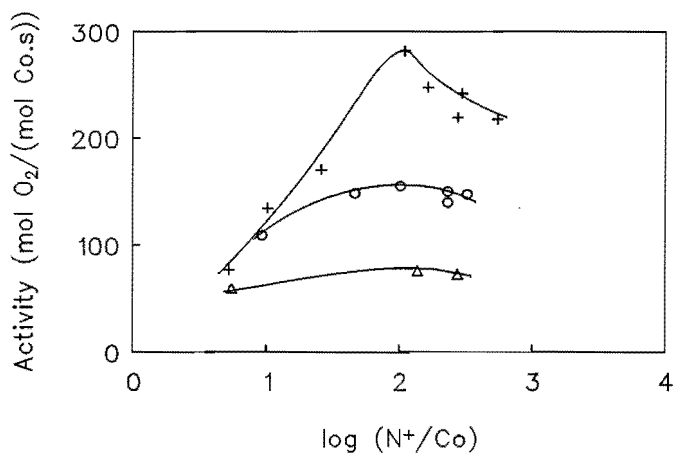


Figure 8.4 Catalytic mercaptoethanol oxidation rate as function of  $[N^+]$ .  
 $[CoPc(NaSO_3)_4] = 4 \cdot 10^{-7} \text{ mol} \cdot \text{dm}^{-3}$ ,  $pH = 9.0$ ,  
 $[ME] = 7.1 \cdot 10^{-2} \text{ mol} \cdot \text{dm}^{-3}$ ;  
 (Δ) E1, (○) E2, (+) E3.

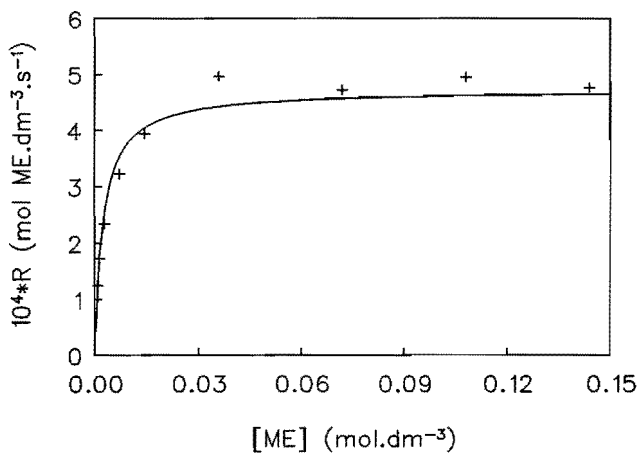


Figure 8.5 Catalytic thiol oxidation rate ( $R$ ) as a function of substrate ( $ME$ ) concentration (latex E3).  
 $N^+/Co = 100$ ,  $[CoPc(NaSO_3)_4] = 4 \cdot 10^{-7} \text{ mol} \cdot \text{dm}^{-3}$ ,  
 $pH = 9.0$ ,  $[ME] = 7.1 \cdot 10^{-2} \text{ mol} \cdot \text{dm}^{-3}$ .

It can be seen (Fig. 8.1, 8.3 and 8.4) that a similar value of the optimal  $N^+/Co$  ratio of about 100 can be observed for the three well-characterized latices (E3, R2 and R8) with relatively long ionene chains. This value is slightly higher than those found for the homogeneous counterparts, but also in the homogeneous system the optimal  $N^+/Co$  ratio is shifted to larger values when relatively short ionene chains are used<sup>47</sup>.

The oxidative coupling of mercaptoethanol to its corresponding disulfide gives rise to an enzyme-like kinetic behaviour. It has been shown before that in the homogeneous as well as in several latex-supported catalytic systems Michaelis-Menten kinetics were observed<sup>34-36,49</sup>. In Fig. 8.5 the ME consumption rate is depicted as a function of the ME concentration using latex E3. These results point to simple Michaelis-Menten kinetics according to eq. 4.1 (zeroth reaction order in  $O_2$ )<sup>49</sup>. The minimum turnover frequency for thiol conversion,  $k'$ , and the apparent Michaelis constant,  $K'_M$ , calculated by plotting  $1/R$  vs  $1/[ME]$ , a so-called Lineweaver Burk plot, are  $1.2 \pm 0.2 \cdot 10^3 \text{ mol ME} \cdot (\text{mol CoPc}(\text{NaSO}_3)_4 \cdot \text{s})^{-1}$  and  $2.4 \pm 0.8 \cdot 10^{-3} \text{ mol ME} \cdot \text{dm}^{-3}$ , respectively. Therefore, we can conclude that the polystyrene-ionene stabilized latices exhibit Michaelis-Menten kinetics in the mercaptoethanol autoxidation.

## 8.5 Conclusions

Monodisperse amphiphilic polystyrene-ionene diblock copolymers act as effective stabilizers during the emulsion polymerization of styrene. Colloidally stable latices with well-defined ionene chains at the particle surface are obtained when diblock copolymers are used with a low polystyrene content and a 2,4-ionene block consisting of at least 7 quaternary ammonium groups. A large part of the  $N^+$  at the latex surfaces consist of AIBA residues, which contribute to the stabilization of the latices.

After immobilization of  $\text{CoPc}(\text{NaSO}_3)_4$  a heterogeneous catalytic system is obtained which is highly active in the autoxidation of mercaptoethanol. Compared with the polymer-free system a fifteen-fold oxidation rate enhancement was observed. Furthermore, it appeared that surface charge density is an important factor but the predominant factor determining the promoting properties is the length of the cationic tails present at the particle surface.



The polystyrene-ionene stabilized latices should be preferred above other latex systems because no leaching of polyelectrolyte of the support occurs. Hence, there is no necessity to perform extensive cleaning techniques: after preparation the reactive latices can immediately be applied in catalysis.

## References

1. L. Rollmann, *J. Am. Chem. Soc.*, **97** (1975) 2132.
2. H. Ledon, Y. Brigandat, *J. Organomet. Chem.*, **165** (1979) C25.
3. A. Skorabogaty, T.D. Smith, *J. Mol. Catal.*, **16** (1982) 131.
4. H. Shirai, A. Maruyama, K. Kobayashi, N. Hojo, K. Urushido, *J. Polym. Sci., Polym. Lett. Ed.*, **17** (1979) 661.
5. M. Gebler, *Inorg. Nucl. Chem.*, **43** (1981) 2759.
6. H. Shirai, S. Higaki, K. Hanabusa, Y. Kondo, N. Hojo, *J. Polym. Sci., Polym. Chem. Ed.*, **22** (1984) 1309.
7. J.H. Schutten, C.H. van Hastenberg, P. Piet, A.L. German, *Angew. Makromol. Chem.*, **89** (1980) 201.
8. W.M. Brouwer, P.A.M. Traa, T.J.W. de Weerd, P. Piet, A.L. German, *Angew. Makromol. Chem.*, **128** (1984) 133.
9. J.W. Hof, *Post-Graduate Research Training Program*, Eindhoven University of Technology, 1990.
10. M.T. Ratering, J. Meuldijk, P. Piet, A.L. German, *React. Polymers*, **19** (1993) 233.
11. R.M. Fitch, in "Macromolecules", H. Benoit, P. Rempp, Eds., Pergamon Press, Oxford, 1982, p. 39.
12. K. Arai, Y. Maseki, Y. Ogiwara, *Makromol. Chem., Rapid Commun.*, **7** (1986) 427.
13. K. Arai, Y. Maseki, Y. Ogiwara, *Makromol. Chem., Rapid Commun.*, **7** (1986) 655.
14. A. Hopkins, A. Williams, *J. Chem. Soc., Perkin Trans. II*, (1983) 891.
15. H. Kitano, Z.-H. Sun, N. Ise, *Macromolecules*, **16** (1983) 1306.
16. Z. Sun, C. Yan, H. Kitano, *Macromolecules*, **19** (1986) 984.
17. E. Ruckenstein, L. Hong, *J. Catal.*, **136** (1992) 378.
18. W.T. Ford, H. Yu, *Langmuir*, **9** (1993) 1999.
19. J.H. Kim, M.S. El-Aasser, A. Klein, J.W. Vanderhoff, *Polym. Mater. Sci. Eng.*, **57** (1987) 819.
20. J.H. Kim, M.S. El-Aasser, A. Klein, J.W. Vanderhoff, *J. Appl. Polym. Sci.*, **35** (1988) 2117.
21. M. Tomoi, W.T. Ford, *J. Am. Chem. Soc.*, **102** (1980) 7140.
22. M. Tomoi, W.T. Ford, *J. Am. Chem. Soc.*, **103** (1981) 3821.
23. M. Bernard, W.T. Ford, T.W. Taylor, *Macromolecules*, **17** (1984) 1812.
24. R.S. Chandran, S. Srinivasan, W.T. Ford, *Langmuir*, **5** (1989) 1061.
25. W. Zhu, W.T. Ford, *J. Mol. Catal.*, **78** (1993) 367.
26. S. Srinivasan, W.T. Ford, *New J. Chem.*, **15** (1991) 693.
27. H. Turk, W.T. Ford, *J. Org. Chem.*, **56** (1991) 1253.

28. H. Turk, W.T. Ford, *J. Org. Chem.*, **53** (1988) 460.
29. H. Kitano, K. Nakamura, N. Ise, *J. Appl. Biochem.*, **4** (1982) 34.
30. M. Hassanein, W.T. Ford, *Macromolecules*, **21** (1988) 525.
31. M. Hassanein, W.T. Ford, *J. Org. Chem.*, **54** (1989) 3106.
32. S. Hari Babu, W.T. Ford, *J. Polym. Sci., Polym. Chem.*, **30** (1992) 1917.
33. K.H. van Streun, W.J. Belt, P. Piet, A.L. German, *Eur. Polym. J.*, **27** (1991) 931.
34. K.H. van Streun, W.J. Belt, E.T.W.M. Schipper, P. Piet, A.L. German, *J. Mol. Catal.*, **71** (1992) 245.
35. F. Twigt, P. Piet, A.L. German, *Eur. Polym. J.*, **27** (1991) 939.
36. F. Twigt, J. Broekman, P. Piet, A.L. German, *Eur. Polym. J.*, **29** (1993) 745.
37. H. van Beek, J.-W. Leclercq, P. Piet, A.L. German, *Makromol. Chem., Rapid Commun.*, **14** (1993) 371.
38. J.H. Fendler, E.J. Fendler, Eds., *"Catalysis in Micellar and Macromolecular Systems"*, Academic Press, New York, 1975.
39. Y. Chonde, I.M. Krieger, *J. Appl. Polym. Sci.*, **26** (1981) 1819.
40. H. Kawaguchi, M. Nakamura, M. Yanagisawa, F. Hishino, *Makromol. Chem., Rapid Commun.*, **6** (1985) 315.
41. A.M. Homola, M. Inoue, A.A. Robertson, *J. Appl. Polym. Sci.*, **19** (1975) 3077.
42. See Chapter 9.
43. I. Piirma, *Makromol. Chem., Macromol. Symp.*, **35/36** (1990) 467.
44. G.L. Jialanella, E.M. Firer, I. Piirma, *J. Polym. Sci., Polym. Chem. Part A*, **30** (1992) 1925.
45. K.H. van Streun, Ph.D. Thesis, Eindhoven University of Technology, Eindhoven, 1990.
46. W.M. Brouwer, P. Piet, A.L. German, *J. Mol. Catal.*, **31** (1985) 169.
47. See Chapter 4.
48. J. van Welzen, A.M. van Herk, A.L. German, *Makromol. Chem.*, **190** (1989) 2477.
49. A.M. van Herk, K.H. van Streun, J. van Welzen, A.L. German, *Br. Polym. J.*, **21** (1989) 125.

## Chapter 9

# Co-Catalytic Properties of Amphiphilic Diblock Copolymers on the Cobalt Phthalocyanine-Catalyzed Oxidation of 1-Dodecanethiol

**SUMMARY:** The co-catalytic properties of monodisperse 2,4-ionene oligomers and diblock copolymers, consisting of an ionene sequence and either a polystyrene block or an alkyl chain, were tested in the  $\text{CoPc}(\text{NaSO}_3)_4$ -catalyzed autoxidation of 1-dodecanethiol. A tremendous rate increase in the dodecanethiol oxidation by a factor of 100, as compared with the polymer-free system, was observed for monodisperse ionene oligomers, with four quaternary ammonium groups and with butylbromide end-groups. By contrast, the same oligomers terminated with the more hydrophilic dimethylamino end-groups showed no enhancement in the catalytic activity. These differences can be ascribed to very effective interactions between the hydrophobic butylbromide end-groups with the hydrophobic thiol, resulting in an enormous increase of the thiol-water interface. The effects of the end-groups decreases with increasing number of  $\text{N}^+$ . 2,4-Ionenes with at least 8 quaternary ammonium groups showed similar co-catalytic properties as the high molecular weight 2,4-ionenes. Moreover, the effect of end-capping of polymeric 2,4- and 3,3-ionenes even with long *n*-alkylbromides is limited. Well-defined amphiphilic diblock copolymers, consisting of an oligomeric quaternary ammonium block, and a polystyrene block, in combination with  $\text{CoPc}(\text{NaSO}_3)_4$  exhibited very high catalytic activities ( $775 \text{ mol O}_2/(\text{mol Co}\cdot\text{s})$ ), *i.e.* 40 times higher as compared with the polymer-free system, due to a combination of the formation of the more active dimers and hydrophobic interactions with the hydrophobic thiol. This hydrophobic interaction resulted in an enhancement of the oxidation rate by a factor of 2.5, as compared with 2,4-ionene.

## 9.1 Introduction

So far all attention has been focused on the effects of polymers on the cobalt phthalocyanine-catalyzed autoxidation of the water-soluble mercaptoethanol. Unfortunately, little is known about the more complex reaction mechanism of the oxidation of hydrophobic thiols. First, Brouwer investigated the effects of surfactants on the 1-dodecanethiol (dodecylmercaptan, DM) oxidation<sup>1</sup>. In the presence of a cationic surfactant (CTAB), a micellar mechanism was proposed with the characteristics of Michaelis-Menten kinetics. Ford *et al.* studied the effects of cationic latices as co-catalyst in the autoxidation of 1-decanethiol catalyzed by  $\text{CoPc}(\text{NaSO}_3)_4$ <sup>2,3</sup>.

Furthermore, Van Welzen studied the use of hydrophilic and hydrophobic ionenes as promoters in the oxidation of the water-insoluble 1-dodecanethiol<sup>4</sup>. It appeared that, when applying the hydrophilic 2,4-ionene as a co-catalyst extremely high catalytic activities were observed. By contrast, the more hydrophobic 2,10-ionene exhibited very low activities, despite the more hydrophobic character of the type of thiol. 2,10-Ionene, with a soap-like character, is incapable of inducing aggregation of  $\text{CoPc}(\text{NaSO}_3)_4$  due to its hydrophobic  $\text{C}_{10}$ -segments<sup>5</sup>. In addition, it was demonstrated that oleyl-3,3-ionene, which is 3,3-ionene extended with a  $\text{C}_{18}$ -alkyl chain, showed further enhancement of the catalytic activity in the oxidation of hydrophobic thiols as compared with the homogeneous 2,4-ionene<sup>4</sup>. This effect was ascribed to the hydrophobic interactions of the alkyl chain with the hydrophobic 1-dodecanethiol.

Our goal is to design an extremely effective polymeric promoter for catalytic hydrophobic thiol autoxidations. The prerequisites should be a hydrophobic chain for efficient interaction with the hydrophobic thiol and an ionene chain for the binding of the  $\text{CoPc}(\text{NaSO}_3)_4$  catalyst in its most active dimeric form. Therefore, it is imperative to know what the length of the hydrophobic as well as the hydrophilic block should be, necessary to achieve the highest possible oxidation rates.

In this chapter we describe the study of the influence of the molecular weight of 2,4-ionene on the autoxidation of 1-dodecanethiol. The 2,4-ionene chain length appeared to have a large influence in the  $\text{CoPc}(\text{NaSO}_3)_4$ -catalyzed oxidation of the hydrophilic mercaptoethanol<sup>6</sup>. The contribution of the end-group of the ionene, the interaction with

the hydrophobic thiol, is examined by testing 2,4- and 3,3-ionene, end-capped with different type of end-groups, as a co-catalyst. Subsequently, the co-catalytic properties of the well-defined amphiphilic polystyrene-ionene diblock copolymers, which synthesis procedure is described in Chapter 7, are studied in order to elucidate the effect of the block lengths. In the end, this will lead to an extremely efficient promoter in the CoPc(NaSO<sub>3</sub>)<sub>4</sub>-catalyzed dodecanethiol autoxidation.

## 9.2 Experimental Procedures

### 9.2.1 Synthesis of End-Capped Ionenes

The preparative procedures of the monodisperse oligomeric ionenes, *i.e.* N-trimer, Br-trimer, N-pentamer, Br-pentamer, N-heptamer and Br-nonamer, have been described in Chapter 3. The polymeric 2,4-ionenes were prepared according to the method developed by Rembaum *et al.*<sup>7)</sup>, which was described in Chapter 3. The number average molecular weights of the dimethylamino terminated 2,4-ionenes used are 1.2, 2.2, 3.1, 6.0, 7.8 and 22 kg/mol. The  $\bar{M}_n$ 's of the butylbromide end-capped 2,4-ionenes are 1.7 and 8.0 kg/mol. 3-(Dimethylamino)propyl chloride (DMAP-Cl), the monomer of 3,3-ionene, was isolated from its hydrochloric salt according to a method described elsewhere<sup>8)</sup>. 3,3-Ionene was synthesized by reacting 22.5 g (0.185 mol) of DMAP-Cl in 53 ml of *N,N*-dimethylformamide (DMF) and 13 ml of water for 24 h at 50 °C. Next, the product was precipitated in acetone, filtered off, washed with acetone and dried at reduced pressure at 50 °C.

2,4-Ionene ( $\bar{M}_n = 7.8$  kg/mol) and 3,3-ionene ( $\bar{M}_n = 8.7$  kg/mol) were extended with different *n*-alkylbromides: 2 g of 2,4- or 3,3-ionene was reacted with a three-fold excess of 1-bromobutane (99+ %) or benzylbromide (98 %) in 20 ml DMF/water (50/50, v/v) for 7 d at 50 °C. The reaction time was increased to three weeks when the ionene was reacted with a three-fold excess of 1-bromodecane (98 %) or 1-bromooctadecane (96 %). In the case of coupling ionene with 1,4-dibromobutane (99 %) a ten-fold excess was used. Titration of the obtained ionenes showed the absence of dimethylamino end-groups.

The synthesis of the amphiphilic polystyrene-ionene diblock copolymers has been extensively described in Chapter 7. All chemicals were obtained from Janssen Chimica and were used without any further purification.

### 9.2.2 Catalytic Activity Measurements

The procedure for the autoxidation of 1-dodecanethiol has been described in Chapter 3. Only in the case of the polystyrene-ionene diblock copolymers a modification of the reaction procedure was utilized. The polystyrene-ionene diblock copolymers were first dissolved in a solution of 2 ml of DMF and placed in the reactor. Then, the catalytic measurements were started by addition of  $\text{CoPc}(\text{NaSO}_3)_4$  to the oxygen-saturated mixture of polystyrene-ionene block copolymer and 1-dodecanethiol in a DMF/water mixture (2/98, v/v) at  $\text{pH} = 13$ .

## 9.3 Influence of the Molecular Weight of 2,4-Ionene on the $\text{CoPc}(\text{NaSO}_3)_4$ -Catalyzed Oxidation of 1-Dodecanethiol

Initially, we examined the influence of the molecular weight of 2,4-ionene on the cobalt phthalocyanine-catalyzed autoxidation of the very sparsely water-soluble 1-dodecanethiol using monodisperse oligomeric 2,4-ionenes. These oligomers already proved to be excellent tools in the study of the influence of the molecular weight on the  $\text{CoPc}(\text{NaSO}_3)_4$ -catalyzed autoxidation of the hydrophilic mercaptoethanol<sup>6)</sup>. In Fig. 9.1 the dodecanethiol oxidation rates are plotted as a function of the polymer/ $\text{CoPc}(\text{NaSO}_3)_4$  ratio, expressed as  $\text{N}^+/\text{Co}$  ratio, for both trimeric 2,4-ionenes, *i.e.* the dimethylamino- (N-trimer) and butylbromide terminated trimer (Br-trimer).

Very low oxidation rates can be observed in the case of the N-trimer as co-catalyst: even at high oligomer concentrations no rate enhancement occurs as compared with the polymer-free system. By contrast, the Br-trimer/ $\text{CoPc}(\text{NaSO}_3)_4$  combination reveals very high catalytic activities. Remarkably, for a  $\text{N}^+/\text{Co}$  ratio higher than 3000 the reaction rate even exceeds the catalytic activity found for the polymeric 2,4-ionene promoting dodecanethiol oxidation<sup>4)</sup>.

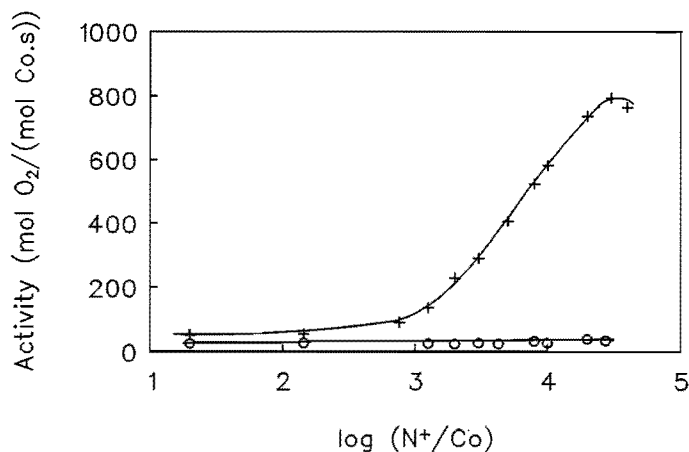


Figure 9.1 Effect of  $N^+/Co$  ratio on the 1-dodecanethiol oxidation rate.  $[CoPc(NaSO_3)_4] = 8 \cdot 10^{-7} \text{ mol} \cdot \text{dm}^{-3}$ ,  $pH = 13$ ,  $[DM] = 2.1 \cdot 10^{-2} \text{ mol} \cdot \text{dm}^{-3}$ ; (+) Br-trimer, (o) N-trimer.

Such tremendous discrepancies between the co-catalytic behaviour of both trimers were not observed in the homogeneous mercaptoethanol oxidation<sup>9</sup>. In that case similar high oxidation rates were observed for both trimeric oligomers. In fact the N-trimer and the Br-trimer differ in their end-group and in their distance between the two quaternary ammonium groups. The difference in distance was illustrated by their ability to stabilize the active dimeric form of the catalyst. Based on the UV-VIS spectroscopic properties of both trimers, the N-trimer appeared to be most effective in inducing aggregation of the catalyst and its spectroscopic behaviour was almost similar as that of polymeric 2,4-ionene<sup>9</sup>. Therefore, the dissimilarity in distance between the ammonium groups in the trimers can not account for the controversy in the dodecanethiol oxidation rates. It must be caused by the difference in hydrophobicity of the end-group of the trimers. Evidently, the dimethylamino end-group of the N-trimer is too hydrophilic to interact with the 1-dodecanethiol. However, the butylbromide end-group of the Br-trimer is more hydrophobic and is therefore capable of interacting with the thiol. Hence, the immense increase in catalytic activity at raising Br-trimer concentrations can be ascribed to the interaction between the butylbromide end-groups and the thiol, which leads to the formation of smaller thiol droplets and, therefore, to an increase in total reaction interface.



In Chapter 4 and 5 it was already demonstrated that the type of end-group had no effect on the maximal mercaptoethanol oxidation rates. However, the optimal  $N^+/Co$  ratios of butylbromide terminated oligomers were lower as compared with the corresponding dimethylamino terminated oligomers. This effect was ascribed to domain formation of the butylbromide end-capped oligomers: lower oligomer concentrations were required to achieve an effective substrate enrichment.

Also, for the two oligomeric ionenes with four quaternary ammonium groups, *i.e.* the N-pentamer and the Br-pentamer (Fig. 3.3), a similar effect of the end-group on the catalytic oxidation of 1-dodecanethiol was found. Keeping the concentration of the catalyst constant and increasing the concentration of the butylbromide terminated pentamer the activity rises to very high values (Fig. 9.2). Moreover, no clear optimum in the catalytic activity was realized, as observed for the Br-pentamer promoted mercaptoethanol oxidation<sup>6</sup>. The activity measured at large amounts of Br-pentamer is even almost a 10-fold as high as that measured for polymeric 2,4-ionene. The N-pentamer shows only a slight increasing activity. For  $N^+/Co$  is  $10^4$  the turnover frequency is 120, which is 5 times lower than that with the Br-pentamer.

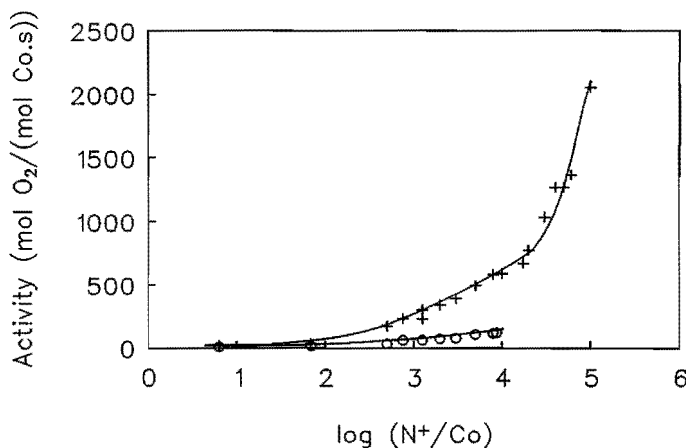


Figure 9.2 Effect of  $N^+/Co$  ratio on the 1-dodecanethiol oxidation rate.  
 $[CoPc(NaSO_3)_4] = 8 \cdot 10^{-7} \text{ mol} \cdot \text{dm}^{-3}$ ,  $pH = 13$ ,  
 $[DM] = 2.1 \cdot 10^{-2} \text{ mol} \cdot \text{dm}^{-3}$ ; (+) Br-pentamer, (o) N-pentamer.

Additionally, we measured for the monodisperse N-heptamer and Br-nonamer oligomers, and for polymeric 2,4-ionenes, comprising the whole range of molecular weights, the effect of varying the  $N^+$ -concentration on the dodecanethiol oxidation rate. In Fig. 9.3 the optimal  $N^+/Co$  ratios at the maximal activities are presented as a function of the chain length of 2,4-ionene. It can be seen that the optimal  $N^+/Co$  ratios of the butylbromide terminated oligomeric 2,4-ionenes are reached at very high values in combination with very high oxidation rates (see Fig. 9.4). Also, the N-terminated oligomers exhibit high optimal  $N^+/Co$  ratios, but as shown in Fig. 9.4 their corresponding maximal activities are rather low. Furthermore, it can be noticed that the Br-nonamer with 8 quaternary ammonium groups and the polymeric 2,4-ionenes exhibit a similar co-catalytic behaviour with respect to the optimal  $N^+/Co$  ratio as well as to the maximal activity. Only when oligomeric ionenes with two, four or six quaternary ammonium groups are used, the end-group significantly affects both the optimal  $N^+/Co$  ratio and the corresponding maximal activity.

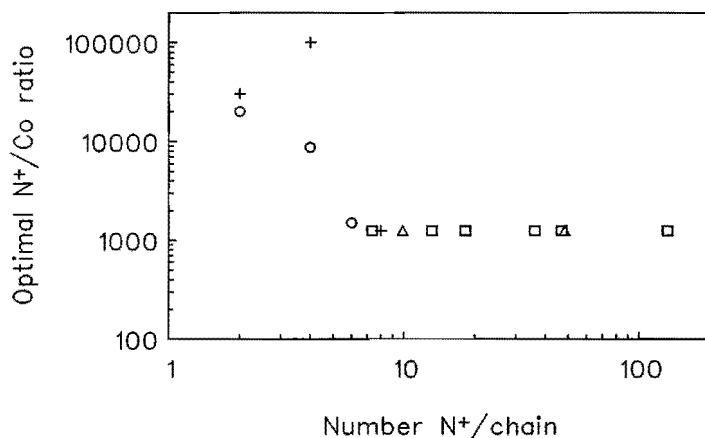


Figure 9.3 The optimal  $N^+/Co$  ratio as a function of the number of quaternary ammonium groups per chain.

$[CoPc(NaSO_3)_4] = 8 \cdot 10^{-7} \text{ mol} \cdot \text{dm}^{-3}$ ,  $pH = 13$ ,

$[DM] = 2.1 \cdot 10^{-2} \text{ mol} \cdot \text{dm}^{-3}$ ;

(+) Br-terminated and (o) N-terminated monodisperse oligomers,

(Δ) Br-terminated and (□) N-terminated polymeric 2,4-ionenes.

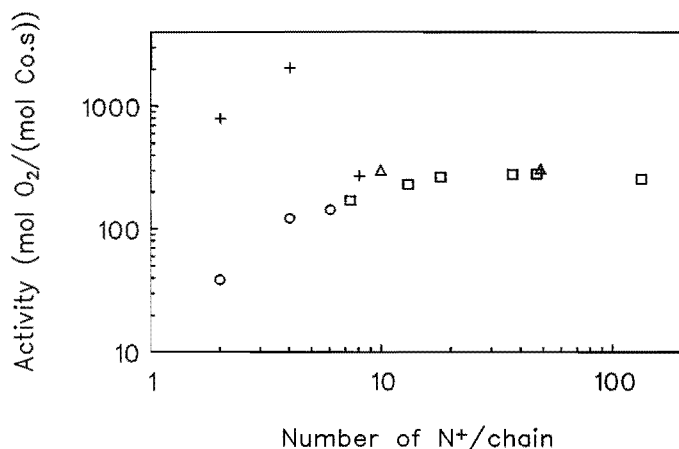


**Figure 9.4** *The maximum catalytic activities at the optimal  $N^+/Co$  ratios as a function of the number of quaternary ammonium groups per chain.  $[CoPc(NaSO_3)_4] = 8 \cdot 10^{-7} \text{ mol} \cdot \text{dm}^{-3}$ ,  $pH = 13$ ,  $[DM] = 2.1 \cdot 10^{-2} \text{ mol} \cdot \text{dm}^{-3}$ ; (+) Br-terminated and (o) N-terminated monodisperse oligomers, (Δ) Br-terminated and (□) N-terminated polymeric 2,4-ionenes.*

Obviously, the interactions between the thiol and the polymer plays a more important role than the formation of the dimeric catalyst species. As proposed by Van Welzen the oxidation proceeds at the interface of the thiol droplet and the water phase<sup>4</sup>). Therefore, an improved interaction between thiol and butylbromide end-groups will lead to smaller thiol droplets and consequently higher oxidation rates. Such an interaction apparently does not occur for oligomers with dimethylamino end-groups.

The influence of the end-group on the dodecanethiol oxidation was already demonstrated by 3,3-ionene, extended with one  $C_{18}$ -alkyl chain, which showed an increase in activity due to hydrophobic interactions<sup>4</sup>). In order to investigate the influence of the end-group, we extended polymeric 2,4-ionene and 3,3-ionene, both with a similar charge density, with different  $n$ -alkylbromides. For 3,3-ionene ( $\bar{M}_n = 8.7 \text{ kg/mol}$ ) terminated at one chain end with the  $n$ -alkylbromides, no rate enhancement was found. Obviously, the 3,3-ionene chain is too long compared with its end-group.

Also, the end-capping of 2,4-ionene ( $\bar{M}_n = 7.8$  kg/mol) has a rather limited effect on the catalytic dodecanethiol oxidation rate, despite the fact that 2,4-ionene is extended at both chain ends. Even with the large *n*-alkyl chains no significant increase in activity was observed. Extension with butylbromide, decylbromide, stearyl bromide or benzylbromide resulted in a small rate increase in the oxidation rate (maximally 50 %), as compared with the dimethylamino terminated 2,4-ionene. Based on these experimental observations and the molecular weight dependence on the DM oxidation, it can be concluded that the influence of the end-group of 2,4-ionene on the thiol oxidation diminishes drastically when the molecular weight of 2,4-ionene increases.

#### 9.4 Influence of Amphiphilic Polystyrene-Ionene Diblock Copolymers on the CoPc(NaSO<sub>3</sub>)<sub>4</sub>-Catalyzed Oxidation of 1-Dodecanethiol

The monodisperse amphiphilic polystyrene-ionene diblock copolymers<sup>9)</sup> which have been applied as surfactant in the emulsion polymerization of styrene<sup>10)</sup>, also give us the opportunity to study their co-catalytic behaviour in the dodecanethiol oxidation. Especially due to their monodisperse character and their relatively short ionene chains, these block copolymers can perfectly be used to investigate the influence of the block length of the ionene block as well as the length of the polystyrene block on the activity.

Catalytic autoxidation experiments of 1-dodecanethiol so far were performed in water<sup>4)</sup>. Using the normal procedure, described in Chapter 3, only very low catalytic activities were achieved, due to the low solubility of the block copolymer B consisting of 9 N<sup>+</sup> (**B-9**,  $\bar{M}_n(\text{polystyrene}) = 2.7$  kg/mol and  $\bar{M}_n(2,4\text{-ionene}) = 1.5$  kg/mol)<sup>9)</sup>, a behaviour characteristic of block copolymers having hydrophobic sequences. Selb *et al.* observed that a polystyrene-poly(vinylpyridinium) block copolymer was completely insoluble in water, despite its very high vinylpyridinium content (94%)<sup>11)</sup>. These results emphasize that the poor solubility arises from a hindering of the penetration of water into the hydrophobic domains of the polystyrene, and therefore cannot sufficiently swell and break up the structure of the solid particles. Several authors have reported before that the dissolution of copolymers apparently insoluble in water can be achieved by first dissolving the copolymer in a better solvent. Selb was able to dissolve the block

copolymer in a water-methanol mixture (1 vol.-% methanol). Schwab dissolved polystyrene-*b*-quaternized poly(2-vinylpyridine) in a THF-water mixture and then stripped off the THF under vacuum<sup>12)</sup>.

A modification of the dissolving procedure of **B-9** had to be developed, which would first destroy the packing of the macromolecules, after which the copolymer can exhibit its real micellar properties. First of all, we tried to swell and dissolve the block copolymer **B-9** in 1-dodecanethiol, but only a low solubility and consequently a low activity was realized. However, it appeared that the applied amount of block copolymer in the catalytic experiments could be dissolved in 2 ml of DMF, after which it was introduced in the reactor.

It should be mentioned here that the phthalocyanine-aggregates, the catalytically most active species, are known to dissociate into monomeric species upon addition of DMF<sup>13)</sup> in an aqueous polymer-free system, but if the mixture of DMF and water also contained ionene, then the aggregates will remain<sup>14)</sup>. The addition of DMF will probably not affect the catalytically active aggregates, but only enhance the solubility of the ionic block copolymer **B-9**. Nevertheless, it is possible that the solubility of 1-dodecanethiol increases and therefore the catalytic activities could be influenced. In order to check these considerations, the catalytic activities of the  $\text{CoPc}(\text{NaSO}_3)_4/2,4\text{-ionene}$  complex for the autoxidation of 1-dodecanethiol in a DMF/mixture were compared with those achieved in water. In Fig. 9.5 the  $\text{N}^+/\text{Co}$  ratio is depicted as a function of the oxidation rate of 1-dodecanethiol in a DMF/water (2/98, v/v) mixture. When comparing the optimal  $\text{N}^+/\text{Co}$  ratio, the corresponding optimal activity and the shape of the curve with the properties of the aqueous systems<sup>4)</sup>, no differences were found. Thus the modification of the reaction procedure, *e.g.* first dissolving the block copolymer in DMF, assures that the entire block copolymer is dissolved and available to interact with the catalyst and substrates. So the assumption is reasonable that DMF does not affect the catalytic experiments.

The effect of the hydrophobic block on the catalytic activity, using block copolymer **B-9** is presented in Fig. 9.5. The maxima in the curves arise because of the electrostatic interaction of the ionene with the thiolate anions present at the thiol-water interface<sup>4)</sup>. At low ionene concentrations, where the oxidation rate is low, only a small part of the thiol droplet interface interacts with the  $\text{CoPc}(\text{NaSO}_3)_4/2,4\text{-ionene}$  complex. Upon increasing

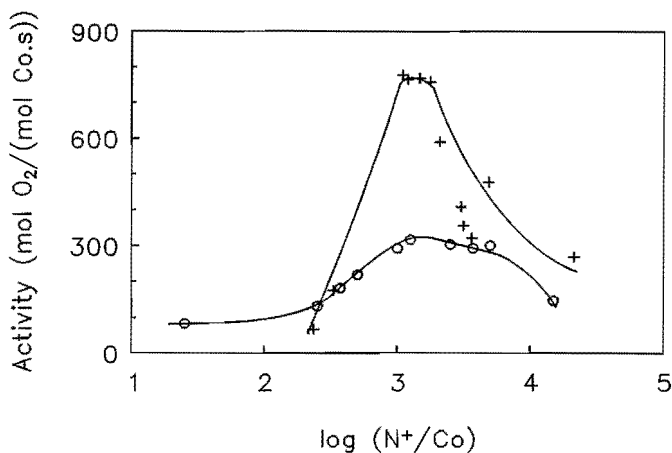


**Figure 9.5** Catalytic activity as function of the  $N^+/Co$  ratio.  
 $[CoPc(NaSO_3)_4] = 2 \cdot 10^{-7} \text{ mol} \cdot \text{dm}^{-3}$ ,  $pH = 13$ ,  
 $[DM] = 2.1 \cdot 10^{-2} \text{ mol} \cdot \text{dm}^{-3}$ ,  $DMF/H_2O = 2/98$  (v/v);  
 (o) 2,4-ionene, (+) polystyrene-2,4-ionene block copolymer **B-9**.

the ionene concentration, the ionene-thiol contact surface also increases, resulting in an increased activity. After reaching a maximum, further addition of ionene leads to an increase of the ionene concentration in the continuous phase, which will probably bind a part of the cobalt-complex, leading to a lower turnover frequency.

Comparing the block copolymer **B-9** with 2,4-ionene, no significant differences can be determined between the optimal  $N^+/Co$  ratios. As a result of the hydrophobic interaction of the polystyrene block with the hydrophobic thiol, the optimal catalytic activity of the block copolymer is 2.5-fold higher than that of 2,4-ionene (Tab. 9.1).

Since such high oxidation rates were reached, even 40 times higher than in the polymer-free system, we also tried to study the influence of the length of the ionene block on the activity. After testing block copolymer **B-4**<sup>9)</sup> with only 4  $N^+$  as co-catalyst, it turned out that under the same conditions similar reaction rates ( $600 \text{ mol O}_2 / (\text{mol Co} \cdot \text{s})$ ) were achieved. Obviously, the quaternary ammonium groups of the ionene are concentrated at the thiol-water interface and several ionene chains collectively contribute to the stabilization of dimers of  $CoPc(NaSO_3)_4$ . If block copolymers were used with a higher polystyrene

Table 9.1 Catalytic DM oxidation rates of several  $\text{CoPc}(\text{NaSO}_3)_4$ -containing systems

	Maximal rate (mol $\text{O}_2$ /(mol Co · s)) at optimal $\text{N}^+/\text{Co}$ ratio
$\text{OH}^-$	20
2,4-ionene	310
<b>B-4</b>	600
<b>B-9</b>	775
<b>F-7</b>	285

Conditions:  $[\text{CoPc}(\text{NaSO}_3)_4] = 2 \cdot 10^{-7} \text{ mol} \cdot \text{dm}^{-3}$ ,  $\text{pH} = 13$ ,  
 $[\text{DM}] = 2.1 \cdot 10^{-2} \text{ mol} \cdot \text{dm}^{-3}$ ,  $\text{N}^+/\text{Co} = 1250$ ,  $\text{DMF}/\text{H}_2\text{O} = 2/98$  (v/v).

content, like **F-7** ( $\overline{M}_n(\text{polystyrene}) = 12.6 \text{ kg/mol}$ ) with 7 quaternary ammonium groups<sup>9</sup>, the resulting activities were comparable with those observed for 2,4-ionene. Due to the high polystyrene/ionene ratio of the block copolymer used, precipitation of the polymer during the catalytic experiments is the reason for such relatively low reaction rates. Therefore, it can be concluded that very high catalytic activities can be achieved when using ionic diblock copolymers, containing a relatively short ionene block necessary for electrostatic interaction with the catalyst, and a hydrophobic polystyrene block, with restricted block length, providing enhanced substrate enrichment by hydrophobic interactions.

## 9.5 Conclusions

The end-group of oligomeric 2,4-ionenes appears to play a dominant role in the  $\text{CoPc}(\text{NaSO}_3)_4$ -catalyzed 1-dodecanethiol autoxidation. Butylbromide terminated oligomers with 2 or 4 quaternary ammonium groups exhibit very high efficient co-catalytic properties. Even higher catalytic activities, as compared with the analogous hydrophilic homopolymer 2,4-ionene, could be achieved. These n-butylbromide end-groups expose very large interactions with the thiol droplets, leading to an enlarged contact interface.

By contrast, the dimethylamino end-capped ionenes exhibit almost no interaction with the thiol, resulting in very low catalytic activities.

Additionally, it has been demonstrated that diblock copolymers, consisting of an ionene sequence and a polystyrene block, show a significant increase in the catalytic activity in the autoxidation of the hydrophobic thiol as compared with the homopolymer of 2,4-ionene. Hence, it can be concluded that polystyrene provided with an ionene sequence consisting of at least four quaternary ammonium groups is a very effective promoter for the CoPc(NaSO<sub>3</sub>)<sub>4</sub>-catalyzed oxidation of 1-dodecanethiol.



## References

1. W.M. Brouwer, P. Piet, A.L. German, *J. Mol. Catal.*, **29** (1985) 347.
2. M. Hassanein, W.T. Ford, *Macromolecules*, **21** (1988) 525.
3. M. Hassanein, W.T. Ford, *J. Org. Chem.*, **54** (1989) 3106.
4. J. van Welzen, A.M. van Herk, A.L. German, *J. Mol. Catal.*, **60** (1990) 351.
5. J. van Welzen, A.M. van Herk, A.L. German, *Makromol. Chem.*, **190** (1989) 2477.
6. See Chapter 4.
7. A. Rembaum, W. Baumgartner, E. Eisenberg, *J. Polym. Sci. Polym. Lett. Ed.*, **6** (1968) 159.
8. S.P.S. Yen, D. Casson, A. Rembaum, in *"Water Soluble Polymers"*, N.M. Bikalis, Ed., Plenum, New York, 1973.
9. See Chapter 7.
10. See Chapter 8.
11. J. Selb, Y. Gallot, *Makromol. Chem.*, **182** (1981) 1775.
12. F.C. Schwab, I.J. Heilweil, *Polym. Prep. (Am. Chem. Soc., Div. Polym. Chem.)*, **24** (1) (1983) 65.
13. J.A. de Bolfo, T.D. Smith, J.F. Boas, J.R. Pilbrow, *J. Chem. Soc., Faraday Trans. II*, **72** (1976) 481.
14. J. van Welzen, A.M. van Herk, A.L. German, *Makromol. Chem.*, **189** (1988) 587.

## Chapter 10

### Effects of Solvents on the Cobalt Phthalocyanine-Catalyzed Oxidation of Hydrophobic Thiols

**SUMMARY:** The use of organic solvents in the oxidation of 1-dodecanethiol, catalyzed by  $\text{CoPc}(\text{NaSO}_3)_4/2,4\text{-ionene}$ , drastically influences the reaction mechanism. Without an organic solvent the reaction proceeds at the thiol-water phase-boundary, where the ionene interacts with the negatively charged dodecanethiol droplets. The degree of complexation between the 2,4-ionene and the thiolate anions diminishes when apolar solvents, like toluene, are added. This leads to a tremendous shift of the  $\text{N}^+/\text{Co}$  ratio, which is a measure of the optimal ionene/ $\text{CoPc}(\text{NaSO}_3)_4$  ratio, from 1250 to 15. Only the maximal catalytic activity is dependent on the amount of apolar solvent used over the whole range of solvent compositions. It is proposed that the reaction proceeds at the phase-boundary, but the degree of complexation between the quaternary ammonium groups of the ionene and the thiolate anions decreases with addition of an apolar solvent. The low optimal  $\text{N}^+/\text{Co}$  ratio of about 15 is apparently sufficient for both binding the ionene to the droplet surface as well as for stabilizing the active dimeric form of the catalyst. When water-insoluble more polar solvents such as 1-octanol are used, the opposite phenomenon is observed: the optimal 2,4-ionene concentration rises. In the latter situation the 2,4-ionene is still able of interacting strongly with the thiolate anions present at the interface of the droplets.

## 10.1 Introduction

In the previous chapter it was illustrated that the addition of monodisperse ionene oligomers, with four quaternary ammonium groups and with butylbromide end-groups, caused a tremendous rate increase in the 1-dodecanethiol (DM) oxidation by a factor of 100 as compared with the polymer-free system. However, some disadvantages of the dodecanethiol oxidation have been reported with  $\text{CoPc}(\text{NaSO}_3)_4/2,4\text{-ionene}$  in water as catalyst<sup>1)</sup>. First, it appeared that  $\text{H}_2\text{O}_2$ , formed at the thiol-water interface, is directly transported to the bulk of the aqueous phase. The non-catalytic consecutive reaction step of  $\text{H}_2\text{O}_2$  reacting with RSH is therefore impossible. Second, accumulation of  $\text{H}_2\text{O}_2$  could be a problem, because  $\text{H}_2\text{O}_2$  may cause breakdown of the  $\text{CoPc}(\text{NaSO}_3)_4$ -complex<sup>2)</sup>. In addition, it was mentioned that during the precipitation of the insoluble disulfide entrainment of the catalyst occurred<sup>1)</sup>. This could lead to a loss of activity in case of continuous operation.

Addition of solvents, in which substrate as well as product are soluble, will probably reduce the drawbacks and will lead to an enhancement of the reaction rate. Generally, organic solvents have been used before because of the insolubility of the thiol in water. For example, Ford *et al.*<sup>3)</sup> added methanol to increase the oxidation rate of 1-decanethiol catalyzed by  $\text{CoPc}(\text{NaSO}_3)_4$  electrostatically bound onto cationic latices. Other examples are known, where the water-insoluble thiol was dissolved in an organic solvent and the catalyst was immobilized onto polymeric supports<sup>4-6)</sup>.

In this chapter, the influence of different solvents on the catalytic oxidation of 1-dodecanethiol will be described. First, in order to study the effect of deactivation that is probably caused by co-precipitation of the disulfide and the catalytic complex, the reaction rate in consecutive runs are examined with and without an organic solvent. It appeared that addition of an apolar solvent, in which 1-dodecanethiol dissolves, had such a drastic influence on the optimal reaction conditions that further attention was focused on gaining a better understanding of the reaction mechanism. The influence of several parameters such as type of ionene and type of solvent and pH was studied. Contrasting effects, obtained with water-insoluble more polar solvents, have also been considered. Additionally, the oxidation of dodecanethiol in a homogeneous medium is discussed.

## 10.2 Experimental Section

### *Catalytic activity measurements*

The catalytic experiments proceeded according to the procedure mentioned in Chapter 3. The total reaction volume, *e.g.* water and organic solvents, was always  $0.1 \text{ dm}^3$ . Unless stated otherwise the 1-dodecanethiol concentration was  $2.1 \cdot 10^{-2} \text{ mol} \cdot \text{dm}^{-3}$  (= 0.5 vol.-%). In all experiments the hydroxide anion concentration was kept constant at  $0.1 \text{ mol} \cdot \text{dm}^{-3}$ , based on the total reaction volume. Toluene (Merck, p.a.), n-hexane (Merck, p.a.), n-dodecane (Janssen Chimica, 99+ %), cyclohexane (Merck, p.a), 1-octanol (Janssen Chimica, 99%), 1-decanol (Janssen Chimica, 99%) and 1-dodecanol (Janssen Chimica, 98 %) were used without any further purification.

### *Characterization*

The  $\text{H}_2\text{O}_2$  concentration was determined spectrophotometrically using  $\text{TiCl}_3\text{-H}_2\text{O}_2$  as reagent<sup>7)</sup>.  $\text{H}_2\text{O}_2$  contents of the reaction mixtures were measured after complete thiol conversion. 1-Dodecanethiol concentrations were determined by gas chromatography (GC) on a Hewlett Packard 5890 II, equipped with an apolar capillar column (5 m, 530  $\mu\text{m}$  HPI). 1-Dodecanol was used as internal standard. A Malvern autosizer IIc was used to measure droplet size distributions. The surface tension properties of DM in water were performed with a Sensa Dyne Bubble Tensiometer and with a Krüss Tensiometer K10T (ring method). The latter method was also used to determine the interfacial tension between an organic phase, consisting of 1-dodecanethiol and/or toluene, and water.

## 10.3 Results and Discussion

During the  $\text{CoPc}(\text{NaSO}_3)_4$ -catalyzed oxidation of 1-dodecanethiol the water-insoluble didodecyldisulfide is formed. This disulfide precipitates in water and is assumed to be able to capture the cobalt complex and the ionene<sup>1)</sup>. We investigated the influence of addition of toluene, in which both the substrate and the disulfide dissolve. This could prevent any possible deactivation. In Fig. 10.1 the oxidation rates are presented in

consecutive runs, with and without toluene. It should be remarked that we can not use the normal reaction procedure for DM oxidations. This leads, in case of DM oxidations in water, to lower activities when the reactions are started by addition of DM instead of cobalt catalyst<sup>1)</sup>.

No significant deactivation can be observed after several runs. The disulfide formed precipitates, but is apparently not able of co-precipitating the catalyst-complex. However, in a toluene-water mixture, with a lower ionene concentration, a decrease in reaction rate can be observed. Nevertheless, higher catalytic activities are observed as compared with the toluene-free system, even after several runs.

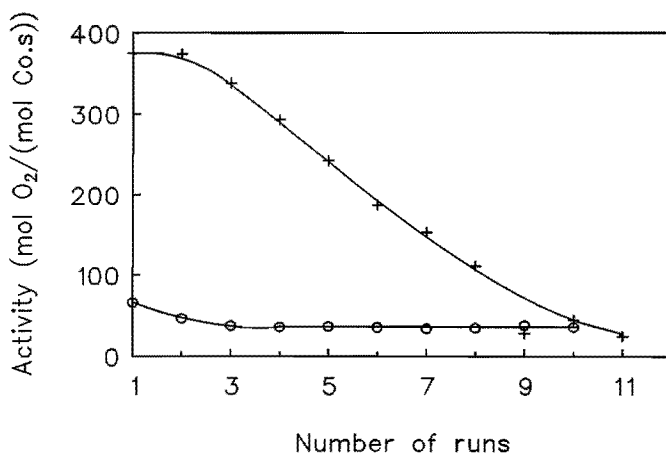


*Figure 10.1* The 1-dodecanethiol oxidation rate in successive runs.  
 $[CoPc(NaSO_3)_4] = 8 \cdot 10^{-7} \text{ mol} \cdot \text{dm}^{-3}$ ,  $[OH^-] = 0.1 \text{ mol} \cdot \text{dm}^{-3}$ ,  
 $[DM] = 2.1 \cdot 10^{-2} \text{ mol} \cdot \text{dm}^{-3}$ , 2,4-ionene ( $\bar{M}_n = 15000 \text{ g} \cdot \text{mol}^{-1}$ ).  
 (+) Toluene/water, vol.-%/vol.-% = 5/94.5,  $[N^+] = 10^{-5} \text{ mol} \cdot \text{dm}^{-3}$ ;  
 (o) no toluene,  $[N^+] = 10^{-3} \text{ mol} \cdot \text{dm}^{-3}$ .

Furthermore, it appeared that less ionene was needed in order to obtain high oxidation rates. In order to study the drastic influence of toluene on the optimal catalytic conditions, the effect of the amount of toluene in toluene/water mixtures on the optimal  $N^+/Co$  ratio and on their corresponding maximal catalytic activities of the dodecanethiol oxidation was examined (Fig. 10.2 and 10.3). It can be seen that addition of a relatively small amount

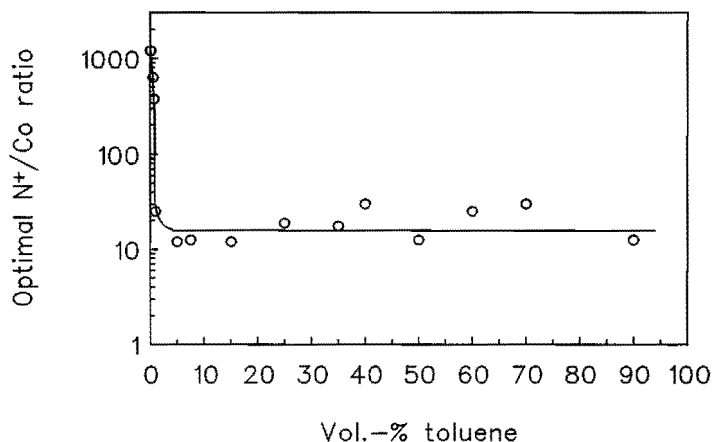


Figure 10.2 Optimal  $N^+/Co$  ratios of the 1-dodecanethiol oxidation as a function of the toluene concentration in toluene/water mixtures.

$$[CoPc(NaSO_3)_4] = 8 \cdot 10^{-7} \text{ mol} \cdot \text{dm}^{-3},$$

$$[DM] = 2.1 \cdot 10^{-2} \text{ mol} \cdot \text{dm}^{-3}, \text{ 2,4-ionene } (\bar{M}_n = 5000 \text{ g} \cdot \text{mol}^{-1}).$$

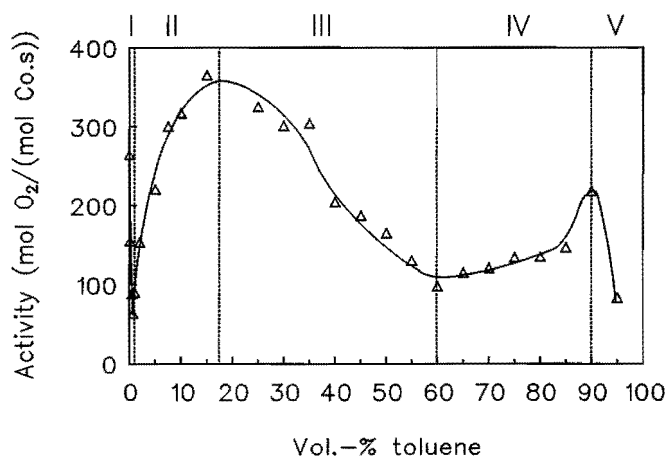
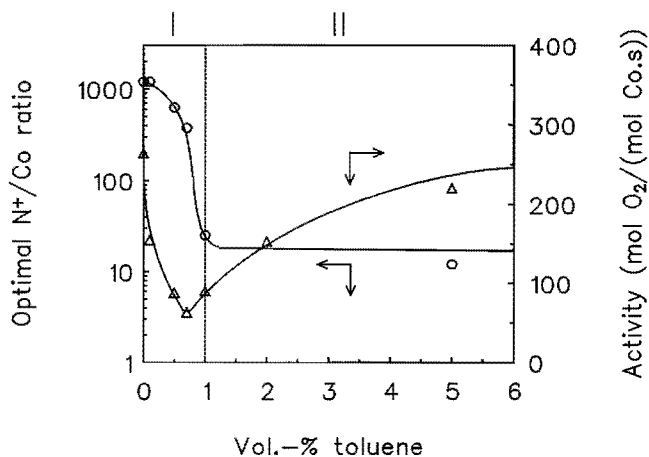


Figure 10.3 Maximal 1-dodecanethiol oxidation rates at optimal  $N^+/Co$  ratios as a function of the toluene concentration in toluene/water mixtures.

$$[CoPc(NaSO_3)_4] = 8 \cdot 10^{-7} \text{ mol} \cdot \text{dm}^{-3},$$

$$[DM] = 2.1 \cdot 10^{-2} \text{ mol} \cdot \text{dm}^{-3}, \text{ 2,4-ionene } (\bar{M}_n = 5000 \text{ g} \cdot \text{mol}^{-1}).$$

of toluene results in a tremendous shift of the optimal  $N^+/Co$  ratio, which is a measure of the optimal 2,4-ionene/ $CoPc(NaSO_3)_4$  ratio, from 1250 to 15. Because of the rapid drop in the optimal  $N^+/Co$  ratio upon addition of a small amount of toluene, in Fig. 10.4 the optimal  $N^+/Co$  ratios and the maximal oxidation rates are plotted comprising the range of 0 to 6 vol.-% of toluene.



**Figure 10.4** Maximal 1-dodecanethiol oxidation rates and their corresponding optimal  $N^+/Co$  ratios as a function of the toluene concentration in toluene/water mixtures.

$$[CoPc(NaSO_3)_4] = 8 \cdot 10^{-7} \text{ mol} \cdot \text{dm}^{-3},$$

$$[DM] = 2.1 \cdot 10^{-2} \text{ mol} \cdot \text{dm}^{-3}, \text{ 2,4-ionene } (\bar{M}_n = 5000 \text{ g} \cdot \text{mol}^{-1}).$$

The optimal  $N^+/Co$  ratio decreases sharply upon addition of toluene to the reaction mixture. Adding more than 1 vol.-% of toluene did not further affect the optimal  $N^+/Co$  ratio: at 1 vol.-% of toluene, where the toluene/DM vol.-%/vol.-% ratio is 2, the optimal  $N^+/Co$  ratio remains constant at a value of about 15. Apparently, less 2,4-ionene is needed to obtain optimal catalytic conditions. By contrast, the maximal thiol oxidation rate changes continuously over the whole range and three maxima can be observed. Five different regions can be distinguished in Fig. 10.3, where the reaction rate decreases or increases upon addition of more toluene to the reaction mixture. If the toluene fraction is larger than 1 vol.-%, no precipitation of disulfide is observed during the catalytic measurements: the disulfide formed dissolves in the toluene.

Before explaining the tremendous drop in the optimal  $N^+/Co$  ratio, it is necessary to look in detail to the reaction mechanism without toluene. Van Welzen proposed the dodecanethiol oxidation in water proceeds at the phase-boundary<sup>1)</sup>. At the interface between the negatively charged thiol droplets and water, the ionene will bind to the thiol. In this boundary layer,  $CoPc(NaSO_3)_4$  bound to the 2,4-ionene, will catalyze the thiol oxidation.

Several observations led to this proposal<sup>1)</sup>. First, in contrast to the reaction procedure followed for the mercaptoethanol oxidations<sup>8)</sup>, the reactions are started by addition of  $CoPc(NaSO_3)_4$  in the case of DM oxidations. Otherwise, a retardation was observed and lower reaction rates were measured, because the system requires some time to reach equilibrium conditions. The fact that the reaction proceeds at this thiol-water contact surface was explained by the dependence of the dodecanethiol oxidation rate on the  $N^+/Co$  ratio. On increasing the ionene concentration, the 2,4-ionene will bind to the thiol droplets. In the maximum the thiol droplets are optimally covered with ionene. Addition of more ionene,  $CoPc(NaSO_3)_4$  will bind to the 2,4-ionene in the continuous phase and as a consequence the oxidation rate decreases. Furthermore, the reaction rate was largely dependent on the impeller speed, which also confirmed that the interface plays a role.

Nevertheless, an emulsion-like system can be observed during the catalytic experiments. The question arises whether 1-dodecanethiol ( $pK_a = \pm 10.8$ )<sup>9)</sup> in water at alkaline conditions ( $pH = 13$ ) is able to form micelles. Therefore, we determined the surface tension properties of DM in water at  $pH = 13$  with two independent techniques. No decrease in surface tension upon increasing concentration of DM could be observed with either of the two methods. However, the thiol-water interfacial tension is influenced by the  $pH$ , indicating surface-active properties of DM. Going from a  $pH$  of 7 to 13, the interfacial tension decreases from 37 mN/m to 7 mN/m. Therefore, it can be assumed that most probably no micelles are present during the catalytic oxidations, but the catalytic reaction will proceed at the thiol droplet-water interface.

In addition, the DM droplet surface area was varied by using different DM concentrations (Fig. 10.5). Reducing the DM concentration, it can be seen that the optimal  $N^+$ -concentration is shifted to lower values and that the oxidation rate decreases simultaneously. A smaller amount of DM will diminish the total droplet surface area, leading to a reduction



of the complexation with 2,4-ionene. Opposite results were observed when larger DM concentrations were applied.

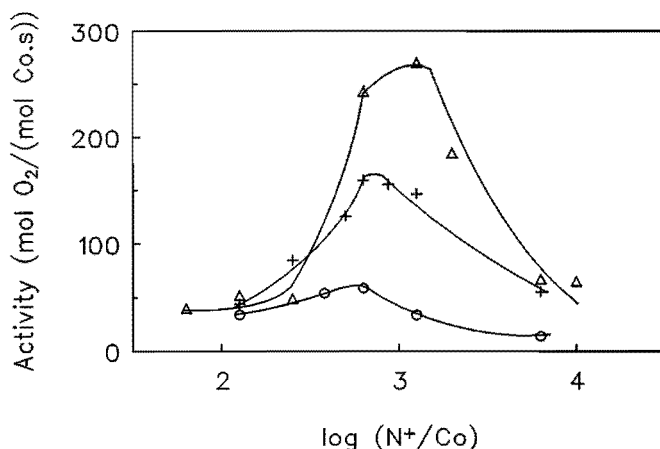


Figure 10.5 Effects of the N<sup>+</sup>-concentration on the 1-dodecanethiol oxidation rate at different DM concentrations.

$$[\text{CoPc}(\text{NaSO}_3)_4] = 8 \cdot 10^{-7} \text{ mol} \cdot \text{dm}^{-3},$$

$$2,4\text{-ionene } (\bar{M}_n = 6600 \text{ g} \cdot \text{mol}^{-1}). [\text{DM}] = 4.2 \cdot 10^{-3} \text{ mol} \cdot \text{dm}^{-3} \text{ (o)},$$

$$1.05 \cdot 10^{-2} \text{ mol} \cdot \text{dm}^{-3} \text{ (+)}, 2.1 \cdot 10^{-2} \text{ mol} \cdot \text{dm}^{-3} \text{ (}\Delta\text{)}.$$

Based on all above mentioned arguments, it can be stated that the mechanism of the dodecanethiol oxidation catalyzed by  $\text{CoPc}(\text{NaSO}_3)_4/2,4\text{-ionene}$  in water proceeds at the thiol-water interface. The high optimal N<sup>+</sup>-concentrations are a result of complexation between the negatively charged thiol droplets and the positively charged 2,4-ionene.

As remarked earlier, 1-dodecanethiol showed surface-active properties, therefore it should be possible to measure the mean droplet size. However, a stirring speed of 2600 r.p.m. makes a simple determination of the droplet size distribution impossible. Despite an emulsion-like system, the DM-droplets are not sufficiently colloiddally stable. Immediately after stopping the impeller, a large part of the thiol droplets coalesces and phase separation is observed. After phase separation, acidification and extraction of the aqueous phase, the DM concentration in the aqueous phase was measured by GC. It appeared that about 40 % of the amount of DM (0.5 vol.-% of DM is added) was present in the water

phase. The DM must be present in droplets in the aqueous phase, because of the extremely low solubility of 1-dodecanethiol in water ( $3 \cdot 10^{-5} \text{ mol} \cdot \text{dm}^{-3}$  at  $50 \text{ }^\circ\text{C}$ )<sup>10</sup>. These droplets are relatively colloidal stable and a volume average diameter of  $10 \text{ }\mu\text{m}$  was measured.

Before returning to the influence of toluene on the dodecanethiol oxidation mechanism, we have to keep in mind that an organic solvent has no influence on the aggregation behaviour of  $\text{CoPc}(\text{NaSO}_3)_4$  in the presence of ionene. It has been demonstrated before that addition of a monomerizing solvent<sup>11,12</sup>, did not affect the dimerization of the cobalt catalyst in the presence of 2,4-ionene<sup>13,14</sup>. Hence, other explanations for the effect of toluene on the optimal catalytic conditions of the oxidation of DM have to be sought.

Therefore, we first examined the effects of the type of organic solvent added. It appeared that apolar solvents, like n-hexane, n-dodecane and cyclohexane showed analogous characteristics, both with regards to the optimal  $\text{N}^+/\text{Co}$  ratios as well as to the maximal oxidation rates, as toluene. On the other hand, with addition of water-insoluble more polar solvents, such as 1-octanol, 1-decanol or 1-dodecanol, a completely different behaviour was noticed (Fig. 10.6). Instead of a radical decrease of the optimal  $\text{N}^+/\text{Co}$  ratio, an increase is observed. Also, the maximal activities are rather unaffected in contrast with those found with toluene. 1-Octanol, which has a similar water solubility as toluene, has a polarity similar to that of 1-dodecanethiol. Therefore, the behaviour with 1-octanol is not unexpected. At the droplet surface the polar heads of the alcohols are mixed with those of DM, thus, the interaction between the droplet surface and the polycation will be similar. Conceivably, the concentration of thiolate anions at the interface increases, because the polar alcohol groups are able of shielding the negatively charged thiol heads. This leads to an enhancement in the amount of  $\text{N}^+$  interacting with the droplets.

The drastic shift in optimal  $\text{N}^+/\text{Co}$  ratio could be a result of a drastic increase in droplet size upon addition of toluene. Hence, this will lead to a decrease in total surface area and, thus, less ionene will be able to interact with the droplets. In order to get insight in this, the DM oxidation in a mixture of 1-octanol, toluene and water was studied (Fig. 10.7). From 1 vol.-% of octanol onwards in Fig. 10.7, the droplet size will not vary much over the whole range. However, the optimal  $\text{N}^+/\text{Co}$  ratio radically drops at a small

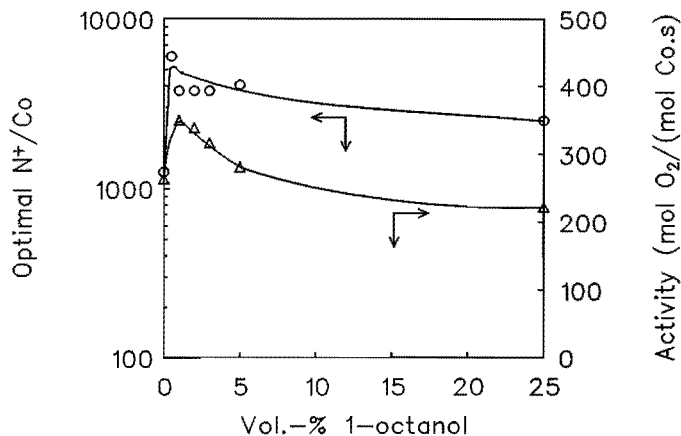


**Figure 10.6** Maximal 1-dodecanethiol oxidation rates and the corresponding optimal  $N^+/Co$  ratios as a function of the 1-octanol concentration in 1-octanol/water mixtures.  $[CoPc(NaSO_3)_4] = 8 \cdot 10^{-7} \text{ mol} \cdot \text{dm}^{-3}$ ,  $[DM] = 2.1 \cdot 10^{-2} \text{ mol} \cdot \text{dm}^{-3}$ , 2,4-ionene ( $\bar{M}_n = 15500 \text{ g} \cdot \text{mol}^{-1}$ ).

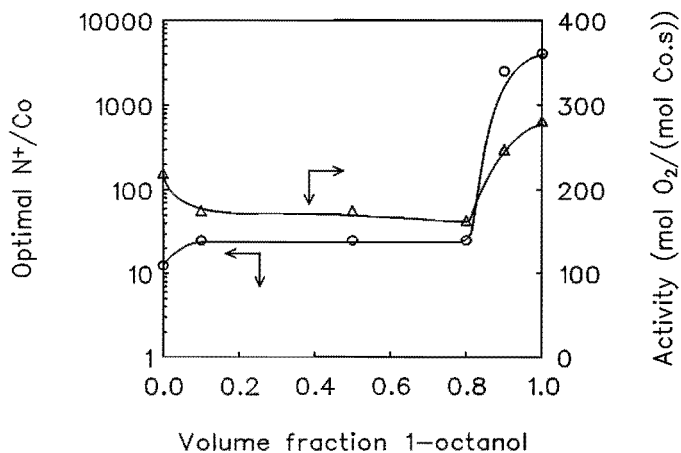


**Figure 10.7** Maximal 1-dodecanethiol oxidation rates and the corresponding optimal  $N^+/Co$  ratios as a function of the volume fraction 1-octanol in the organic phase in a toluene/1-octanol/water mixture. (Total volume percentage toluene and 1-octanol is kept constant at 5 vol. %).  $[CoPc(NaSO_3)_4] = 8 \cdot 10^{-7} \text{ mol} \cdot \text{dm}^{-3}$ ,  $[DM] = 2.1 \cdot 10^{-2} \text{ mol} \cdot \text{dm}^{-3}$ , 2,4-ionene ( $\bar{M}_n = 4900 \text{ g} \cdot \text{mol}^{-1}$ ).

toluene fraction, thus, it is unlikely that the optimal  $N^+/Co$  is determined by differences in droplet sizes. Another important observation is that in an 1-octanol/toluene mixture the catalytic properties are dominated by the apolar solvent toluene: even at high octanol concentrations the optimal  $N^+/Co$  ratio is still relatively low and the effect on the catalytic activity is rather limited.

Also, the interfacial tension, which is an important parameter for the droplet size, between an organic phase, consisting of toluene and dodecanethiol (4/1, v/v) and water at pH = 13 (9 mN/m), did not differ from the interfacial tension measured between DM and water. Nevertheless, we tried to determine the droplet size distribution. It appeared that in the presence of 5 vol.-% of toluene, 10 % of the amount of DM added (= 0.5 vol.-%) still was present in the aqueous phase in droplets after phase separation. The volume average droplet diameter was comparable with that measured without toluene. If 25 vol.-% of toluene is added only 1 % of the amount of DM is present in the aqueous phase. Thus, it can be concluded that the droplet size is not the determining factor in the drastic fall of the optimal  $N^+/Co$  ratio upon addition of an apolar solvent.

In addition, the molecular weight of polymeric 2,4-ionenes appeared to have no effect on the optimal  $N^+/Co$  ratio in region I-V. The application of different types of ionenes, like 2,6-, 2,10- and oleyl-ionene, resulted in a similar decrease of the optimal  $N^+$ -concentration by a factor of 100 upon introduction of toluene. In the presence of toluene, variation of the pH only led to a decrease of the maximum catalytic activity. From region II onwards, no influence could be observed whether the reaction was started by addition of  $CoPc(NaSO_3)_4$  or DM. The  $H_2O_2$ -concentration after complete reaction in all five regions indicated that no consecutive reaction between  $H_2O_2$  and DM occurred as in homogeneous thiol oxidations.

When the DM oxidation is homogeneously performed in a methanol/water mixture (Fig. 10.8), a relatively low optimal  $N^+/Co$  ratio can be observed. This is in agreement with the mercaptoethanol autoxidations<sup>15</sup>, because the reaction proceeds according to a completely different mechanism.

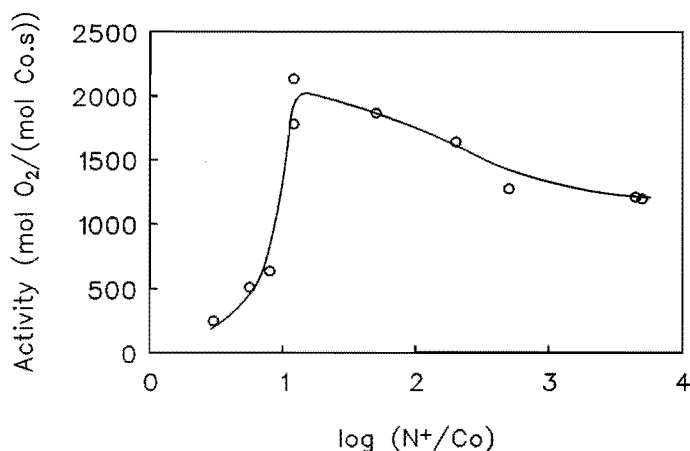


**Figure 10.8** The effect of the  $N^+/Co$  ratio on the 1-dodecanethiol oxidation rate in a methanol/water (80/20, vol.-%/vol.-%) mixture.  $[CoPc(NaSO_3)_4] = 10^{-7} \text{ mol} \cdot \text{dm}^{-3}$ ,  $[DM] = 2.1 \cdot 10^{-2} \text{ mol} \cdot \text{dm}^{-3}$ , 2,4-ionene ( $\bar{M}_n = 15000 \text{ g} \cdot \text{mol}^{-1}$ ).

Based on all results, a reaction model can be proposed, where the dodecanethiol oxidation in toluene-water mixtures proceeds at the phase-boundary. The low optimal  $N^+/Co$  ratio suggests that the primary function of the ionene has become the formation of the catalytically active dimers of  $CoPc(NaSO_3)_4$ . Already from a  $N^+/Co$  ratio of 4, dimeric catalyst species are formed and further addition of 2,4-ionene has no effect on the dimerization of  $CoPc(NaSO_3)_4$ <sup>14</sup>. Apparently, only a small part of the polycation seems to be necessary for interaction with the droplets.

Now we are able to clarify the different regions (Fig. 10.2 and 10.3). In region I, the  $N^+/Co$  ratio drops because of a decrease of the degree of complexation between the quaternary ammonium groups of the ionene and the thiolate anions. The decrease in activity is most probably a result of a decrease in total surface area. The dodecanethiol-toluene droplets are less colloiddally stable as compared with dodecanethiol droplets. This leads to coalescence of the droplets, resulting in larger droplet diameters.

From region II onwards the total surface area increases because of the increase in toluene concentration and, thus, the reaction rate rises. The main function of 2,4-ionene is the

stabilization of the catalytically active dimeric form of the catalyst. Only a small part of the 2,4-ionene interacts with the thiolate anions at the outside of the droplets. When increasing the toluene concentration further a larger fraction of DM will be present inside the toluene droplets, which will lead to a depletion of the DM concentration at the outside of the droplets (region III). Hence, lower reaction rates are observed.

At a toluene/water ratio of 1 the system turns from a toluene in water dispersion into a water in toluene dispersion. For similar reasons as for region II, the activity in region IV increases, because the reaction interface between toluene and water increases. In the last region V, the pH has increased to pH values of 14 and larger. These high ionic strengths result in lower DM oxidation rates.

It can be concluded that addition of organic solvents affects drastically the dodecanethiol oxidations. The amount of polyelectrolyte necessary to obtain optimal catalytic conditions can be decreased enormously upon addition of an organic solvent.

## 10.4 Conclusions

Addition of water-insoluble apolar solvents to the  $\text{CoPc}(\text{NaSO}_3)_4/2,4\text{-ionene}$ -catalyzed oxidation of the hydrophobic 1-dodecanethiol has an enormous effect on the reaction mechanism. Without an apolar solvent there is a high degree of complexation between the thiolate anions and the 2,4-ionene, which leads to a high optimal  $\text{N}^+/\text{Co}$  ratio. However, in the presence of small amounts of toluene the optimal  $\text{N}^+/\text{Co}$  ratio decreases drastically from 1250 to 15. Introducing more solvent to the system appeared to have no effect on the polycation/catalyst ratio. The maximal oxidation rates vary over the whole solvent composition range and are determined by differences in droplet sizes. Presumably, only a small part of the 2,4-ionene interacts with the thiolate anions at the outside of the droplets and the main function of the ionene is the formation of the active dimeric catalyst species.

Contrasting results are realized when more polar solvents are added. If octanol is present the optimal  $\text{N}^+$ -concentration rises. Apparently, without apolar solvents 2,4-ionene strongly interacts with the negatively charged droplets.

Deactivation of the catalytic system only takes place during dodecanethiol oxidations in toluene-water mixtures.

## References

1. J. van Welzen, A.M. van Herk, A.L. German, *J. Mol. Catal.*, **60** (1990) 351.
2. J.H. Schutten, T.P.M. Beelen, *J. Mol. Catal.*, **10** (1981) 85.
3. M. Hassanein, W.T. Ford, *J. Org. Chem.*, **54** (1989) 3106.
4. L. Rollmann, *J. Am. Chem. Soc.*, **97** (1975) 2132.
5. A. Skorobogaty, T.D. Smith, *J. Mol. Catal.*, **12** (1982) 131.
6. D. Wöhrle, T. Buck, G. Schneider, G. Schulz-Ekloff, H. Fischer, *J. Inorg. Organomet. Polym.*, **1** (1991) 115.
7. A.C. Egerton, A.J. Everett, G.J. Minkoff, S. Rudrakanthana, K.C. Salooja, *Anal. Chim. Acta*, **10** (1954) 422.
8. See Chapter 3.
9. H. Chaimovich, R.M.V. Aleixo, I.M. Cuccovia, D. Zanetta, F.H. Quina, in "Solution Behavior of Surfactants", K.L. Mittal, E.J. Fendler, Eds., New York, 1982, pp. 949-973.
10. I.M. Kolthoff, I.K. Miller, *J. Am. Chem. Soc.*, **73** (1951) 5118.
11. J.A. de Bolfo, T.D. Smith, J.F. Boas, J.R. Pilbrow, *J. Chem. Soc., Faraday Trans. II*, **72** (1976) 481.
12. Y.-C. Yang, J.R. Ward, R.P. Seiders, *Inorg. Chem.*, **24** (1985) 1765.
13. J. van Welzen, A.M. van Herk, A.L. German, *Makromol. Chem.*, **189** (1988) 587.
14. J. van Welzen, A.M. van Herk, A.L. German, *Makromol. Chem.*, **190** (1989) 2477.
15. See chapter 4.



## Chapter 11

# Molecular Mechanics Calculations on Cobalt Phthalocyanine Dimers

**SUMMARY:** In order to obtain insight into the structure of cobalt phthalocyanine dimers molecular mechanics calculations were performed on dimeric cobalt phthalocyanine species. First, in this chapter molecular mechanics calculations are presented on monomeric cobalt(II) phthalocyanine. Using the Tripos force field for the organic part of the molecule and parameters derived from literature and subsequently optimized to describe the Co<sup>II</sup> force field resulted in a geometry that is in very good agreement with experimental data from literature. Optimization of the dimeric structure leads to a geometry in which both phthalocyanines are separated by 3.2 Å and one of the molecules is shifted 2.38 Å in both X- and Y-direction with respect to the other. This geometry is in excellent agreement with literature data on  $\beta$ -Co(pc) crystals and with other calculated and experimental data on similar systems. All calculations have been performed with three possible charge distributions in the phthalocyanine molecule and it was shown that varying the used charge distribution had no significant effect on the final dimeric structure. The presented method provides valuable insight in the most important energetic interactions leading to dimer formation.

### 11.1 Introduction

As pointed out before, addition of 2,4-ionene to a solution containing the cobalt(II) phthalocyaninetetrasodiumsulfonate catalyst results in a 40-fold rate enhancement in the mercaptoethanol oxidation as compared with the polymer-free system<sup>1-3</sup>. Visible

light spectroscopy indicates that in the presence of 2,4-ionene dimerization of the phthalocyanine species occurs, which is assumed to play a major role in the observed rate enhancement<sup>4,5</sup>. In order to get insight into the interaction between 2,4-ionene and the dimeric cobalt phthalocyanine (Co(pc)) species, we studied the structure of a dimeric Co(pc) species, before modelling the interaction of this species with 2,4-ionene.

A good method for the investigation of molecular structures and geometries is molecular mechanics (MM), which has been applied successfully to organic molecules for many years<sup>6</sup>. The last decade, a growing interest is occurring for the use of MM in inorganic and metallo-organic chemistry<sup>7-16</sup>. A problem with the use of MM for the description of metal-ligand interactions is the absence of optimized force field parameters for most metals, including cobalt, in most commercial MM software packages.

In this study, force field parameters from similar studies<sup>9,11,13-15</sup> were used to estimate the required Co<sup>II</sup> force field parameters. The modelling of the Co(pc) dimer was performed in two subsequent steps: first we modelled a Co(pc) molecule and second we modelled the interaction between two of these molecules, which is merely determined by electrostatic and Van der Waals interactions<sup>17-21</sup>. Since these interactions are explicitly taken into account in the MM method, MM calculations are very likely to result in rather good geometric predictions for the Co(pc) dimer.

## 11.2 Experimental Section

All calculations were performed with the Molecular Mechanics software package SYBYL<sup>22</sup>) on the Convex C120 computer of the CAOS/CAMM Centre of Nijmegen University, The Netherlands. Force field parameters used for the description of the organic part of the molecule were taken from the Tripos force field<sup>23</sup>) and the following atom types were used: C.ar for all carbon atoms, N.ar for N<sub>b</sub> and N.pl3 for N<sub>a</sub> (see Fig. 11.1). Parameters for the description of the Co<sup>II</sup> force field were estimated from literature as described in the following sections and are listed in Tab.

11.2. All extra parameters for bonds and angles arising in the dimeric structure were set to zero.

## 11.3 Results and Discussion

### 11.3.1 Modelling of Cobalt(II) Phthalocyanine

The modelling of Co(pc) consisted of two parts, *i.e.* finding good force field parameters for the description of the organic part of the molecule and estimating good parameters for the Co-ligand interactions. Force field parameters for the organic part of the molecule were taken from the Tripos force field<sup>23)</sup> without modifications. The chosen atom types (Fig. 11.1) yielded overall the best geometry as compared with experimental data<sup>24)</sup>.

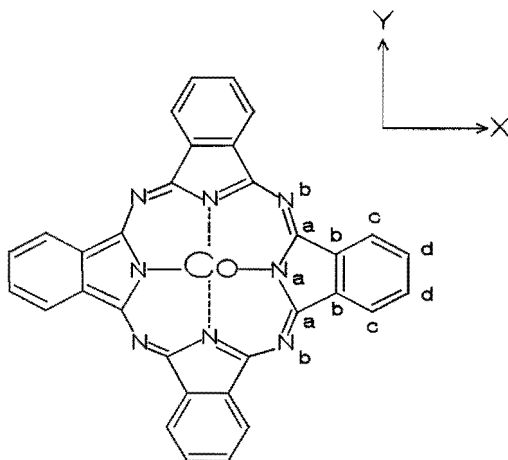


Figure 11.1 Labelling scheme of Co(pc) and definition of the coordinate axes.

In order to investigate the effect of charge distribution on the final geometry of both the monomer and dimer, we did calculations with three possible charge distributions. As a lower bound for the charge on Co, +1.48e was chosen<sup>24)</sup> and as an upper bound +2e. The most likely charge on Co seems to be +1.88e<sup>25,26)</sup>, so the results of the calculations for these three cases should cover nearly all possibilities. In the case of

$\text{Co}^{1.48+}$  and  $\text{Co}^{1.88+}$  experimental data were used for the corresponding charge distributions in the phthalocyanine ligands<sup>25,26)</sup> (see Tab. 11.1). The charge distribution in  $\text{Co}^{2+}(\text{pc})^{2-}$  was calculated by means of the Gasteiger-Hückel<sup>27,28)</sup> option within the SYBYL<sup>22)</sup> software package. In these calculations we assigned a charge of  $+2e$  to Co and the net charge of  $-2e$  was distributed within the phthalocyanine ligand. The overall trend of the charge distribution in all three cases is similar and agrees with the trends of an Extended Hückel calculation on  $\text{Co}(\text{pc})$ <sup>29)</sup> and of an *ab initio* calculation on cobalt porphine, in which the charge on Co was calculated to be  $+1.78$  to  $+1.88$ <sup>30)</sup>.

Table 11.1 Used charge distributions for  $\text{Co}(\text{pc})$  ( $e$ )

Atom	$\text{Co}^{1.48+}(\text{pc})^{1.48-}$ Figgis <i>et al.</i> <sup>24,26)</sup>	$\text{Co}^{1.88+}(\text{pc})^{1.88-}$ Figgis <i>et al.</i> <sup>25,26)</sup>	$\text{Co}^{2+}(\text{pc})^{2-}$ calculated
Co	+1.48	+1.880	+2.000
N <sub>a</sub>	-0.39	-0.337	-0.167
C <sub>a</sub>	+0.36	+0.261	+0.095
N <sub>b</sub>	-0.42	-0.497	-0.348
C <sub>b</sub>	-0.05	-0.065	-0.027
C <sub>c</sub>	-0.25 <sup>a)</sup>	-0.266	-0.080
C <sub>d</sub>	-0.24 <sup>a)</sup>	-0.239	-0.083
H <sub>c</sub>	+0.16 <sup>a)</sup>	+0.239	+0.053
H <sub>d</sub>	+0.24 <sup>a)</sup>	+0.252	+0.049

<sup>a)</sup> estimated from :  $(\text{C}_c + \text{H}_c) = -0.09$  and  $(\text{C}_d + \text{H}_d) = 0.0$  and charges of  $\text{Co}^{1.88+}$  case<sup>24-26)</sup>.

A first approximation of the equilibrium Co-N<sub>a</sub> bond length was determined by the method described by Drew *et al.*<sup>10)</sup>. We first assigned a very high value of 7000 kcal/(mol·Å<sup>2</sup>) to the Co-N stretching force constant and varied the equilibrium Co-N bond length from 1.80 Å to 2.05 Å. Due to the very high stretching force constant of the Co-N bond, the phthalocyanine ligand will adapt its conformation to suit the fixed Co-N bond length. The bond length at which the strain energy of the  $\text{Co}(\text{pc})$  molecule

shows a minimum is a good estimate for the equilibrium Co-N bond length. In Fig. 11.2 these results are presented for the  $\text{Co}^{2+}$  case and a deep well is shown at a distance of 1.95 Å. In order to investigate whether this strain energy vs Co-N distance relation still holds for more realistic stretching force constants, we performed the same calculations with a stretching force constant of 200 kcal/(mol·Å<sup>2</sup>)<sup>12-15,31</sup>. As can be seen from Fig. 11.2, again a minimum occurs at 1.95 Å, although the well itself is shallower than in the case of the very high force constant. A similar pattern was found in the cases of  $\text{Co}^{1.88+}$  and  $\text{Co}^{1.48+}$  and the results for the stretching force constant of 200 kcal/(mol·Å<sup>2</sup>) are also depicted in Fig. 11.2. It can be seen that in all cases a minimum in the strain energy occurs at a distance of 1.95 Å. Furthermore, it can be seen that the curvature in the region of the minimum is small and that the strain ener-

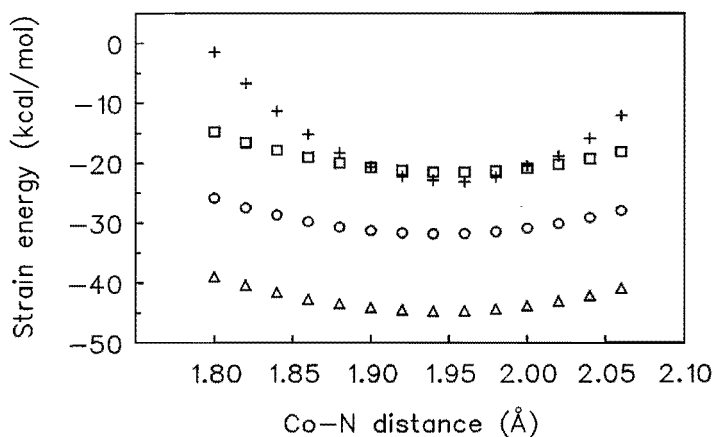


Figure 11.2 Plot of steric strain energy (kcal/mol) against  $\text{Co-N}_a$  distance (Å) for  $\text{Co}(\text{pc})$ .

(+)  $\text{Co}^{2+}(\text{pc})^{2-}$ ,  $\text{Co-N}_a$  stretching force constant = 7,000 kcal/(mol·Å<sup>2</sup>),

(□)  $\text{Co}^{2+}(\text{pc})^{2-}$ ,  $\text{Co-N}_a$  stretching force constant = 200 kcal/(mol·Å<sup>2</sup>),

(Δ)  $\text{Co}^{1.88+}(\text{pc})^{1.88-}$ ,  $\text{Co-N}_a$  stretching force constant = 200 kcal/(mol·Å<sup>2</sup>),

(o)  $\text{Co}^{1.48+}(\text{pc})^{1.48-}$ ,  $\text{Co-N}_a$  stretching force constant = 200 kcal/(mol·Å<sup>2</sup>).

gy at a bond length of 1.92 Å is less than 0.3 kcal/mol higher than the minimum. Further optimization of the equilibrium bond length was carried out with a starting bond length of 1.95 Å.

Initial estimates for the Co<sup>II</sup> force field parameters were taken from literature data on similar molecules<sup>11-15,32</sup>. Since many of these data are MM2 values, they seem to be good first estimates for their use in the Tripos force field, which is very similar to the MM2 force field.

The Co-N<sub>a</sub> bond stretching force constant, equilibrium bond length and Co-N<sub>a</sub>-C<sub>a</sub> angle bending force constant were varied simultaneously and the optimal combination was found to be: a stretching force constant of 250 kcal/(mol·Å<sup>2</sup>), an equilibrium bond length of 1.92 Å and an angle bending force constant of 1 kcal/(mol·degree<sup>2</sup>). With these parameters the calculated Co-N<sub>a</sub> distance was found to be 1.938 Å for the Co<sup>I,88+</sup> case, which could be improved to 1.931 Å if the angle bending force constant was lowered to 0.01 kcal/(mol·degree<sup>2</sup>), but then the overall geometry was worse compared to the case of an angle bending force constant of 1 kcal/(mol·degree<sup>2</sup>).

Torsional parameters for torsion angles containing Co were assigned by SYBYL<sup>22</sup> using default values. No attention was paid to these parameters because of their minor importance due to the very rigid structure of Co(pc). Van der Waals parameters for Co(pc) were estimated from the parameters used in low-spin Ni<sup>II</sup> and Co<sup>II</sup> studies. The Van der Waals radius for Co<sup>II</sup>, was chosen to be 2.35 Å, which seems to be a good estimate<sup>13</sup>. In contrast to the high  $\epsilon$  value of 1.65 kcal/mol reported in the same paper, we used a value of 0.25 kcal/mol, which seemed to be more reasonable when compared with other reported  $\epsilon$  values<sup>11,14,23,33</sup>.

The Co<sup>II</sup> out-of-plane-bending parameter was shown to have a minor effect on the overall energy. This was concluded from the optimization results obtained by energy minimizations using values for the out-of-plane bending force constant of 200 and 10,000 kcal/(mol·Å<sup>2</sup>). In all further calculations a value of 200 kcal/(mol·Å<sup>2</sup>) was used. This seemed to be a good estimate, because Adam *et al.*<sup>14</sup> used a value of 158 kcal/(mol·Å<sup>2</sup>) in Ni<sup>II</sup> tetraaza macrocycles, so no further optimizations for this

constant were carried out. A summary of the used Co<sup>II</sup> force field parameters is given in Tab. 11.2.

Table 11.2 Used force field for Co<sup>II</sup> in Co(pc)

Bond stretching		
Bond	$r^0/\text{\AA}$	$k/(\text{kcal}/(\text{mol} \cdot \text{\AA}^2))$
Co-N <sub>a</sub>	1.92	250
Angle bending		
Angle	$\theta^0/\text{degree}$	$k/(\text{kcal}/(\text{mol} \cdot \text{degree}^2))$
Co-N <sub>a</sub> -C <sub>a</sub>	126.50	1
N <sub>a</sub> -Co-N <sub>a</sub>	90	0.0013
Van der Waals		
Atom	$r^0/\text{\AA}$	$\epsilon/(\text{kcal}/\text{mol})$
Co	2.35	0.25
Out-of-plane bending		
Atom		$k/(\text{kcal}/(\text{mol} \cdot \text{\AA}^2))$
Co		200
Torsion	periodicity	$V_0/(\text{kcal}/(\text{mol} \cdot \text{degree}^2))$
All torsions involving Co	3	0.200

Optimization of the Co(pc) molecule with the parameters of Tab. 11.2 yields geometries that are in excellent agreement with the geometry published by Figgis *et al.*<sup>24)</sup>. The RMS difference in bond lengths for all three investigated charge distribution cases was found to be 0.062 Å if the C-H bond lengths are included and 0.029 Å if they are excluded. The calculated C-H bond lengths in Tab. 11.3 converge to the equilibrium C-H bond lengths assigned by SYBYL<sup>22)</sup> and are of minor importance for

the overall geometry, so it is not necessary to consider them explicitly. Also a good agreement was found for the bond angles, where the RMS differences were found to be  $0.60^\circ$ ,  $0.49^\circ$  and  $0.61^\circ$  for the  $\text{Co}^{1.48+}$ ,  $\text{Co}^{1.88+}$  and  $\text{Co}^{2+}$  cases respectively (if the C-C-H angles were excluded, otherwise the RMS values were  $0.72^\circ$ ,  $0.58^\circ$  and  $0.57^\circ$  respectively). The calculated bond lengths and bond angles are compared with the experimental values in Tab. 11.3 and 11.4.

Table 11.3 Comparison of calculated and experimental bond lengths ( $\text{\AA}$ )

Bond	calculated	calculated	calculated	experimental
	$\text{Co}^{1.48+}(\text{pc})^{1.48-}$	$\text{Co}^{1.88+}(\text{pc})^{1.88-}$	$\text{Co}^{2+}(\text{pc})^{2-}$	Figgis <i>et al.</i> <sup>24)</sup>
$\text{Co-N}_a$	1.935	1.938	1.941	1.919
$\text{N}_a\text{-C}_a$	1.346	1.345	1.349	1.380
$\text{N}_b\text{-C}_a$	1.337	1.337	1.338	1.325
$\text{C}_a\text{-C}_b$	1.394	1.394	1.393	1.457
$\text{C}_b\text{-C}_b$	1.386	1.386	1.387	1.398
$\text{C}_b\text{-C}_c$	1.395	1.395	1.396	1.397
$\text{C}_c\text{-C}_d$	1.401	1.402	1.401	1.396
$\text{C}_d\text{-C}_d$	1.404	1.404	1.404	1.410
$\text{C}_c\text{-H}_c$	1.086	1.086	1.085	0.96
$\text{C}_d\text{-H}_d$	1.087	1.088	1.086	0.98



Table 11.4 Comparison of calculated and experimental bond angles (°)

Angle	calculated	calculated	calculated	experimental
	Co <sup>1.48+</sup> (pc) <sup>1.48-</sup>	Co <sup>1.88+</sup> (pc) <sup>1.88-</sup>	Co <sup>2+</sup> (pc) <sup>2-</sup>	Figgis <i>et al.</i> <sup>24)</sup>
N <sub>a</sub> -Co-N <sub>a</sub>	90.0	90.0	90.0	90.0
Co-N <sub>a</sub> -C <sub>a</sub>	126.60	126.60	126.59	126.50
C <sub>a</sub> -N <sub>b</sub> -C <sub>a</sub>	122.46	122.86	122.90	121.07
C <sub>a</sub> -N <sub>a</sub> -C <sub>a</sub>	106.79	106.78	106.81	107.00
N <sub>b</sub> -C <sub>a</sub> -N <sub>a</sub>	127.09	126.97	126.88	127.93
N <sub>b</sub> -C <sub>a</sub> -C <sub>b</sub>	122.44	122.65	122.74	121.93
N <sub>a</sub> -C <sub>a</sub> -C <sub>b</sub>	110.44	110.49	110.38	110.14
C <sub>a</sub> -C <sub>b</sub> -C <sub>c</sub>	132.44	132.40	132.22	132.06
C <sub>a</sub> -C <sub>b</sub> -C <sub>b</sub>	106.14	106.15	106.23	106.36
C <sub>b</sub> -C <sub>b</sub> -C <sub>c</sub>	121.45	121.44	121.43	121.58
C <sub>b</sub> -C <sub>c</sub> -C <sub>d</sub>	117.50	117.58	117.45	117.06
C <sub>c</sub> -C <sub>d</sub> -C <sub>d</sub>	121.03	120.94	121.02	121.36
C <sub>b</sub> -C <sub>c</sub> -H <sub>c</sub>	120.48	119.81	120.95	121.2
C <sub>d</sub> -C <sub>c</sub> -H <sub>c</sub>	122.04	122.54	121.54	121.7
C <sub>c</sub> -C <sub>d</sub> -H <sub>d</sub>	119.21	119.41	119.44	119.9
C <sub>d</sub> -C <sub>d</sub> -H <sub>d</sub>	119.86	119.67	119.54	118.8

### 11.3.2 Modelling of Cobalt(II) Phthalocyanine Dimer

Modelling of the Co(pc) dimer was carried out by finding the mutual position of two phthalocyanine molecules for which the dimeric strain energy displays a minimum. In order to find this minimum we connected both molecules by a dummy bond and varied the bond length and the torsion angle around this bond. This was done for several different connections, of which the following cases will be discussed here: *i.e.*

$\text{Co}_{\text{Co}(\text{pc})1}-\text{Co}_{\text{Co}(\text{pc})2}$ ,  $\text{Co}_{\text{Co}(\text{pc})1}-\text{N}_{\text{a,Co}(\text{pc})2}$  and  $\text{Co}_{\text{Co}(\text{pc})1}-\text{N}_{\text{b,Co}(\text{pc})2}$ . Also calculations where Co was attached to the carbon atoms were performed, but these all lead to higher energies than the Co-N linked dimers.

All new force constants occurring due to the several new bonds and angles formed in this "super molecule" were set to zero, so no additional parameters have been added. This enables us to compare the energies of the several conformations objectively. Calculations on these dimeric structures have been performed for cobalt phthalocyanines with the three charge distributions mentioned. Only the results of  $\text{Co}^{1.88+}(\text{pc})^{1.88-}$  will be shown in the figures for clarity and the differences with the other two cases will be discussed.

#### *Case I: dimers through Co-Co linkage*

For  $\text{Co}^{1.88+}(\text{pc})^{1.88-}$ , a minimum of -94.5 kcal/mol was found in the overall dimeric strain energy upon decreasing the defined Co-Co bond from 6 to 2 Å, as can be seen in Fig. 11.3. However, the actual inter planar separation does not correspond to the defined Co-Co distance. As can be seen from Fig. 11.4a and 11.4b, the Co-Co distance converges to about 4.1 Å whereas the inter ligand distance converges to about 3.3 Å upon decreasing the defined Co-Co bond length. Optimizations of starting conformations in which the connecting bond length is smaller than about 3.6 Å lead to almost the same energy and geometry irrespective to the starting conformation. Only very small defined separations (~1.5 Å) do not lead to a realistic optimized structure. For the two other charge distribution cases a similar pattern was found. In the case of  $\text{Co}^{2+}(\text{pc})^{2-}$ , the energy decreases from -40.9 to -54.2 kcal/mol for the dimer and the final Co-Co distance is 4.2 Å. The  $\text{Co}^{1.48+}(\text{pc})^{1.48-}$  dimer shows an energy decrease from -64.3 to -75.2 kcal/mol and the final Co-Co distance is 3.9 Å. The final inter ligand distance for the latter two cases is the same as in the  $\text{Co}^{1.88+}(\text{pc})^{1.88-}$  case. The fact that the Co-Co distance does not converge to the same value as the inter ligand distance is due to the strong electrostatic repulsion between the two relatively high charges on the Co centres and even a stretching force constant of 10,000 kcal/(mol·Å<sup>2</sup>) used for the Co-Co bond had no influence on this optimized distance.

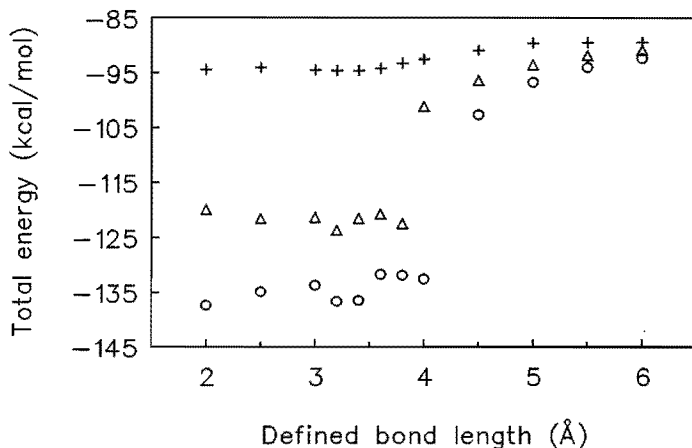


**Figure 11.3** Total energy (kcal/mol) as a function of the defined connecting bond length (Å) in a  $\text{Co}^{1.88+}(\text{pc})^{1.88-}$  dimer. (+) Case I: Co-Co linkage, ( $\Delta$ ) Case II: Co- $N_a$  linkage, (o) Case III: Co- $N_b$  linkage. Calculation results for defined bond lengths  $< 1.5 \text{ \AA}$  are not depicted, because the "optimized" geometries were completely deformed structures with very high energies.

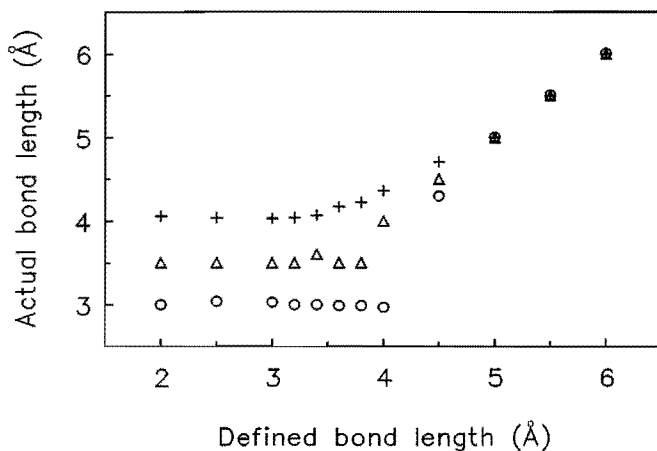


**Figure 11.4a** Plot of the length of the connecting bond (Å) in the  $\text{Co}^{1.88+}(\text{pc})^{1.88-}$  dimer after optimization against the defined connecting bond length (Å). (+) Case I: Co-Co linkage, ( $\Delta$ ) Case II: Co- $N_a$  linkage, (o) Case III: Co- $N_b$  linkage.

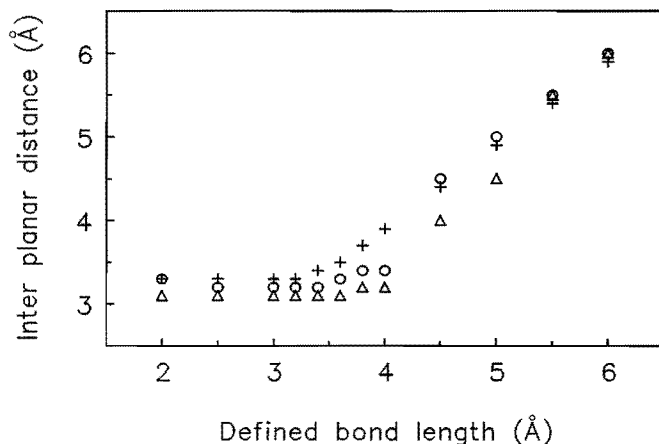


Figure 11.4b Plot of the average inter planar distance ( $\text{\AA}$ ) in the  $\text{Co}^{1.88+}(\text{pc})^{1.88-}$  dimer after optimization against the defined connecting bond length ( $\text{\AA}$ ). (+) Case I: Co-Co linkage, ( $\Delta$ ) Case II: Co- $N_a$  linkage, (o) Case III: Co- $N_b$  linkage.

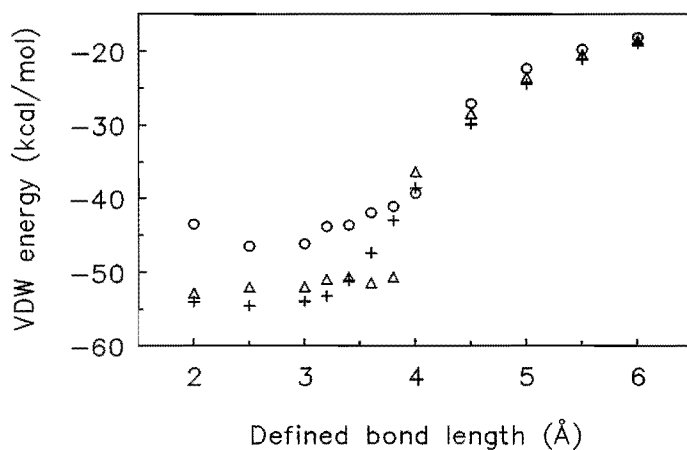


Figure 11.5 Plot of the VDW energy (kcal/mol) against the defined connecting bond length ( $\text{\AA}$ ) in a  $\text{Co}^{1.88+}(\text{pc})^{1.88-}$  dimer. (+) Case I: Co-Co linkage, ( $\Delta$ ) Case II: Co- $N_a$  linkage, (o) Case III: Co- $N_b$  linkage.

The main energetic contributions to the stabilization of the dimer consist of Van der Waals and electrostatic interactions. A plot of these energies against the defined Co-Co bond length is given in Fig. 11.5 and 11.6. If the sum of the energy changes in electrostatic and Van der Waals contributions going from the monomer to the dimer (see Tab. 11.5a) is considered, then it can be seen that on average the stabilizing effect is about 3 kcal/mol larger than the calculated energy of dimerization, here defined as the energy difference between the stable dimer and a pair of phthalocyanine molecules at 6 Å distance. This extra stabilization is compensated by a slight increase of the internal strain of a monomeric phthalocyanine arising from the dimer formation.

From these results it can be concluded that by optimizing the electrostatic and Van der Waals interactions in the dimer, a more favourable dimer conformation can be obtained.

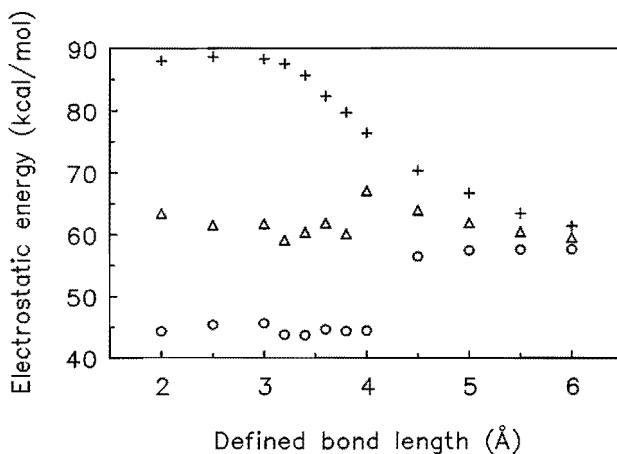


Figure 11.6 Plot of the electrostatic energy (kcal/mol) against the defined connecting bond length (Å) in a  $\text{Co}^{1.88+}(\text{pc})^{1.88-}$  dimer. (+) Case I: Co-Co linkage, ( $\Delta$ ) Case II: Co- $N_a$  linkage, (o) Case III: Co- $N_b$  linkage.

*Table 11.5a Comparison of the results for the dimers of  $\text{Co}^{2+}(\text{pc})^{2-}$ ,  $\text{Co}^{1.88+}(\text{pc})^{1.88-}$  and  $\text{Co}^{1.48+}(\text{pc})^{1.48-}$ .  
Case I : dimers through Co-Co linkage*

	$\text{Co}^{2+}(\text{pc})^{2-}$	$\text{Co}^{1.88+}(\text{pc})^{1.88-}$	$\text{Co}^{1.48+}(\text{pc})^{1.48-}$
Optimized Co-Co length/Å	4.2	4.1	3.9
Inter planar separation/Å	3.3	3.3	3.3
Dimerization energy/(kcal/mol)	-13.3	-5.1	-10.9
Change in Van der Waals energy/(kcal/mol)	-32.8	-32.1	-33.0
Change in electrostatic energy/(kcal/mol)	15.0	24.3	19.9
Torsion angle about Co-Co bond/degree	0	0	0

In order to find a better conformation within the Co-Co bond approach, we varied the  $\text{N}_a\text{-Co-Co-N}_a$  torsion angle, but the lowest energy was obtained for the eclipsed face-to-face dimeric conformation. The staggered conformation (rotated by  $45^\circ$  about the Z-axis) has an energy of about 3 kcal/mol higher than the eclipsed conformation.

*Case II: dimers through Co- $\text{N}_a$  linkage*

In the case of linkage between Co and  $\text{N}_a$ , a minimum of -123.8 kcal/mol was found upon decreasing the defined Co- $\text{N}_a$  bond length from 6 Å to 2 Å, which is depicted in Fig. 11.3. As can be seen from Fig. 11.4a and b, the inter planar distance in these dimers converges to about 3.1 Å, whereas the Co- $\text{N}_a$  distance converges to about 3.5 Å. Rotation of the two molecules with respect to each other via the linkage does not lead to an energetically more favourable conformation. Similar as in the case of the Co-Co linked dimers, the most favourable conformation is an eclipsed face-to-face conformation, but now one of the molecules has been moved 1.94 Å in the X- (or Y-)

direction parallel to the other molecule. Compared to the most favourable dimer via Co-Co linkage, these dimers are energetically more favourable, as was to be expected, because of a smaller electrostatic repulsion (see Fig. 11.6). The behaviour of the other two charge distribution cases is similar and the final geometries are the same as found in the  $\text{Co}^{1.88+}(\text{pc})^{1.88-}$  case (see Tab. 11.5b).

*Table 11.5b Comparison of the results for the dimers of  $\text{Co}^{2+}(\text{pc})^{2-}$ ,  $\text{Co}^{1.88+}(\text{pc})^{1.88-}$  and  $\text{Co}^{1.48+}(\text{pc})^{1.48-}$ .  
Case II : dimers through Co- $N_a$  linkage*

	$\text{Co}^{2+}(\text{pc})^{2-}$	$\text{Co}^{1.88+}(\text{pc})^{1.88-}$	$\text{Co}^{1.48+}(\text{pc})^{1.48-}$
Optimized Co- $N_a$ length/Å	3.5	3.5	3.5
Inter planar separation/Å	3.1	3.1	3.1
Dimerization energy/(kcal/mol)	-23.4	-32.8	-25.7
Change in Van der Waals energy/(kcal/mol)	-35.2	-32.3	-34.5
Change in electrostatic energy/(kcal/mol)	8.5	-0.4	7.2
Torsion angle about Co- $N_a$ bond/degree	0	0	0

*Case III: dimers through Co- $N_b$  linkage*

Linkage of the two phthalocyanine molecules via a Co- $N_b$  linkage resulted in an energy that was much lower than obtained in both other cases. As can be seen from Fig. 11.3, the minimum energy is -136.6 kcal/mol in the case of  $\text{Co}^{1.88+}(\text{pc})^{1.88-}$ . This lower energy cannot be explained by a difference in Van der Waals interactions, because these are of comparable magnitude in all three cases and are even higher in this case (see Fig. 11.5). As can be seen from Fig. 11.6, the reason for the extra stabilization lies in the fact that the electrostatic repulsion is significantly lower as in the other two cases and even decreases going from 6 Å to 2 Å.

As can be seen from Fig. 11.4a and b, the final inter planar distance is 3.2 Å and the final Co-N<sub>b</sub> distance is 3.0 Å. This geometry thus is consisting of two phthalocyanines at a separation of 3.2 Å and one phthalocyanine moved parallel with respect to the other 2.38 Å in the X- and 2.38 Å in the Y-direction. In the case of Co<sup>2+</sup>(pc)<sup>2-</sup> both the inter planar distance and the Co-N<sub>b</sub> distance converge to 3.1 Å, whereas the Co-N<sub>b</sub> distance converges to 3.2 Å and the inter planar distance to 3.1 Å in the case of Co<sup>1.88+</sup>(pc)<sup>1.88-</sup> (see Tab. 11.5c). As in cases I and II we tried to optimize the structure by rotation about the connecting bond, but again the non rotated conformation was most stable. A representation of the optimal geometry is given in Fig. 11.7.

*Table 11.5c Comparison of the results for the dimers of Co<sup>2+</sup>(pc)<sup>2-</sup>, Co<sup>1.88+</sup>(pc)<sup>1.88-</sup> and Co<sup>1.48+</sup>(pc)<sup>1.48-</sup>.  
Case III : dimers through Co-N<sub>b</sub> linkage*

	Co <sup>2+</sup> (pc) <sup>2-</sup>	Co <sup>1.88+</sup> (pc) <sup>1.88-</sup>	Co <sup>1.48+</sup> (pc) <sup>1.48-</sup>
Optimized Co-N <sub>b</sub> length/Å	3.1	3.0	3.2
Inter planar separation/Å	3.1	3.2	3.2
Dimerization energy/(kcal/mol)	-38.9	-44.3	-34.3
Change in Van der Waals energy/(kcal/mol)	-28.2	-25.7	-32.0
Change in electrostatic energy/(kcal/mol)	-11.5	-13.8	-3.5
Torsion angle about Co-N <sub>b</sub> bond/degree	0	0	0



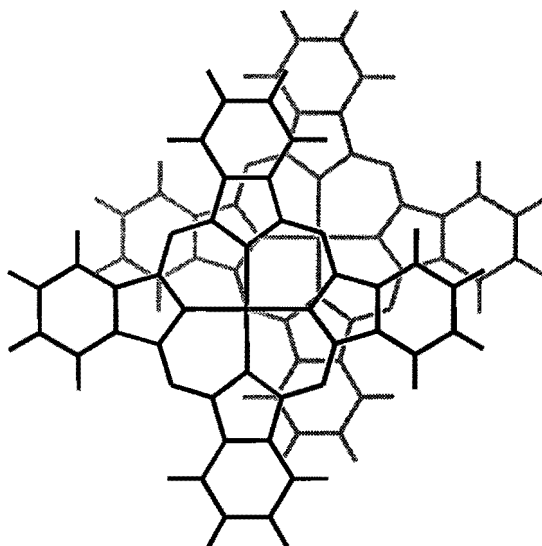


Figure 11.7 Optimized geometry of Co(pc) dimer.

#### Comparison of the three linkage cases

A summary of the most important results obtained in this study is given in Tab. 11.5a-c. As can be seen from these tables and Fig. 11.3, the dimers of case III geometry are more stable than both other dimers. Since the Van der Waals stabilization is almost the same in all three cases, the main cause of the difference in dimerization energy is the lower electrostatic repulsion in case III. It may be concluded that the Van der Waals interaction is the predominant factor in the stabilization of the dimer, but the final geometry is determined by the electrostatic interactions, which is in agreement with other studies<sup>34,35</sup>.

Furthermore, the most favourable conformation is a conformation that has been translated just in the X- and Y-directions and not been rotated about the Z-axis. This is in agreement with the fact that  $\pi$ -stacked porphyrins are not found in a rotated conformation<sup>34</sup>, but in disagreement with other MM calculations which predicted geometries in which one phthalocyanine or porphine ring was rotated about the Z-axis<sup>35</sup>. However, these authors did not present the energy difference between the eclipsed and staggered conformations, so it is not clear if this rotation contributes

much to an extra stabilization of the dimer. Anderson *et al.*<sup>36)</sup> performed MO calculations on Si(pc)-O-Si(pc) dimers and found that a dimer, in which the phthalocyanines were rotated 45° with respect to each other, was favoured over an eclipsed conformation by only 1 kcal/mol. This difference was not enough to conclude that the rotated dimer was more favourable than the eclipsed face-to-face conformation. Also the calculations of Sudhindra and Fuhrhop on porphine dimers<sup>17)</sup> showed a very small energy difference (0.7 kcal/mol) between an eclipsed face-to-face dimer and a dimer in which one molecule was rotated about the Z-axis by 60°, which was the optimal geometry.

The parallel shifts in X- and Y-directions leading to more stable geometries are in good agreement with earlier experimental and calculated data. Hunter and Sanders<sup>34)</sup> stated that rotations are not likely to occur, but an optimization of the energy can be achieved by parallel shifts of one molecule in both X- and Y-directions. They ascribe these shifts to  $\pi$ - $\pi$  repulsion terms. Similar shifts are observed in phthalocyanine crystals. Our results are in excellent agreement with experimental data published on  $\beta$ -Co(pc) crystals<sup>37,38)</sup>. X-Ray diffraction results at 295 K indicate a dimeric structure, similar to our structure, in which the Co of one phthalocyanine faces the N<sub>b</sub> of another phthalocyanine molecule at a separation of 3.219 Å<sup>37)</sup>. Single-crystal neutron diffraction methods at 4.3 K give the same structure in which the Co-N<sub>b</sub> distance is now 3.154 Å<sup>38)</sup>. Crystallographic studies on other phthalocyanine structures indicate comparable X- and Y-shifts. In stacked  $\alpha$ -Cu(pc) crystals, the phthalocyanines are shifted in the X- (or Y-) direction by 1.7 Å and have an inter planar separation of 3.4 Å<sup>39)</sup>. A similar geometry was found for  $\beta$ -Cu(pc) where the shift in the X- (or Y-) direction is 3.43 Å and the inter planar distance is 3.34 Å<sup>39)</sup>. In Mg(pc) crystals precipitated in pyridine, dimers were found in which one phthalocyanine was shifted along the Mg-N axis and the Mg centre of this molecule was positioned between the two C<sub>b</sub> atoms (convention of Fig. 11.1) of the other<sup>40)</sup>. The minimum separation between the two phthalocyanine molecules was found to be 3.239 Å.

## 11.4 Conclusions

The modelling of a cobalt(II) phthalocyanine molecule was very successful using the Tripos force field and some additional parameters estimated from literature. Excellent agreement with earlier reported crystallographic data on  $\beta$ -Co(pc) was obtained. Our results are also in agreement with calculated and experimental data on similar systems, which indicates the successful applicability of MM to these systems. Our method for modelling the dimeric structure of Co(pc) resulted in an optimized structure in which one of the molecules was shifted 2.38 Å in both the X- and Y-direction with respect to the other. The inter planar separation in this geometry is 3.2 Å, which is the same as found in  $\beta$ -Co(pc) crystals.

Furthermore, it was shown that the three used charge distributions yielded qualitatively comparable results, which indicates that the trend in the charge distribution is more important than the absolute values. The results also indicate that the Van der Waals interactions are the predominant factor in stabilizing the dimer, whereas the electrostatic interactions mainly determine the final geometry. Since our method is very straightforward we believe that it is very useful to model the interactions between larger molecules and that this will lead to (at least qualitatively) good results.

## References

1. W.M. Brouwer, P. Piet and A.L. German, *J. Mol. Catal.*, 1985, **31**, 169.
2. J. van Welzen, A.M. van Herk, A.L. German, *Makromol. Chem.*, **190** (1989) 2477.
3. See Chapter 4.
4. J. van Welzen, A.M. van Herk and A.L. German, *Makromol. Chem.*, 1987, **188**, 1923.
5. See Chapter 6.
6. U. Burkert and N.L. Allinger, "*Molecular Mechanics*", A.C.S. Monograph **177**, American Chemical Society, Washington D.C., 1982.
7. G.R. Brubaker, D.W. Johnson, *Coord. Chem. Rev.*, **53** (1984) 1.
8. V.J. Thöm, J.C.A. Boeyens, G.J. McDougall, R.D. Hancock, *J. Am. Chem. Soc.*, **106** (1984) 3198.
9. A.M. Bond, T.W. Hambley, M.R. Snow, *Inorg. Chem.*, **24** (1985) 1920.
10. M.G.B. Drew, S. Hollis, P.C. Yates, *J. Chem. Soc., Dalton Trans.*, (1985) 1829.
11. M.G.B. Drew, D.A. Rice, S. bin Silong, P.C. Yates, *J. Chem. Soc., Dalton Trans.*, (1986) 1081.
12. R.D. Hancock, J.S. Weaving, H.M. Marques, *J. Chem. Soc., Chem. Commun.*, (1989) 1176.
13. C. Harding, D. McDowell, J. Nelson, S. Raghunathan, C. Stevenson, M.G.B. Drew, P.C. Yates, *J. Chem. Soc., Dalton Trans.*, (1990) 2521.
14. K.R. Adam, M. Antolovich, L.G. Brigden, L.F. Lindoy, *J. Am. Chem. Soc.*, **113** (1991) 3346.
15. W.A. Kaplan, K.S. Suslick, R.A. Scott, *J. Am. Chem. Soc.*, **113** (1991) 9824.
16. T.N. Mali, P.W. Wade, R.D. Hancock, *J. Chem. Soc., Dalton Trans.*, (1992) 67.
17. B.S. Sudhindra, J.-H. Fuhrhop, *Int. J. Quant. Chem.*, **20** (1981) 747.
18. E.S. Dodsworth, A.B.P. Lever, P. Seymour, C.C. Leznoff, *J. Phys. Chem.*, **89** (1985) 5698.
19. Z. Gasyna, N. Kobayashi, M. Stillman, *J. Chem. Soc., Dalton Trans.*, (1989) 2397.
20. K. Kano, T. Hayakawa, S. Hashimoto, *Bull. Chem. Soc. Jpn.*, **64** (1991) 778.
21. T.H. Tran-Thi, J.F. Lipskier, P. Maillard, M. Momenteau, J.-M. Lopez-Castillo, J.-P. Jay-Gerin, *J. Phys. Chem.*, **96** (1992) 1073.
22. Tripos Associates, Inc., *SYBYL 6.0, Theory Manual*, St. Louis, November 1992.
23. M. Clark, R.D. Cramer III, N. Van Opdenbosch, *J. Comp. Chem.*, **10** (1989) 982.

24. B.N. Figgis, E.S. Kucharski, P.A. Reynolds, *J. Am. Chem. Soc.*, **111** (1989) 1683.
25. P.A. Reynolds, B.N. Figgis, *Inorg. Chem.*, **30** (1991) 2294.
26. P.A. Reynolds, B.N. Figgis, personal communication.
27. J. Gasteiger, M. Marsili, *Tetrahedron*, **36** (1980) 3219.
28. A. Streitwieser Jr., "*Molecular Orbital Theory for Organic Chemists*", Wiley, New York, 1961.
29. A.M. Schaffer, M. Gouterman, E.R. Davidson, *Theor. Chim. Acta*, **30** (1973) 9.
30. H. Kashiwagi, T. Takada, S. Obara, E. Miyoshi, K. Ohno, *Int. J. Quant. Chem.*, **14** (1978) 13.
31. P.V. Bernhardt, P. Comba, *Inorg. Chem.*, **31** (1992) 2638.
32. K.R. Adam, M. Antolovich, D.S. Baldwin, L.G. Brigden, P.A. Duckworth, L.F. Lindoy, A. Bashal, M. McPartlin, P.A. Tasker, *J. Chem. Soc., Dalton Trans.*, (1992) 1869.
33. N.L. Allinger, *Adv. Phys. Org. Chem.*, **13** (1976) 1.
34. C.A. Hunter and J.K.M. Sanders, *J. Am. Chem. Soc.*, **112** (1990) 5525.
35. T.G. Gantchev, F. Beaudry, J.E. van Lier, A.G. Michel, *Int. J. Quant. Chem.*, **46** (1993) 191.
36. A.B. Anderson, T.L. Gordon, M.E. Kenney, *J. Am. Chem. Soc.*, **107** (1985) 192.
37. R. Mason, G.A. Williams, P.E. Fielding, *J. Chem. Soc., Dalton Trans.* (1979) 676.
38. G.A. Williams, B.N. Figgis, R. Mason, S.A. Mason, P.E. Fielding, *J. Chem. Soc., Dalton Trans.*, (1980) 1688.
39. D. Wöhrle, G. Meyer, *Kontakte (Darmstadt)*, **3** (1985) 38.
40. M.S. Fischer, D.H. Templeton, A. Zalkin, M. Calvin, *J. Am. Chem. Soc.*, **93** (1971) 2622.

## Epilogue

The objective of this thesis was to obtain a better understanding of the role of polycation promoters in the cobalt phthalocyanine-catalyzed autoxidation of thiols. This study was concentrated on the use of poly(quaternary ammonium)salts (ionenes) in the  $\text{CoPc}(\text{NaSO}_3)_4$ -catalyzed autoxidation of thiols, because previous research showed that these polycations are the most promising promoters.

We first succeeded in separating the different promoting contributions polycations exhibit on the catalytic thiol oxidation.

The use of monodisperse oligomeric 2,4-ionenes showed that already small units of 2,4-ionene, with only two quaternary ammonium groups separated by four methylene groups, are capable of suppressing the formation of the inactive  $\mu$ -peroxo complexes and simultaneously inducing dimerization of the cobalt phthalocyanines. This was rather unexpected because this behaviour was thought to be characteristic of polymeric 2,4-ionene only. The chain length of the ionene appeared to have a minor effect on its excellent co-catalytic activity. Only the optimal polymer/catalyst ratio, expressed as  $\text{N}^+/\text{Co}$ , appeared to be dependent on the molecular weight of the ionene.

The concentrational promoting effect of 2,4-ionenes, *i.e.* substrate enrichment, which leads to higher local thiolate anion concentrations near the catalytically active centra, appeared to be responsible for a rate increase by a factor of 2-3 upon addition of 2,4-ionene. It appears that the optimal  $\text{N}^+/\text{Co}$  ratio as a function of the molecular weight of the ionene for the  $\text{CoPc}(\text{COOH})_8/2,4\text{-ionene}$  system is similar as for the  $\text{CoPc}(\text{NaSO}_3)_4/2,4\text{-ionene}$  system. This leads to the conclusion that the optimal 2,4-ionene/ $\text{CoPc}(\text{NaSO}_3)_4$  ratio is predominantly determined by substrate enrichment.

The catalytic properties of mixtures of oppositely charged water-soluble cobalt(II) phthalocyanines offered the possibility to study the sole contribution of dimerization of the catalyst to the overall activity. These mixtures exerted reaction rates, which are the highest measured so far for any phthalocyanine-catalyzed mercaptoethanol oxidation in the absence of polycations. Upon addition of 2,4-ionene to these stoichiometric hetero-dimeric and hetero-trimeric cobalt phthalocyanine complexes, reaction rates are obtained lower than those achieved for the conventional  $\text{CoPc}(\text{NaSO}_3)_4/2,4\text{-ionene}$  system.

Based on all insights acquired an improved reaction mechanism could be obtained, in which the ionene-induced  $\text{CoPc}(\text{NaSO}_3)_4$ -dimers are the most active species, which most probably break up during the catalytic cycle.

The next objective was to immobilize the catalytic system in order to make reuse and separation of products possible, and to simplify eventual practical applications. The catalytic system could be immobilized on polystyrene-ionene stabilized latex particles whilst maintaining high mercaptoethanol oxidation rates.

With that object, amphiphilic monodisperse polystyrene-ionene diblock copolymers with controlled block lengths have been synthesized according to a new synthetic route. The strategy of coupling end-functionalized polystyrene, prepared by anionic polymerization using a functional initiator, and small oligomeric units of 2,4-ionene, proved to be successful.

The catalytic oxidation of hydrophobic thiols proceeds according to a more complex mechanism. Besides the ionene promoting effects a significant effect of the end-group of the ionenes can be noticed. A tremendous rate increase in the 1-dodecanethiol oxidation by a factor of 100, as compared with the polymer-free system, is observed for monodisperse ionene oligomers, with four quaternary ammonium groups and with butylbromide end-groups.

Remarkably, the addition of apolar organic solvents to the oxidation of 1-dodecanethiol shows a drastic effect on the optimal catalytic reaction conditions. Addition of a

small amount of toluene leads to a sharp decrease of the optimal  $N^+/Co$  ratio from 1250 to 15. When the reaction is carried out in the presence of water-insoluble, more polar solvents, such as 1-octanol or 1-dodecanol, the opposite phenomenon is observed: the optimal  $N^+/Co$  ratio rises.

A first attempt was made to obtain insight into the optimal geometry of the dimeric cobalt phthalocyanine species by means of molecular mechanics calculations. The optimized structure of a cobalt phthalocyanine dimer we calculated is in agreement with literature data. However, it is impossible to determine the optimal structure of a dimeric cobalt phthalocyanine species in a polycationic environment.

In future, research should be concentrated on solving the question why ionene-induced dimeric cobalt phthalocyanine complexes are more active in the thiol oxidation as compared with the monomeric species. More evidence for the proposed mechanism postulated in Chapter 6 could be obtained by quantum chemical calculations on the reactivity of both monomeric and dimeric cobalt phthalocyanine species. The role of dimeric species during the catalytic cycle can also be further unravelled by synthesizing and studying the catalytic properties of a water-soluble covalently linked dimeric cobalt phthalocyanine species, which can function as a realistic model for a  $CoPc(NaSO_3)_4$ -dimer.



## Summary

This thesis describes a study on the role of polycation promoters in the cobalt phthalocyanine-catalyzed autoxidation of hydrophilic, as well as hydrophobic thiols. Previous studies demonstrated that, with 2-mercaptoethanol as substrate, the addition of poly(quaternary ammonium)salts, so-called ionenes, to the catalyst cobalt(II) phthalocyaninetetrasodiumsulfonate ( $\text{CoPc}(\text{NaSO}_3)_4$ ) resulted in a forty-fold enhancement of the reaction rate.

One of the main objectives was to obtain insight into the contribution of the separate promoting effects of ionenes on the catalytic thiol oxidation. First of all, the influence of the molecular weight of 2,4-ionene on the catalytic oxidation of 2-mercaptoethanol to its disulfide has been examined. For that purpose, several monodisperse oligomers of 2,4-ionene have been synthesized. From spectroscopic measurements it appears that trimeric 2,4-ionenes, containing two quaternary ammonium groups separated by four methylene groups, are already capable of suppressing the formation of the catalytically inactive oxygen-bridged dimeric complexes, the so-called  $\mu$ -peroxo complexes, and are able to stimulate the formation of active  $\text{CoPc}(\text{NaSO}_3)_4$ -dimers. It is surprising that this behaviour can be noticed for oligomeric ionenes, as till now this was only observed for high molecular weight 2,4-ionene. These oligomers also showed high co-catalytic properties, comparable with those of polymeric 2,4-ionene. The optimal polymer/catalyst ratio, expressed as  $\text{N}^+/\text{Co}$ , decreases with increasing chain length of 2,4-ionene and reaches a constant value of 50 for a 2,4-ionene with 8  $\text{N}^+$ . Furthermore, the optimal  $\text{N}^+/\text{Co}$  ratio appears to be dependent on the end-group of the ionene.

The water-soluble cobalt(II) phthalocyanineoctacarboxylic acid ( $\text{CoPc}(\text{COOH})_8$ ) forms no aggregates or  $\mu$ -peroxo complexes in the presence of 2,4-ionene under catalytic conditions. Hence, this catalyst complex offers the possibility to study exclusively the

effect of 2,4-ionene-induced substrate enrichment, *i.e.* a higher local thiolate anion concentration near the catalytically active centra. Addition of 2,4-ionene to an aqueous  $\text{CoPc}(\text{COOH})_8$  solution results in a rate enhancement by a factor of 2-3, which can entirely be ascribed to substrate enrichment. The optimal  $\text{N}^+/\text{Co}$  ratio as a function of the molecular weight of the ionene for the  $\text{CoPc}(\text{COOH})_8/2,4\text{-ionene}$  system is similar to that of the  $\text{CoPc}(\text{NaSO}_3)_4/2,4\text{-ionene}$  system. This leads to the conclusion that the optimal ionene/ $\text{CoPc}(\text{NaSO}_3)_4$  ratio is predominantly determined by substrate enrichment.

In addition, the spectroscopic and catalytic properties of mixtures of oppositely charged water-soluble cobalt phthalocyanines have been studied, which offer the possibility to elucidate exclusively the contribution of dimerization of the catalyst to the overall activity. A mixture of equimolar amounts of cobalt(II) phthalocyanine-tetra(trimethylammonium)iodide ( $\text{CoPc}[\text{N}(\text{CH}_3)_3\text{I}]_4$ ) and  $\text{CoPc}(\text{NaSO}_3)_4$  shows an increase in reaction rate for the 2-mercaptoethanol autoxidation as compared with an equal amount of one of the catalyst species separately. A mixture of  $\text{CoPc}(\text{COOH})_8$  and  $\text{CoPc}[\text{N}(\text{CH}_3)_3\text{I}]_4$  exhibits its maximum activity at a ratio of 1:2. The catalytic activities of these dimeric and trimeric catalyst complexes are the highest measured so far for any phthalocyanine-catalyzed mercaptoethanol autoxidation in the absence of polycations. Upon addition of 2,4-ionene, to an equimolar dimeric  $\text{CoPc}[\text{N}(\text{CH}_3)_3\text{I}]_4/\text{CoPc}(\text{NaSO}_3)_4$  complex lower reaction rates are obtained as those achieved for the conventional  $\text{CoPc}(\text{NaSO}_3)_4/2,4\text{-ionene}$  system. It can be concluded that the  $\text{CoPc}(\text{NaSO}_3)_4$ -dimers, which are the most catalytically active species, most probably break up during the catalytic cycle.

In order to make separation of products and catalyst after the thiol oxidation possible, the catalytic system was immobilized on latices. With that object, tailor-made amphiphilic monodisperse polystyrene-ionene diblock copolymers have been synthesized according to a new synthetic route. The preparation starts with the anionic polymerization of styrene using 3-(dimethylamino)propyllithium as initiator. This results in tertiary amino end-functionalized polystyrenes of molecular weights, which could be varied over a wide range (from 1 to 100 kg/mol), and of relatively low polydispersities ( $\bar{M}_w/\bar{M}_n = 1.1 - 1.4$ ). The crucial step in this method is the stepwise coupling of the reactive end-group of the polystyrene with bromo and tertiary amino terminated monodisperse oligomeric 2,4-ionenes. In this manner, amphiphilic block copolymers with a monodisperse ionene block consisting of up to 10 quaternary ammonium groups, could be obtained.

The polystyrene-ionene block copolymers act as surfactants and are built in latex particles during the emulsion polymerization of styrene. The latices with ionene chains at the particle surface extending into the water phase, are stabilized electrostatically as well as sterically. An important advantage of the applied preparative procedure is that no extensive cleaning techniques need to be used in order to remove free polyelectrolyte. After electrostatic immobilization of  $\text{CoPc}(\text{NaSO}_3)_4$  onto the cationic latices high mercaptoethanol oxidation rates are measured. Apparently, the short ionene chains at the particle surface are flexible and long enough to form  $\text{CoPc}(\text{NaSO}_3)_4$ -dimers and to induce substrate enrichment.

The polystyrene-ionene diblock copolymers as well as the monodisperse 2,4-ionene oligomers are excellent promoters in the oxidation of the water-insoluble 1-dodecanethiol. High catalytic activities are achieved with the block copolymers, because of hydrophobic interactions of the polystyrene blocks with 1-dodecanethiol. The use of the ionene oligomers shows that for the  $\text{CoPc}(\text{NaSO}_3)_4/2,4$ -ionene system the reaction rate is largely dependent on the molecular weight of 2,4-ionene. A tremendous acceleration of the oxidation rate by a factor of 100 ( $2000 \text{ mol O}_2/(\text{mol Co}\cdot\text{s})$ ), as compared with the polymer-free system, is observed for 2,4-ionene oligomers, with 4 quaternary ammonium groups and with butylbromide end-groups. No enhancement in the catalytic activity is found when the oligomers are equipped with the hydrophilic dimethylamino end-groups. These differences in activity can be ascribed to a very effective hydrophobic interaction between the butylbromide end-groups and the 1-dodecanethiol, resulting in an enormous increase in the reaction interface.

The oxidation of 1-dodecanethiol in water proceeds at the thiol-water phase-boundary: 2,4-ionene strongly interacts with the negatively charged dodecanethiol droplets. This leads to a very high optimal  $\text{N}^+/\text{Co}$  ratio of 1250. The addition of apolar organic solvents to the oxidation of 1-dodecanethiol has a remarkable effect on the optimal catalytic reaction conditions. For example, addition of a small amount of toluene leads to a sharp decrease of the optimal  $\text{N}^+/\text{Co}$  ratio from 1250 to 15. The low  $\text{N}^+/\text{Co}$  ratio indicates that the main function of the ionene is to stabilize the active dimeric form of the catalyst. Only a small percentage of the ionene is bonded to the droplet surface. When the reaction is carried out in the presence of water-insoluble, more polar solvents, such as 1-octanol

or 1-dodecanol, the opposite phenomenon is observed: the optimal  $N^+/Co$  ratio rises. Apparently, in the latter situation the 2,4-ionene interacts to a large extent with the thiolate anions present at the surface of the droplets.

In order to obtain insight into the structure of the catalytically active dimeric cobalt phthalocyanine complex, molecular mechanics calculations have been used to calculate the optimal geometry of a cobalt phthalocyanine dimer. Optimization of the dimeric structure leads to a geometry in which the phthalocyanines are separated by 3.2 Å and one of the molecules is shifted 2.38 Å in both X- and Y-direction with respect to the other. These results are in agreement with literature data. The presented method provides valuable insight in the most important energetic interactions leading to dimer formation.

## Samenvatting

Dit proefschrift beschrijft een studie naar de rol van polykationen in de kobalt-ftalocyanine gekatalyseerde autoxidatie van zowel hydrofiele als hydrofobe thiolen. Eerder onderzoek toonde aan dat bij het substraat 2-mercaptoethanol het toevoegen van poly(quaternaire ammoniumzouten), zogenaamde ionenes, aan de katalysator kobalt(II)-ftalocyanine-tetra-natriumsulfonaat ( $\text{CoPc}(\text{NaSO}_3)_4$ ) resulteerde in een 40-voudige verhoging van de reactiesnelheid.

Eén van de voornaamste doelstellingen is inzicht te verkrijgen in de bijdrage van de verschillende promoterende effecten van ionenes op de katalytische thiooxidatie. Allereerst is gekeken naar de invloed van het molecuulgewicht van 2,4-ionene op de katalytische oxidatie van het hydrofiele 2-mercaptoethanol tot disulfide. Voor dit doel zijn verschillende monodisperse oligomeren van 2,4-ionene gesynthetiseerd. Uit spectroscopische metingen blijkt dat trimere 2,4-ionenes, bestaande uit twee quaternaire ammoniumgroepen gescheiden door vier methyleengroepen, al in staat zijn om de vorming van katalytische inactieve zuurstofgebrugde dimeren, de zogenaamde  $\mu$ -peroxo-complexen, te onderdrukken en vorming van actieve dimeren van  $\text{CoPc}(\text{NaSO}_3)_4$  te bevorderen. Het is verwonderlijk dat dit gedrag al bij oligomere ionenes voorkomt, aangezien dit voorheen alleen was waargenomen voor hoog-moleculair 2,4-ionene. Ook zijn met deze oligomere ionenes hoge co-katalytische eigenschappen gevonden vergelijkbaar met die voor het polymere 2,4-ionene. De optimale polymeer/katalysator-verhouding, uitgedrukt als  $\text{N}^+/\text{Co}$ -verhouding, daalt met toenemende ketenlengte van 2,4-ionene en bereikt een constant niveau van 50 voor een 2,4-ionene met 8  $\text{N}^+$ . Deze verhouding blijkt verder afhankelijk te zijn van de eindgroep van het ionene.

Het water-oplosbare kobalt-ftalocyanine-octa-carbonzuur ( $\text{CoPc}(\text{COOH})_8$ ) vertoont in de aanwezigheid van 2,4-ionene onder katalytische condities geen aggregatie of  $\mu$ -peroxo-

complexvorming. Daardoor biedt dit katalysatorcomplex de mogelijkheid om alleen het door 2,4-ionene geïnduceerde effect van substraatverrijking, d.w.z. een hogere lokale thiolaat-anionconcentratie in de buurt van de katalytische actieve centra, te bestuderen. Toevoeging van 2,4-ionene aan een  $\text{CoPc}(\text{COOH})_8$ -oplossing resulteert in een activiteitsverhoging met een factor 2 à 3, die volledig kan worden toegeschreven aan substraatverrijking. Het verloop van de optimale  $\text{N}^+/\text{Co}$ -verhouding als functie van het molecuulgewicht van ionene is voor het  $\text{CoPc}(\text{COOH})_8/2,4$ -ionene-systeem gelijk aan die voor het  $\text{CoPc}(\text{NaSO}_3)_4/2,4$ -ionene-systeem. Geconcludeerd kan worden dat de optimale ionene/ $\text{CoPc}(\text{NaSO}_3)_4$ -verhouding hoofdzakelijk wordt bepaald door substraatverrijking.

Tevens zijn de spectroscopische en katalytische eigenschappen bestudeerd van tegengesteld geladen water-oplosbare kobalt-ftalocyanine-complexen, welke de mogelijkheid bieden om uitsluitend de bijdrage van dimerisatie van de katalysator tot de totale activiteit op te helderen. Een mengsel van equimolaire hoeveelheden van kobalt-ftalocyanine-tetra(trimethylammonium)jodide ( $\text{CoPc}[\text{N}(\text{CH}_3)_3\text{I}]_4$ ) en  $\text{CoPc}(\text{NaSO}_3)_4$  blijkt katalytisch actiever in de autoxidatie van mercaptoethanol dan één van de katalysatorcomplexen afzonderlijk. De maximale activiteit van een combinatie van  $\text{CoPc}(\text{COOH})_8$  en  $\text{CoPc}[\text{N}(\text{CH}_3)_3\text{I}]_4$  wordt bereikt bij een verhouding van 1:2. De activiteiten van deze dimere en trimere complexen zijn de hoogste tot nu toe gemeten in afwezigheid van polykationen. Door het toevoegen van 2,4-ionene aan het dimere  $\text{CoPc}[\text{N}(\text{CH}_3)_3\text{I}]_4/\text{CoPc}(\text{NaSO}_3)_4$ -complex zijn echter lagere reactiesnelheden verkregen als met het conventionele  $\text{CoPc}(\text{NaSO}_3)_4/2,4$ -ionene-systeem. Geconcludeerd kan worden dat de  $\text{CoPc}(\text{NaSO}_3)_4$ -dimeren, welke het meest katalytisch actief zijn, hoogstwaarschijnlijk tijdens de katalytische cyclus openbreken.

Om scheiding van de produkten en het katalysatorsysteem na de thioloxydatie mogelijk te maken, werd het katalysatorcomplex geïmmobiliseerd op latices. Hiervoor zijn amfifiele monodisperse polystyreen-ionene diblokcopolymeren gesynthetiseerd volgens een nieuwe route. De bereiding start met de anionische polymerisatie van styreen, gebruikmakend van 3-(dimethylamino)propyl-lithium als initiator. Dit resulteert in polystyreenen met tertiaire amino-eindgroepen en met molecuulgewichten van 1 tot 100 kg/mol en relatief lage dispersiegraden ( $\bar{M}_w/\bar{M}_n = 1.1 - 1.4$ ). De cruciale stap bij deze methode is de stapsgewijze koppeling van de reactieve eindgroep van het polystyreen met broom en tertiaire amino-getermineerde monodisperse oligomere 2,4-ionenes. Op deze

wijze zijn amfifiele blok-copolymeren met een monodispers ionenblok van maximaal tien quaternaire ammoniumgroepen verkregen.

De polystyreen-ionene blokcopolymeren kunnen dienen als surfactant en worden tijdens de emulsiepolymerisatie van styreen ingebouwd in de latex-deeltjes. De latices met ionene-ketens aan het latexoppervlak die in de waterfase steken, worden zowel elektrostatisch als sterisch gestabiliseerd. Een belangrijk voordeel van de gevolgde syntheseprocedure is dat geen arbeidsintensieve schoonmaaktechnieken behoeven te worden toegepast om vrij polyelektrolyet te verwijderen. Na elektrostatische immobilisatie van  $\text{CoPc}(\text{NaSO}_3)_4$  op de kationische latices zijn hoge oxidatiesnelheden voor mercaptoethanol gemeten. Blijkbaar zijn de korte ionenblokken aan het oppervlak flexibel en lang genoeg om  $\text{CoPc}(\text{NaSO}_3)_4$ -dimeren te vormen en substraatverrijking te induceren.

Zowel de polystyreen-ionene diblokcopolymeren als de monodisperse 2,4-ionene oligomeren zijn uitstekende promotoren bij de oxidatie van het water-onoplosbare 1-dodecaanhiol. Hoge katalytische activiteiten worden gemeten met de blokcopolymeren, dankzij hydrofobe interacties van het polystyreenblok met het 1-dodecaanhiol. Het gebruik van ionene oligomeren toont aan dat voor het  $\text{CoPc}(\text{NaSO}_3)_4/2,4$ -ionene-systeem een sterke molecuulgewichtsaafhankelijkheid van ionene op de katalytische activiteit wordt gemeten. Een gigantische versnelling van de oxidatiesnelheid en wel met een factor 100 ( $2000 \text{ mol O}_2/(\text{mol Co}\cdot\text{s})$ ) ten opzichte van het polymeer-vrije systeem, wordt bereikt met 2,4-ionene oligomeren, met 4 quaternaire ammoniumgroepen en butyl-brómide-eindgroepen. Er is geen verhoogde katalytische activiteit gevonden wanneer de oligomeren zijn uitgerust met hydrofiele dimethylamino-eindgroepen. Deze verschillen in activiteit kunnen worden verklaard door de zeer effectieve hydrofobe interactie van de butyl-bromide-eindgroepen met het 1-dodecaanhiol, resulterend in een enorme toename van het reactie-grensvlak.

De oxidatie van 1-dodecaanhiol in water verloopt aan het thiol-water fasegrensvlak: 2,4-ionene complexeert zeer sterk met het negatief geladen thiol druppeloppervlak. Dit heeft als gevolg een zeer hoge optimale  $\text{N}^+/\text{Co}$ -verhouding van 1250. Het toevoegen van apolaire organische oplosmiddelen tijdens de oxidatie van 1-dodecaanhiol heeft evenwel een opmerkelijk effect op de optimale katalytische reactiecondities. Een kleine

hoeveelheid toluen bijvoorbeeld zorgt voor een drastische daling van de optimale  $N^+/Co$ -verhouding van 1250 naar 15. De lage ionene/ $CoPc(NaSO_3)_4$ -verhouding duidt erop dat de belangrijkste functie van het ionene is het vormen van Co-dimeren. Verder is slechts een klein percentage van het ionene gebonden aan het druppeloppervlak. Wanneer de reactie wordt uitgevoerd in aanwezigheid van water-onoplosbare meer polaire solvents zoals 1-octanol, vindt het tegengestelde fenomeen plaats: de optimale  $N^+/Co$ -verhouding stijgt. Blijkbaar is het ionene in het laatste geval in hoge mate gecomplexed met de thiolaat-anionen aan de buitenkant van de druppels.

Om een inzicht te verkrijgen in de uiteindelijk structuur van het meest katalytisch actieve dimeer-complex van kobalt-ftalocyanine, is met molecular mechanics de optimale geometrie van een kobalt-ftalocyanine-dimeer berekend. Optimalisatie van de dimere structuur leidt tot een geometrie waarin de afstand tussen de moleculen  $3.2 \text{ \AA}$  is en de moleculen  $2.38 \text{ \AA}$  verschoven zijn in zowel de x- als y-richting. Deze resultaten komen overeen met data uit de literatuur. De gepresenteerde methode levert verder waardevolle informatie op over de verschillende energetische interacties die leiden tot dimeervorming.



## Dankwoord

Graag wil ik iedereen bedanken die op een of andere wijze een bijdrage heeft geleverd aan het tot stand komen van dit proefschrift. Enkelen wil ik met name noemen.

Op de eerste plaats wil ik mijn eerste promotor Ton German bedanken voor de stimulerende begeleiding, het in mij gestelde vertrouwen en de grote mate van vrijheid.

Mijn co-promotor Pieter Piet wil ik graag bedanken voor de motiverende en plezierige begeleiding en voor de vele nuttige, vaak pragmatische, discussies die we hebben gevoerd.

Grote erkentelijkheid gaat uit naar mijn afstudeerders, Jan van Hest, Hans Heuts, Hein Hopstaken, Tijs Nabuurs, Ralph Pinckaers en Alexander Roelofs voor hun inzet en hun enthousiaste manier van samenwerken.

In het bijzonder wil ik ook mijn kamergenoten Henno van Beek, Paul Cools en Lodewijk van de Heuvel bedanken voor de gezellige tijd en plezierige samenwerking.

Speciale dank gaat uit naar Wieb Kingma (GPC) en Herman Ladan (TEM en SEM) voor de experimentele ondersteuning.

Theo Beelen (Vakgroep Anorganische Chemie en Katalyse) dank ik voor zijn bijdrage aan Hoofdstuk 6.

Prof. Hirofusa Shirai of the Department of Functional Polymer Science of the Shinshu University (Ueda, Japan) is acknowledged for kindly providing cobalt phthalocyanine-octacarboxylic acid.

Verder wil ook Steven van Es, Alex van Herk, Ton Janssens, Jan Meuldijk, Harold Schoonbrood, Rik ter Veen en Tonnie Willems bedanken voor hun inbreng aan het onderzoek. Ook dank ik de vele praktikanten voor hun experimentele werk.

Tenslotte dank ik alle (ex-)collega's, familie en vrienden voor de door hen getoonde belangstelling tijdens mijn promotieonderzoek.

## **Curriculum Vitae**

Eugène Schipper werd geboren op 30 juli 1966 te Helmond. Hij behaalde in 1984 het VWO diploma aan het dr. Knippenbergcollege te Helmond. In datzelfde jaar begon hij met de studie Scheikundige Technologie aan de Technische Universiteit Eindhoven en legde een jaar later het propaedeutisch examen af. In juni 1989 studeerde hij af bij de vakgroep Anorganische Chemie en Katalyse onder leiding van prof.dr. R.A. van Santen. In augustus 1989 begon hij het in dit proefschrift beschreven onderzoek bij de vakgroep Polymeerchemie en Kunstoftechnologie aan de Technische Universiteit Eindhoven onder leiding van prof.dr.ir. A.L. German.

# STELLINGEN

behorende bij het proefschrift

## Role of Polycation Promoters in the Cobalt Phthalocyanine-Catalyzed Autoxidation of Thiols

van

Eugène Theodorus Wilhelmus Maria Schipper

1. Polymere katalyse is oligomere katalyse.  
Dit proefschrift.
2. Het is zeer twijfelachtig dat Takahashi *et al.* 3,3-ionene-tetrahydrofuran triblok copolymeren hebben kunnen vervaardigen in een methanol/benzeen mengsel, aangezien de oplosbaarheid van 3,3-ionene in dit mengsel zeer laag is.  
A. Takahashi, M. Kawaguchi, T. Kato, M. Kuno, S. Matsumoto, *J. Macromol. Sci.-Phys.*, **B17** (1980) 747.  
Hoofdstuk 7 uit dit proefschrift.
3. De conclusie van Li *et al.*, dat één CH<sub>2</sub>CH<sub>2</sub>- en vier CH<sub>3</sub>-groepen een hydrofoob domein vormen in 2,10-ionene, is niet juist. De hydrofobe domeinen van 2,10-ionene worden gevormd door de (CH<sub>2</sub>)<sub>10</sub>-segmenten.  
Z.M. Li, X.X. Zhang, Y.P. Chen, Y.Z. Zhong, *Macromolecules*, **25** (1992) 450.
4. De bewering van Shirai *et al.* dat zij het eerste bewijs presenteren voor een "enzyme-like" gekatalyseerde oxidatie van thiol, die verloopt via een radicaal mechanisme, is onterecht.  
H. Shirai, H. Tsuiki, E. Masuda, T. Koyama, K. Hanabusa, N. Kobayashi, *J. Phys. Chem.*, **95** (1991) 417.  
J. Zwart, proefschrift, Technische Universiteit Eindhoven, 1978.  
W.M. Brouwer, P. Piet, A.L. German, *J. Mol. Catal.*, **22** (1984) 297.  
A.M. van Herk, A.H.J. Tullemans, J. van Welzen, A.L. German, *J. Mol. Catal.*, **44** (1988) 269.

5. Bajpai en Otsu baseren hun hele artikel op een verkeerde suggestie, namelijk dat de polymerisatie van methylmethacrylaat met benzyltrifenylfosfonium bromide als initiator verloopt via een levend radicaalpolymerisatie mechanisme, terwijl het een gewone radicaalpolymerisatie betreft. Dit draagt niet bij tot de helderheid van het artikel.  
U.D.N. Bajpai, T. Otsu, *Eur. Polym. J.*, **29** (1993) 517.
6. Na een gedegen inventarisatie van de visfauna in Zuid-Amerika zou het aantal Rivulus-soorten wel eens groter kunnen zijn dan het aantal Aphyosemion-soorten.  
*Killi Nieuws*, **22** (1992) 105.
7. Sinds de invoering van het setpunten-systeem door de NTTB is de teamopstelling van ondergeschikt belang geworden.
8. Het wordt tijd dat een officiële tijdwaarnemer zijn intrede doet bij het professionele veldvoetbal.
9. Het feit dat een stelling in iemands proefschrift staat, betekent niet dat de auteur van het proefschrift de stelling zelf heeft verzonnen.
10. De term initiële opleiding past beter aan het begin van het rijtje basisonderwijs, basisvorming en voorbereidend wetenschappelijk onderwijs, dan aan het eind.
11. Het is een schande voor de mensheid dat overal ter wereld wel wapens te verkrijgen zijn, maar geen voedsel.
12. Deze stelling wordt het meest gelezen.

Eindhoven, 19 januari 1994